Evaluation of Structured Light Plethysmography for lung function monitoring in pediatric respiratory disorders

Hamzah Hmeidi

This thesis is submitted in partial fulfilment of the requirement for the degree of Doctor of Philosophy

Supervised by

Dr. Edward Chadwick & Prof. Warren Lenney

Keele University

June 2019

Abstract

Current Lung function assessments in children can be clinically challenging and even inapplicable in preschool children, this is due to the test requirements of cooperation and understanding. Hence, there is a need for new techniques that can overcome these limitations. Structured Light Plethysmography (SLP) is a new non-invasive technique to measure tidal breathing by capturing the movement of the thoraco-abdominal wall. This technique requires minimal subject cooperation as it does not require the subject to perform any breathing manoeuvres but to sit still and breathe normally. The usefulness of SLP in adults has been shown in previous studies, specifically in detecting abnormal breathing patterns in adults diagnosed with Chronic Obstructive Pulmonary Disease (COPD). SLP is arguably a more suitable method for young children and infants. Therefore, the main aim of this study was to determine the reliability of SLP for lung function monitoring in paediatric population. The first part of this project aimed to investigate the use of SLP in assessing tidal breathing parameters in: (1) school-age children (7-16 years) with stable Asthma, (2) younger children (2-12 years) recovering from acute asthma/wheeze and (3) infants recovering from acute viral bronchiolitis (0-1 year). Whereas, the second part aimed to assess the robustness of the parameter estimation algorithm against interferences that might be introduced to the SLP signal during data acquisition.

The results obtained from the studies conducted in this work illustrated the feasibility of SLP procedure in obtaining a reliable assessment of lung function in children aged 0 to 17 years. This is true for children presenting with normal lung function and lung function affected by stable asthma, acute asthma/wheeze and acute viral bronchiolitis. The method proved sensitive enough to detect differences in clinically important measures in healthy, asthmatic and recovering populations. This suggests that the potential use of SLP in monitoring asthma and bronchiolitisworth further investigation. However, more refinements in data analysis techniques are required. The robustness of the algorithm to possible interferences also needs to be further investigated before being introduced clinically.

Acknowledgements

I would like to generously thank many people, who participated in the work presented in this thesis.

Firstly, I would like to express my sincere gratitude to my supervisors Dr. Ed Chadwick & Prof. Warren Lenny for their continuous support, patience, motivation and immense knowledge. Their guidance helped me in all the time of research and writing of my thesis.

Similar, many thanks to Eric Roe for his continuous support during my data collection at the hospital, the successful completion of the clinical studies owed much to his active input.

I would also like to express my gratitude to Dr Caroline Stewart, Prof Anand Pandyan, Dr Dimitra Blana and Dr Charles Day for sharing their expertise so willingly, especially during the PhD lab meetings which was of a great value.

Many thanks also to the ISTM rehabilitation research PhD students: Ali, Mohammad, Ahmad, Fraser, Amnah, Badrieh and Shallum. Thank you all for the useful discussions and delicious meal that we had in the office.

A special thanks to Marina Alarcon Garcia for everything. Your love and support provided me with the strength that I needed to carry on and could not have accomplished this work without you.

Finally, but by no means least, Mom and Dad you were my source of inspiration. Thank you so much for believing in me and for your ongoing love and support throughout this journey. Many thanks also to my family and friends for their support.

Statement of interest and funding acknowledgment

Funding for the PhD (including stipend, tuition fees and project costs) is gratefully acknowledged from Pneumacare Ltd and the Guy Hilton Astham Trust.

Hamzah Hmeidi was employed by PneumaCare Ltd after data collection and analysis was completed.

Contents

1 Introduction 1

2 Literature review 3

2.1 Anatomy of respiratory system 3

2.2 Respiratory system structure and function 4

2.2.1 Nose and Nasal Cavity 4

2.2.2 Mouth 4

2.2.3 Pharynx 4

2.2.4 Larynx 4

2.2.5 Trachea 5

2.2.6 Bronchi and Bronchioles 5

2.2.7 Lungs 6

2.3 Development of the respiratory system 7

2.4 Natural physiology of breathing 8

2.4.1 Pulmonary Ventilation 8

2.4.2 External Respiration 9

2.4.3 Internal Respiration 9

2.4.4 Transportation of Gases 9

2.4.5 Homeostatic Control of Respiration 10

2.5 Respiratory Disease in Childhood 10

2.5.1 Childhood Asthma 10

2.5.2 Pre-school wheeze 12

2.5.3 Acute Viral Bronchiolitis (AVB) 13

2.5.4 Pathophysiological alterations in obstructive lung disease 14

2.6 Measures of the Lung Functions 15

2.6.1 Spirometry 15
2.6.2 Whole-Body Plethysmography 18
2.6.3 Measurements of Chest Wall Movement 19
2.7 Summary 26
3 Study Aims 28
4 Structured Light Plethysmography (SLP) 29
4.1 Introduction 29
4.2 Tidal Breathing 29
4.2.1 Flow-based tidal breathing parameters 30
4.3 Structured Light Plethysmography - Thora3Di™ 30
4.3.1 Thora3Di™ Working Principle 31
4.3.2 Thora3Di™ tidal Breathing Parameters 35
4.3.3 Thora3Di™ Software and Data Analysis 41
5 Tidal breathing parameters in healthy children and those with stable asthma 42
5.1 Introduction 43
5.2 Study Aims 44
5.3 Methods 44
5.3.1 Study participants and design 44
5.3.2 Study devices and procedures 45
5.3.3 Parameters 45
5.3.4 Statistical Analysis 45
5.4 Results 46
5.4.1 Study population 46
5.4.2 Spirometry 46
5.4.3 Tidal breathing parameters' magnitudes and within-subject variabilities 46

5.5 Discussion 54
5.6 Conclusions 56
6 Tidal breathing parameters in Children recovering from acute asthma 57
6.1 Introduction 58
6.2 Materials and Methods 58
6.2.1 Participants 58
6.2.2 Study design 59
6.2.3 SLP procedure and data analysis 59
6.2.4 Statistical Analysis 59
6.3 Results 60
6.4 Discussion 66
7 Acute Viral Bronchiolitis (AVB) Study 75
7.1 Introduction 76
7.2 Materials and methods 76
7.2.1 Participants 76
7.2.2 Study design 77
7.2.3 SLP procedure and data analysis 77
7.2.4 Statistical Analysis 77
7.3 Results 78
7.4 Discussion 82
7.5 Conclusion 84
8 Investigating the effect of upper-body movements and coughs on SLP quantified parameters 85
8.1 Introduction 86
8.2 Digital Filters 89

8.2.1 Frequency Domain Parameters....90
8.3 Discrete Fourier Transform (DFT) 91
8.4 Wavelet Transformation 93
8.4.1 Introduction....93
8.4.2 Continuous-time Wavelet Transformation (CWT)....94
8.5 Spectral Subtraction 96
8.5.1 Spectral Subtraction Principle 96
8.6 Abnormalities-Removal Algorithm 97
8.7 Methodology 99
8.7.1 Study Participants and design 99
8.7.2 Study Devices and Procedures....99
8.7.3 Study divisions....100
8.8 Study Aims....102
8.9 Software and Data Analysis....102
8.9.1 Pre-processing....102
8.9.2 Calculation of Tidal Breathing Parameters....103
8.9.3 Statistical Analysis....104
8.9.4 Results....105
8.10 Discussion 128
8.10.1 Sitting Still and Breathing 128
8.10.2 The Effect of Upper-Body Movements on the Derived Tidal Breathing Parameters....130
8.10.3 The Effect of Coughing on SLP-Derived Parameters 133
9 General Discussion 135
9.1 Limitations 139

10 Conclusion and Future Work 140

11 References: 143

12 Appendices 158

Appendix - A Matlab codes 158

Appendix - B Clinical Studies Demographic 165

12.1 Healthy Subjects 165

12.2 Acute Asthma: 167

12.3 Stable asthma: 168

Appendix - C Bland-Altman Agreement Plots 169

List of Figures

Figure 2-1. Main respiratory system structures 3

Figure 2-2. Normal Airway vs an airway with asthma.....11

Figure 2-3. Forced expired volume in one second (FEV1) and forced vital capacity (FVC), displayed on a spirometry output.....16

Figure 2-4. Maximal expiratory and inspiratory flow-volume loop.....16

Figure 2-5. A flow-based spirometer.....17

Figure 2-6 The device developed by Konno and Mead to measure chest and abdominal wall displacements.....21

Figure 2-7 Respiratory inductance plethysmography, band are used to measure change in the cross-sectional area enclosed by the bands.....23

Figure 2-8 Electromagnetic inductive plethysmography. Upper shows a single coil representation of the device and lower shows a vest (containing the RC and B coils) placed on a new born infant 24

Figure 2-9 Optoelectronic plethysmography 26

Figure 4-1. A child undergoing an SLP assessment in a seated position 30

Figure 4-2. A child undergoing an SLP assessment in a supine position.....31

Figure 4-3. Basic Layout for a Parallel-optical axes Stereo Imaging system.....31

Figure 4-4. Two stereo Images of a Cube.....32

Figure 4-5. Parallel geometry system 32

Figure 4-6. Grids identification on a patient's TA wall.....35

Figure 4-7. SLP-traces of tidal breathing and the derived parameters. 37

Figure 4-8. The anterior TA wall split into two sections,.....38

Figure 4-9. Thoracic and abdominal components of one breath as calculated using SLP 38

Figure 4-10. A representation of Konno and Mead method of quantifying thoracoabdominal asynchrony for a single breath. 39

Figure 4-11. A single breath representation using Konno-Mead approach. 40

Figure 5-1. Box plots showing $mIE50_{SLP}$(A) and $vIE50_{SLP}$(B) in healthy children and those with asthma (pre- and postbronchodilator). 48

Figure 5-2 Box plots showing mtI/tE(A), mtI/tTot(B), $vtPTEF_{SLP}$/tE(C) in healthy children and in those with asthma (pre- and postbronchodilator). 51

Figure 5-3. Correlation between $mIE50_{SLP}$ and FEV1 (% predicted) in children with asthma (prebronchodilator) 54

Figure 6-1. Distribution of ages in both groups: (A) Healthy and (B) Acute asthma/wheeze .62

Figure 6-2. Comparison between SLP-estimated parameters in health and acute asthma pre and post-bronchodilation administration. 65

Figure 6-3. Asynchrony parameters mTAA (A), vTAA (B), mHTA (C), and vHTA (D) differences in healthy children compared with those with asthma/wheeze which remained after bronchodilator administration (Hmeidi et al., 2018, p.6). 67

Figure 6-4. mTAA in healthy children and with those with asthma/ wheeze, classified by age groups.....67

Figure 6-5. Changes in mrCT (A), mTAA (B) and vTAA (C) after bronchodilator administration in children with asthma/wheeze, classified by age group.....69

Figure 7-1. SLP assessment on an infant with AVB during sleeping.....78

Figure 7-2. $vIE50_{SLP}$ differed in healthy infants compared with those with AVB at admission and discharge. 82

Figure 8-1. Biomedical signal processing steps: 86

Figure 8-2. Filter characteristics. 90

Figure 8-3. The Four common filter types (frequency responses). 91

Figure 8-4. Real and complex DFT. 92

Figure 8-5. Constructing a Scalogram in CWT. 95

Figure 8-6. Time-Frequency plane of the Continuous Wavelet transform. 95

Figure 8-7. A block diagram representation of spectral subtraction.....97

Figure 8-8. Markers placement on the subject's shoulder and C7.....100

Figure 8-9. Study setup. The subject is sitting as far back in a high-backed chair as possible with his arms on the chair arms. The PNT suspended from the ceiling to avoid blocking SLP-grid. 101

Figure 8-10. Tidal volume signal (PNT), with the peaks and troughs localized. 103

Figure 8-11. Continuous wavelet transformation of a PNT signal recorded from Subject_03 in Sitting still session. 106

Figure 8-12. Continuous wavelet transformation of a SLP signal recorded simultaneously from Subject_03 in Sitting still session. 106

Figure 8-13. Mean differences between RR_{SLP} and RR_{PNT} and CIs at 10, 20, 30, 40 and 47 breaths. 107

Figure 8-14. Mean differences between tI_{SLP} and tI_{PNT} and CIs at 10, 20, 30, 40 and 47 breaths. 108

Figure 8-15. Mean differences between tE_{SLP} and tE_{PNT} and CIs at 10, 20, 30, 40 and 47 breaths. 108

Figure 8-16. Mean differences between $tTot_{SLP}$ and $tTot_{PNT}$ and CIs at 10, 20, 30, 40 and 47breaths. 109

Figure 8-17. Mean differences between tI/tE_{SLP} and tI/tE_{PNT} and CIs at 10, 20, 30, 40 and 47 breaths. 110

Figure 8-18. Mean differences between $tI/tTot_{SLP}$ and $tI/tTot_{PNT}$ and CIs at 10, 20, 30, 40 and 47 breaths 110

Figure 8-19 Mean differences between $IE50_{SLP}$ and $IE50_{PNT}$ and CIs at 10, 20, 30, 40 and 47 breaths. 111

Figure 8-20. The effect of upper-body movement on SLP and PNT signals measured simultaneous. 113

Figure 8-21. Continuous wavelet representation of a still SLP signal for Sub_01.....116

Figure 8-22. Continuous wavelet representation of a still PNT signal for Sub_01 116

Figure 8-23. Continuous wavelet representation of SLP-signal with five upper-body movements for Sub_01. 117

Figure 8-24. Continuous wavelet representation of a PNT-signal with five upper-body movements for Sub_01. 117

Figure 8-25. Continuous wavelet representation of the Vicon signal with the five body movements sub_01 118

Figure 8-26. Spectral subtraction outcome for Sub_06. 119

Figure 8-27. Upper-body movements identification and removal from SLP signal (Sub_10) using abnormalities removal algorithm. 120

Figure 8-28. A comparison between PNT and SLP signals for one subject, both traces were normalized to facilitate visual comparison. 123

Figure 8-29. Continuous wavelet representation of SLP signal with five coughs from Sub_01. 124

Figure 8-30. Continuous wavelet representation of a PNT signal with five coughs from Sub_01. 124

Figure 8-31. Coughs identification and removal from SLP signal using abnormalities-removal algorithm. 125

Figure 8-32. Power spectrums of an SLP signal before and after coughs removal. 127

List of Tables

Table 2-1 Methods Used for chest wall motion measurements.....20

Table 5-1. Comparison of spirometry measures in children with asthma 46

Table 5-2. Comparison of tidal breathing parameters measured with SLP between healthy children and children with asthma (prebronchodilator).....49

Table 5-3. Comparison of tidal breathing parameters measured with SLP in children with asthma before and after bronchodilator administration. 50

Table 5-4. Comparison of tidal parameters measured with SLP between healthy children and children with asthma (postbronchodilator). 51

Table 5-5. CLES evaluation of SLP and spirometry-obtained breathing parameters. 53

Table 6-1. Participants demographics from both groups. Data are mean (standard deviation) unless otherwise specified. 62

Table 6-2. SLP-estimated tidal breathing parameters in healthy children versus children with acute asthma/wheeze (before bronchodilator administration). 64

Table 6-3. SLP-estimated tidal breathing parameters in children with acute asthma/wheeze before and after bronchodilator administration. 70

Table 6-4. SLP-estimated tidal breathing parameters in children with acute asthma/wheeze (after bronchodilator administration) versus healthy children.....72

Table 6-5. CLES evaluation of SLP-estimated tidal breathing parameters. 73

Table 7-1. Participants demographics from both groups. 79

Table 7-2. Comparison of clinical measures in infants with AVB (N=30) on admission and discharge. Heart Rate; Respiratory Rate; Oxygen saturation. 79

Table 7-3. Comparison of tidal breathing parameters measured with SLP between healthy children and infants with AVB (Admission). 80

Table 7-4. Comparison of tidal breathing parameters measured with SLP in infants with AVB on admission and discharge. 81

Table 7-5. CLES evaluation of SLP-estimated tidal breathing parameters which have shown significant differences. 84

Table 8-1. Participants demographics; 105

Table 8-2 Absolute and Percentage differences between tidal breathing parameters measured simultaneously by SLP and PNT at 40 breaths. 112

Table 8-3. The agreement between PNT and SLP in both study conditions. 115

Table 8-4. Changes in the estimated parameters between both study conditions observed from both machines. 115

Table 8-5. The sensitivity and specificity of the abnormalities-removal algorithm in detecting upper-body movements for subjects Sub_01-14. 121

Table 8-6. The agreement between tidal breathing parameters measured by PNT and SLP at still, movement, post spectral subtraction and post movement removal. 122

Table 8-7. The sensitivity of abnormalities-removal algorithm in detecting coughs. 125

Table 8-8. Differences in tidal breathing parameters measured by SLP_{Still} and SLP_{Cough}. 126

Table 8-9. Differences in tidal breathing parameters measured by SLP_{Still} and SLP_{Cough} post the removal of coughs using the abnormalities-removal algorithm. 126

Abbreviations

WHO: World Health Organization

COPD: Chronic Obstructive Pulmonary Disease

PFT: Pulmonary Function Test

FRC: Functional Residual Capacity

FEV1: Forced Expiratory Volume in one second

FVC: Forced Vital Capacity

PIF: Peak inspiratory flow

PEF: Peak expiratory flow

$FEF_{50\%}$: Forced expiratory flow at 50% of the forced vital capacity curve

PNT: Pneumotachograph

RSV: Respiratory Syncytial Virus

TAA: Thoracoabdominal asynchrony

AVB: Acute Viral Bronchiolitis

P_A : Alveolar Pressure

ΔP_A : Change in alveolar pressure

R_{aw} : Airways Resistance

TA: Thoraco-abdominal wall

PTIF: Peak tidal inspiratory flow

tPTIF: Time to reach peak tidal inspiratory flow

PTEF: Peak tidal expiratory flow

tPTEF: Time to reach peak tidal expiratory flow

TEF50: Tidal expiratory flow at 50% of tidal volume

TIF50: Tidal inspiratory flow at 50% of tidal volume

IE50: the ratio between TIF50 and TEF50

tI: Inspiratory time

tE: Expiratory time

tTot: Total breath time

tI/tE: the ratio between inspiratory and expiratory times

tI/tTot: the ratio between inspiratory and total breath times

RR: Respiratory rate

$TIF50_{SLP}$: Tidal inspiratory TA displacement rate at 50% of inspiratory displacement

$TEF50_{SLP}$: Tidal expiratory TA displacement rate at 50% of expiratory displacement

$IE50_{SLP}$: Inspiratory to expiratory TA displacement rate ratio

mRCt: Relative contribution of the thorax to each breath

HTA: Left–right hemithoracic asynchrony

CWT: Continuous wavelet transformation

SLP: Structured Light Plethysmography

NICE: The National Institute for Health and Care Excellence

FFT: Fast Fourier Transform

TA: Thoraco-abdominal region

SaO2: Oxygen Saturation

AVB: Acute Viral Bronchiolitis

FRSH: Front right shoulder

FLSH: Front left shoulder

BRSH: Back right shoulder

BLSH: Back left shoulder

ULOA: Upper limit of agreement

LLOA: Lower limit of agreement

CIs: Confidence intervals

SLP_{Still}: SLP-signal in a still session

SLP_{Mov}: SLP-signal in a session with introduced upper-body movements

SLP_{Cough}: SLP-signal in a session with introduced coughs

CLES: Common Language Effect Size

WSR: Wilcoxon signed-rank test

MWU: Mann–Whitney U test

The addition of the suffix “SLP” beside any of the above-mentioned tidal breathing parameters is to indicate that the origin of the signal is TA displacement based.

1 Introduction

Lung diseases are a prevalent group of long-term conditions and are one of the leading causes of emergency hospital admissions in adults and particularly in children. World Health Organisation (WHO) estimated that 65 million people were diagnosed with Chronic Obstructive Pulmonary Disease (COPD) by 2004 and that 3 million people died of COPD in 2005 alone. According to Asthma-UK, 5.4 million people in the UK are diagnosed with asthma of which 1.1 million are children (1 in 11), and the rest 4.3 million are adults. According to Asthma UK (Asthma UK, 2018), someone has a dangerous asthma attack every 10 seconds, and three individuals die every single day in the UK because of an asthma attack. Two-thirds of these deaths are preventable (Asthma UK, 2018).

Acute respiratory illnesses are the largest single cause of death in infants and children less than five years of age: intermittent problems with ‘’wheezy chest’’ in the first year of life occur in more than a third of all children. Asthma is the most common chronic disease during childhood which starts very early in life in the majority of cases, and it is under-diagnosed and under-treated (World Health Organisation, 2013).

Respiratory conditions such as asthma and COPD are typically identified by distressing symptoms, mainly breathlessness, chest pain, wheeze, dyspnoea and cough (Leach, 2008); those symptoms can markedly reduce the quality of a patient’s life (Weldam et al., 2014).

Many respiratory diseases are not curable and are progressive, however accurate diagnosis and treatment can help in managing the symptoms and slowing the progression of the disease, thus improving quality of life.

Lung function tests are examinations used to evaluate or give an interpretation of respiratory function (Quanjer, 2003). Most commonly used techniques require the patient to breathe through a mouthpiece, to provide a measurement of flow and volume. This requires the patient’s understanding and cooperation and can be challenging to perform and to obtain accurate measures in infants and preschool children (Williams *et al.*, 2014)

Pulmonary function testing (PFT) is a general term that covers a wide range of clinical tests to assess the respiratory status of a patient. A device employed in carrying out pulmonary function tests may broadly be classified as belonging to either one of two categories. In the first category, airflow is measured, and it is referred to as Pneumotachography. The second category is referred to as Plethysmography, and it involves the measurements of lung volume.

Global lung function is assessed using a pulmonary function test (PFT), which offers essential information for diagnosing and monitoring lung disorders. The PFT data include: Functional Residual Capacity (FRC) which is the amount of air at the end of a normal quiet respiration, Forced Expiratory Volume (FEV1) which represents the amount of air measured during the first second of a forced exhalation, and Forced Vital Capacity (FVC) which is the maximum amount of air during the measurement of forced expiratory volume.

Various techniques have also been developed and validated which measure the chest wall movement (Respiratory Inductance Plethysmography). These techniques can provide useful information relating to ventilatory effort and can also provide an estimation of changes in volume. All of these techniques require physical contact with the patients, and the positioning of physical markers which can be encumbering and time-consuming (Stocks, 1996).

A group of clinicians and scientists in Cambridge have developed a new technique, known as Structured Light Plethysmography (SLP), which is a non-contact light-based technique that measures the movement of the chest and abdominal wall during tidal breathing (Boer *et al.*, 2010). SLP provides valuable information about patients' lung function (Ghezzi *et al.*, 2017). In addition, SLP offers advantages over conventional lung function assessment, as it provides information about the regional changes in ventilation and also the relative contributions of different thoraco-abdominal regions in breathing across ages. The zero-contact environment minimises altered breathing mechanics, introduced from breathing into a measurement device. Thus, it allows more natural breathing patterns to be observed. One of the limitations of SLP is that an accurate data acquisition requires the patient to remain still and breathe quietly for a given period of time, which is sometimes difficult to achieve in young children (Almazaydeh *et al.*, 2013).

In order to overcome the limitations of traditional lung function assessment, SLP usage was investigated in this thesis as a possible alternative modality for lung function monitoring in paediatric population. This was done by firstly investigating the use of SLP in assessing tidal breathing in (1) school-age children (7-16 years) with stable Asthma, (2) younger children (2-12 years) recovering from acute asthma/wheeze and (3) infants recovering from acute viral bronchiolitis (0-1 year). And secondly, by assessing the robustness of the parameter estimation algorithm against interferences that might be introduced to the SLP signal during data acquisition.

In this thesis, Chapter 2 presents a literature review covering the anatomy and physiology of the respiratory system and its development. Natural physiology of breathing is also discussed with an introduction to respiratory diseases in childhood (mainly asthma/wheeze and Acute Viral Bronchiolitis). In addition, traditional measures of lung functions are illustrated. Specific aims of the thesis are articulated in chapter 3. Chapter 4 gives a technical overview of the working principle of SLP and defines core terminologies. Chapters 5,6 and 7 evaluate the use of SLP in monitoring lung function in healthy and sick children/infants. Chapter 8 investigates the effects of upper-body movements and coughs, as artefacts, on SLP signal and its estimated tidal breathing parameters. In addition, various signal processing and statistical techniques were applied to remove those artefacts. A general discussion of common themes is given in chapter 9, and chapter 10 gives a final conclusion and recommendations.

2 Literature review

2.1 Anatomy of respiratory system

A constant supply of oxygen is required by the cells of the human body to stay alive (The Pt Group: Physical Therapy, 2015). The respiratory system acts in such a way that it provides the needed oxygen to the body as well as removes carbon dioxide, the accumulation of which is lethal. The process of moving gas into and out of the lungs (ventilation) and moving oxygen and carbon dioxide between air and blood (respiration) requires an elaborate organ system (Taylor, 2013; Beachey, 2018).

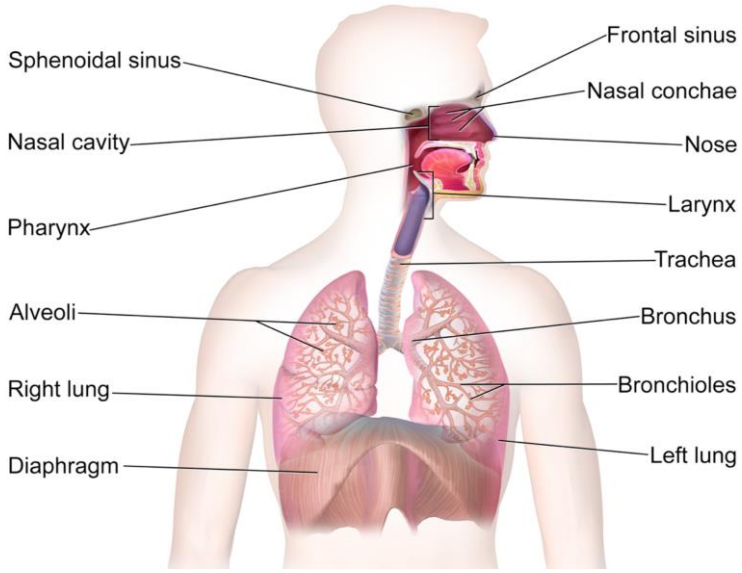

Figure 2-1. Main respiratory system structures

(Anatomy-medicine, 2018)

The respiratory system is comprised of three major parts: the lungs, the muscles of respiration, and the airways (Figure 2-1). As the functional unit of the respiratory system, the lungs pass the oxygen into the body and remove the carbon dioxide. The muscles of respiration, including the intercostal muscles and the diaphragm, drive ventilation by pushing the air in and out of the lungs during breathing. The airway (the mouth, nose, pharynx, larynx, trachea, bronchi and bronchioles) passes air between the exterior of the body and the lungs (Taylor, 2013). These parts make up the conductive zone of the respiratory system wherein no gaseous exchange takes place, which only occurs in the alveoli and alveolar ducts as explained in the next section.

2.2 Respiratory system structure and function

2.2.1 Nose and Nasal Cavity

The nose and the nasal cavity together form the main respiratory system's external opening, and they are the first section of the airway of the body, the respiratory tract which is responsible for the air movement. The nasal cavity, lined with mucus membrane and hairs, works as a filtering device, moisturising and warming air before it enters the lungs. The mucus and the hair help in the trapping of dust, pollen, mould and any other hazardous substances from the environment, preventing them from reaching the inner parts of the body. Air coming out of the body through the nose returns heat and moisture to the nasal cavity before it is finally exhaled to the environment (Taylor, 2013; Beachey, 2018).

2.2.2 Mouth

The secondary external opening for the respiratory tract is the mouth. Normal breathing occurs predominantly through the nasal cavity, and the mouth is mostly used as a supplement replacing the functions of the nasal cavity when the need arises. However, the disadvantages associated with breathing through the mouth include:

a) The mouth cannot moisturise or warm the air entering the lungs as effectively as the nose, because the pathway of air entering the body through the mouth is shorter than the path of air that enters through the nose.
b) The hairs and the sticky mucus, which are responsible for filtering the air that passes through the nasal cavity, are missing in the mouth (Taylor, 2013).

2.2.3 Pharynx

The Pharynx, commonly known as the throat, is made up of a muscular funnel extending from the posterior end of the nasal cavity and ends at the superior end of the Larynx and the Oesophagus. It is divided into three: The Oropharynx (located in the oral cavity's posterior), the Nasopharynx (the largest region located in the posterior nasal cavity), and the Laryngopharynx. When inhaled from the nasal cavity, air passes into the Nasopharynx and then descends through the Oropharynx, but when inhaled through the mouth, air enters the Pharynx through the Oropharynx. The air that is inhaled descends right into the Laryngopharynx where Epiglottis, an elastic flap of cartilage, acts as a switch between the Oesophagus and the Trachea, diverts it into the Larynx's opening (Taylor, 2013). This, a defence mechanism, ensures correct passage of air and food, avoiding choking (Beachey, 2018).

2.2.4 Larynx

The Larynx, commonly referred as the voice box, is the short length of the airway connecting the Trachea and the Laryngopharynx. It is positioned in the neck's anterior portion, above the

trachea and below the hyoid bone and is a cylindrical structure, acting as a valve. The Larynx is comprised of several cartilage structures, hence its structural properties, and includes the Epiglottis. Just below the Epiglottis is the Thyroid cartilage, which is commonly known as Adam's apple due to its enlarged size and visibility in male adults. The Thyroid offers protection to the vocal folds. The ring-shaped cricoid cartilage, which is located just below the thyroid cartilage, holds the larynx open and supports its posterior end. Other than the cartilage, the larynx also bears unique structures called the vocal folds, which are responsible for sounds. The tension, as well as the vibration speed of the vocal folds, can be changed so as the pitch that they produce (Taylor, 2013; Beachey, 2018).

2.2.5 Trachea

The Trachea, or windpipe, is a tube, 10-11 cm tube in length, and 1.5 - 2 centimetres in inner diameter. It is made up of C-shaped hyaline cartilage rings, lined with the Pseudostratified Ciliated Columnar Epithelium. The larynx is connected to the Bronchi by the Trachea which allows the passage of air into the Thorax through the neck. The Trachea, with the help of rings of cartilage that are contained in it, always remains open to air. The Oesophagus is allowed to expand into the space that is occupied by the trachea to accommodate the masses of food that are moving through the Oesophagus because the open end of the cartilage rings face posteriorly to the oesophagus (Taylor, 2013; Beachey, 2018). The Trachea ensure a clear airway passage of air to the lungs. Mucus, a defence mechanism, produced by the Epithelium lining the Trachea, helps to trap dust and other contaminants, preventing them from reaching the lung. On the surface of Epithelial cells, there are microscopic, slender, hair-like organelles. The mucus is moved toward the Pharynx superiorly where it can then be swallowed and finally digested in the Gastrointestinal tract (Taylor, 2013).

2.2.6 Bronchi and Bronchioles

Towards the end of the Trachea, there is a left and right division into branches called the primary bronchi. These bronchi enter each lung and branch off into relatively smaller secondary bronchi, carrying the air into the lobes of the left and right lungs. The secondary bronchus then split into smaller third bronchi in each lobe. The resulting tertiary bronchi further split into numerous bronchioles which then spread throughout the lungs. Each of the bronchioles then split into numerous smaller branches called terminal bronchioles whose diameters are less than one millimetre. Millions of tiny terminal bronchioles finally conduct air into the alveoli of the lungs. The structure of the airway's wall also starts to change during the splitting of the airway into the tree-like branches of bronchi and bronchioles (Beachey, 2018). The primary function of both bronchi and bronchioles is to transmit air from the trachea into the lungs. The quantity of the air flowing into the lungs is regulated by the smooth muscle tissue found in the surrounding walls of the bronchi and the bronchioles (Taylor, 2013).

2.2.7 Lungs

The pair of lungs, large and spongy, are found in the thorax just lateral to the heart and above the diaphragm. Each lung has a pleural membrane surrounding it to provide the space for the Lung to expand and a negative pressure space in relation to the exterior of the body. The negative pressure always allows for the passive filling of the Lungs with air as they relax. Because of the heart points to the left side of the body, the left and right lungs consequently have slightly different size and shape with the right lung being slightly bigger than the left lung. It is made up of three lobes while the left lung is made up of two lobes (Beachey, 2018).

The lungs' interior is made up of spongy tissues which contain many capillaries and numerous (around thirty million) tiny sacs called alveoli. These are cup-shaped structures, are surrounded by capillaries and are found at the end of the terminal bronchioles. The alveoli contain a thin simple and squamous epithelium lining that allows air entering the alveoli to be able to exchange its gases with the blood that is passing through the capillaries (Taylor, 2013).

2.3 Development of the respiratory system

In this section, the development of the respiratory system is addressed, as this work has assessed breathing of infants (< two years) and children between 2 and 17 years of age. Human infants and mature adults have similar lungs in structure, but a difference in the number of airways and the components of airway walls (Greenough, 2003). There is a continuous development of the lung from birth until adolescence with its maximum in the first few months after birth. Newborn lungs have around 150 million alveoli. It was believed for a long time that alveolarisation stops by 7-8 years of age when this number almost quadruples (Angus and Thurlbeck, 1972; Langston *et al.*, 1984; Malina, Bouchard and Bar-Or, 2004). Recent studies, though, suggested that alveolarisation continues after that age and during adolescence resulting in an increase in lung volume from 7 years to adulthood (Narayanan *et al.*, 2012).

The number of pulmonary capillaries surrounding the alveoli increases with age in childhood, increasing the gas exchange per unit of body mass (Zeltner *et al.*, 1987; Greenough, 2003). Airways increase in size during childhood (Morgan *et al.*, 1982; Zapletal, Samanek and Paul, 1982), which result in a decrease in airways resistance with a linked rise in lung compliance (Stocks, 1999).

The ribcage of a new-born is very compliant, consisting mainly of cartilage (Bryan and Wohl, 2011). Ossification changes the structure of the ribcage into mineralised bone, which is a process that continues until 25 years of age (Glass et al., 2002). The high compliance of an infant chest wall decreases to almost one third in adulthood, because of both ossification and the increase of muscle mass (Papastamelos et al., 1995).

In infants, the ribs are more horizontally oriented relative to the vertebra than in adults. The thoracic cage of an infant is triangular due to the shorter ribs length in the upper part of the rib cage, while it has a dome shape in an adult (Devlieger *et al.*, 1991). This configuration causes flattening of the diaphragm in infants and children, which leads to a reduction in the load of lower rib cage on the abdominal content in diaphragm contraction (Devlieger *et al.*, 1991), this means that the rib cage movement has a small contribution in tidal volume (Hershenson *et al.*, 1990). The raised orientation of the ribs changes with age, as the ribs tilt downward to reach the adult configuration by the age of ten years (Haddad, Abman and Chernick, 2002).

2.4 Natural physiology of breathing

2.4.1 Pulmonary Ventilation

Pulmonary ventilation is the process involving the movement of air in and out of the lungs to facilitate the exchange of gases. In order to achieve pulmonary ventilation, the respiratory system uses not only the negative pressure system but also the contraction of muscles (Ratnovsky, Elad and Halpern, 2008). In the negative pressure system, a negative pressure gradient is established between the alveoli and the external atmosphere. The lungs are sealed by the pleural membrane to maintain the pressure of the lungs slightly below the atmospheric pressure when the lungs are at rest. Consequently, the air is made to follow with the pressure gradient to passively fill the lungs which are at rest. The pressure within the lungs rises as the lungs fill with air until it matches the atmospheric pressure. More air can still be inhaled, albeit by the contraction of the diaphragm as well as the external intercostal muscles, leading to the increase in the volume of the thorax and resulting in the reduction of the pressure of the lungs below the atmospheric pressure once again (Taylor, 2013).

In order to exhale air, the diaphragm and the external intercostal muscles relax, as the internal intercostal muscles contract leading to the reduction of the volume of the thorax and consequently increasing the pressure inside the thoracic cavity. The pressure gradient is reversed, leading to the exhalation of air which continues until the pressure inside the lungs and the pressure outside the body match (are equal). The elastic nature of the lungs then causes them to recoil back to their original volume, leading to the restoration of the negative pressure gradient which was present during the inhalation (Beachey, 2018).

There are sets of muscles surrounding the lungs that have the ability to cause air from the lungs to be inhaled or exhaled. Diaphragm, a thin sheet of skeletal muscle which forms the bottom of the thorax, is the principal muscle of respiration that is found in the human body. During inhalation, the diaphragm contracts making it move a few inches lower into the abdominal cavity, thus expanding the space inside the thoracic cavity and, therefore, pull air into the lungs. By moving down, the thoracic cavity's volume increases which drops the pressure inside the thoracic cavity with respect to the atmosphere, this difference in the pressure generates the flow of air (air rushes inside the lungs). The intercostal muscles further increase the volume of the thoracic cavity by moving the ribs forward and up (Taylor, 2013).

The flow of air is directly proportional to the difference in the pressure between the thoracic cavity and the atmosphere, and inversely proportional to the airway resistance.

On the other hand, when the diaphragm relaxes, air is allowed to flow back out of the lung leading to exhalation. When the diaphragm relaxes it moves up, and this decreases the volume of the thoracic cavity which increases the pressure inside and pushes the air out of the lungs. The relaxation of the intercostal muscles moves the ribs back and down which further reduces the volume (Taylor, 2013).

There are numerous small intercostal muscles between the ribs that assist the diaphragm with compressing and expanding the lungs. These muscles are generally divided into two groups: the internal intercostal muscles and the external intercostal muscles. The internal intercostal muscles which are the deeper lying sets of muscles act by depressing the ribs to help in the compression of the thoracic cavity which consequently forces the air from the lungs to be exhaled. The external intercostals, on the other hand, are found superficial to the internal intercostals, and they act to elevate the ribs, leading to the expansion of the volume of the thoracic cavity and consequently cause the air to be inhaled into the lungs (Beachey, 2018). Accessory muscles of the upper chest and neck contribute to different levels in the inspiration phase, whereas the abdominal muscles contribute in the expiration phase (MacBean, 2014).

The contraction of abdominal muscles causes the abdominal wall to move inward, pushing the abdominal content and causing the diaphragm to move upward (Ratnovsky, Elad and Halpern, 2008). The increase in both intra-abdominal and intra-thoracic pressures pushes the air out of the lungs. Abdominal muscles may also act as an accessory muscle set in the inspiratory phase, to further support the elastic recoil of the chest wall (Hamid, Shannon and Martin, 2005).

2.4.2 External Respiration

External respiration involves the exchange of gases between the air that fills the alveoli and blood in the capillaries that surround the walls of the alveoli. Air from the atmosphere entering the lungs has a higher partial pressure of oxygen and a relatively lower partial pressure of carbon dioxide than the blood found in the capillaries. This difference in partial pressure makes the gases diffuse passively from high to low pressure along their pressure gradient through the simple squamous epithelium lining of the alveoli. The net result of the external respiration, therefore, is the absorption of oxygen from the air into the blood and the expulsion of the carbon dioxide from the blood into the air. The oxygen is then transported to the tissues of the body while carbon dioxide is released out of the body during exhalation (Taylor, 2013).

2.4.3 Internal Respiration

Internal respiration involves the exchange of gases between the blood inside the capillaries and the body tissues. In the capillary, blood consists of higher partial pressure and a relatively lower pressure of carbon dioxide than the tissues it passes through. This means that the resulting partial pressure difference results in the diffusion of gases from high to low pressure along their pressure gradients, and this often happens through the endothelium lining of the capillaries. The net result of the internal respiration is, therefore, the diffusion of oxygen into the body tissues and the removal of carbon dioxide in the blood (Beachey, 2018).

2.4.4 Transportation of Gases

There are two major respiratory gases, they are, oxygen and carbon dioxide, and both of them are transported by blood through the body. Blood plasma is able to transport some of the dissolved oxygen and carbon dioxide, although a bigger percentage of the gases transported

within the blood are usually bonded to transport molecules. One of the most important transport molecules is the Hemoglobin that is found in the red blood cells that carry nearly ninety-nine percent (99%) of the oxygen in the blood. A small quantity of carbon dioxide can also be carried by the Hemoglobin from the tissues back to the lungs. The carbonic anhydrase enzyme always catalyses a reaction between water and the existing carbon dioxide to form carbonic acid whenever there is a high partial pressure of the carbon dioxide in tissues. Carbonic acid then dissociates to form hydrogen ion and bicarbonate ion. The low partial pressure of carbon dioxide in the lungs leads to the reverse reaction, and carbon dioxide is, therefore, liberated into the lungs to be exhaled (Taylor, 2013).

2.4.5 Homeostatic Control of Respiration

The body, under normal resting conditions, maintains a quiet breathing rate as well as depth which are referred to as Eupnoea (tidal breathing). Eupnoea is always maintained until there is a demand for oxygen by the body and the production of carbon dioxide rises as a result of greater exertion. The partial pressures of oxygen and carbon dioxide in the blood are monitored by autonomic chemoreceptors in the body which then send signals to the respiratory centre of the brain stem. The respiratory centre eventually adjusts the rate as well as the depth of breathing to return the blood to its usual levels of partial gas pressures (Beachey, 2018).

2.5 Respiratory Disease in Childhood

According to the British Thoracic Society statistics in 2006, respiratory disease is the most common reason for both acute and chronic illness in children in the United Kingdom, covering 14% of all hospital consultant appointments and 42% of all inpatient admissions (BTS, 2006). Although most of the acute episodes of respiratory illness resolve spontaneously and do not have a long-lasting effect (Bush and Thomson, 2007), chronic disease place a significant burden on healthcare systems worldwide and causes significant morbidity and mortality. It is also well known that most of the burden of disease in later life has its origin in childhood (Piippo-Savolainen *et al.*, 2004; Pittman *et al.*, 2011).

2.5.1 Childhood Asthma

Asthma is the most prevalent chronic ailment in childhood according to the World Health Organization, and the leading cause of morbidity among chronic diseases in this group (Pedersen *et al.*, 2011). Asthma causes a significant burden on healthcare systems internationally, and the prevalence and incidence of asthma are growing worldwide (Bateman *et al.*, 2008; Nunes, Pereira and Morais, 2017).

Chronic inflammation of the airways and increasing activity of the smooth muscles surrounding them indicate asthma, causing the lining of the airways (epithelial) to swell and secrete more mucus. Consequently, the air becomes difficult to move in and out of the lungs. Asthma most

common symptoms are wheezing, coughing, shortness of breath and, in some cases, chest tightness.

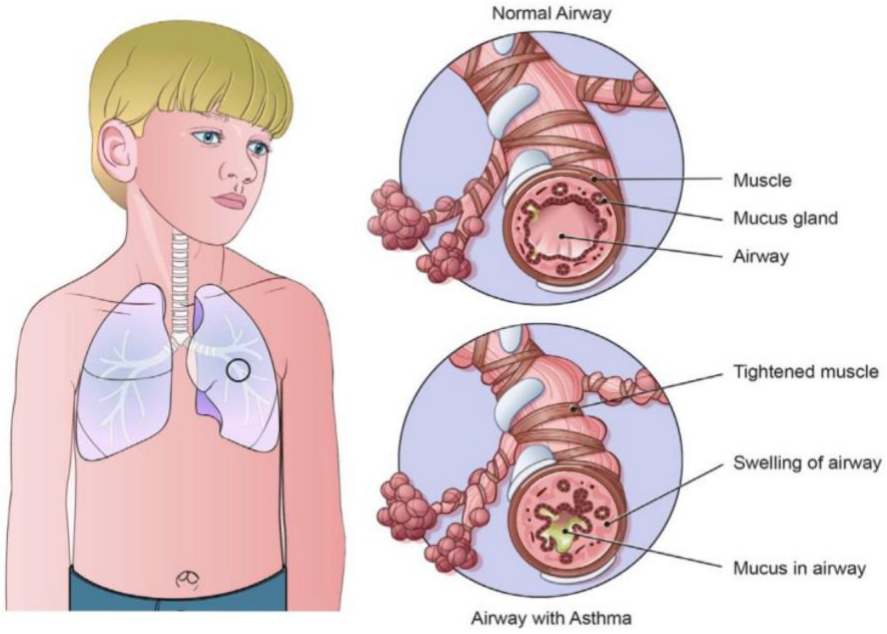

Figure 2-2. Normal Airway vs an airway with asthma

(Nationwide Children's Hospital, 2018).

Asthma type, severity or frequency of symptoms have no standard definition (Papadopoulos *et al.*, 2012), but among all definitions, many symptoms are in common mainly wheeze, cough, chest tightness and breathlessness, in addition to airflow obstruction and hyperresponsiveness (Monitoring, 2008; Pedersen *et al.*, 2011; Turner *et al.*, 2011).

Clinical history obtained from the patient is used to confirm the diagnosis, lung function tests are then used to determine the severity of asthma, which could be used in school-age children. In younger children, clinical history provided by the parents is used to describe the symptoms which is a subjective method of information acquisition, this makes identification of the symptoms accurately hard to obtain in younger children, clinical observation is then used to confirm the diagnosis (Castro-Rodriguez, Rodriguez-Martinez and Custovic, 2012).

An objective assessment of lung function is needed to identify airflow obstruction. Spirometer and peak expiratory flow are conventional techniques used in identifying airflow obstruction, its severity and response to treatments, but those techniques are used with children over five years of age (Spycher *et al.*, 2008). Although there exist some guidelines suggesting the use of a spirometer to obtain objective measures from children below five (Pedersen *et al.*, 2011; Turner *et al.*, 2011), this age group is usually considered unsuitable for this test (Tidy, 2016).

The history of wheeze episodes and the accompanying symptoms are considered as the basis for asthma diagnosis in children. Taking the family history of asthma into consideration further

support the possibility of the child having asthma. Various treatments are then tried to confirm the diagnosis, which may result in a late accurate-treatment for a child with asthma, and a non-needed exposure of a treatment to a non-asthmatic child (Papadopoulos *et al.*, 2012).

2.5.2 Pre-school wheeze

Pres-school wheeze is defined as whistling sounds happening in the inspiratory or expiratory parts of breathing due to increased work of breathing; it is also divided into two types: episodic viral and multiple trigger, depending on the symptoms and child's history; identifying the type is then used to direct the treatment. The episodic viral type happens in the existence of a viral infection only, whereas the multiple trigger type is caused by triggers such as environmental allergies, tobacco smoke and exercise (Brand *et al.*, 2008; Bush, Grigg and Saglani, 2014). One of the limitations of this classification is that there is not enough evidence that both types are pathologically different, this could be reasoned to the absence of an objective measure of pulmonary function in this young age group (Schultz *et al.*, 2010; Castro-Rodriguez, Rodriguez-Martinez and Custovic, 2012).

In this thesis 'wheeze' will refer to both types of pre-school wheeze.

2.5.3 Acute Viral Bronchiolitis (AVB)

Acute Viral Bronchiolitis is an infection affecting the lower respiratory tract, which usually affects infants and young children (Green *et al.*, 2016). AVB is common in winter and is usually caused by the respiratory syncytial virus (RSV) (Moodley *et al.*, 2010). Almost 70% of all infants have had an RSV infection in their first year of life (Glezen *et al.*, 1986), Although many bronchiolitis infections disappear without a treatment being necessary, symptoms can develop. Moreover, in 2-3% of primary infections, they result in admission to hospital for assessment and possibly for specific treatment (Deshpande and Northern, 2003; Hall *et al.*, 2009).

In England, hospital admissions of bronchiolitis have increased in the past three decades and are higher than estimates from similar industrialised countries. In 2011 259,044 infants less than 1 year of age were admitted to hospital because of bronchiolitis, which places a considerable strain on hospital resources especially during winter season. The high number of emergency admissions and the lack of universal preventive measures shines a light on the importance of controlling bronchiolitis (Green *et al.*, 2016). There is also a reported relationship between early bronchiolitis in infancy and a higher chance of developing wheeze and asthma later in life (Sigurs *et al.*, 2010; Blanken *et al.*, 2013; Régnier and Huels, 2013).

Coughing, wheezing and increased work of breathing are common symptoms of bronchiolitis, and there is insufficient evidence on the best treatment to use with infants with bronchiolitis, but providing patients with oxygen and fluids is the cornerstone of the therapy used currently. Conventionally, oxygen saturation is measured in AVB infants to monitor the progression of the condition and the response to treatment (NICE, 2015).

Thoracoabdominal asynchrony (TAA) occurs in infants with acute and chronic lower airway obstruction such as bronchiolitis with the degree of asynchrony associated with the degree of the abnormality of pulmonary resistance and elastance (Rome *et al.*, 1987; Allen *et al.*, 1990). The quantification of TAA could be a promising approach in classifying the severity of the AVB. SLP could be used as an objective measure of the increased work of breathing and respiratory load even when a normal oxygen saturation levels exist (Allen *et al.*, 1990).

2.5.4 Pathophysiological alterations in obstructive lung disease

Obstructive lung diseases affect the respiratory system in different ways, but they have physiological features in common such as airway narrowing which occurs at different levels within the airway tree as a result of hyperactivity of smooth muscles or excessive secretion of mucous (Kim *et al.*, 2007). In around 90% of asthma cases airway obstruction happens in large airways (internal diameter >2mm), which are above the 8th generation of the airways (Burgel *et al.*, 2009; Thien, 2013), while in acute viral bronchiolitis (AVB) lower respiratory tract is mainly affected (Webb *et al.*, 1985), obstruction in distal airways may cause their collapse in the expiratory phase of breathing, this can result in gas trapping or so-called hyperinflation, which is expressed as a high volume of air staying in the lungs at the end of breathing cycles. Gas trapping was also detected in acute exacerbation of respiratory conditions even with the absence of severe airflow obstruction (Muller, Bryan and Zamel, 1980). Hyperinflation introduces elastic load on the respiratory muscles, because of the excessive stretching of lung tissues caused by the increased residual lung volume (Moxham and Jolley, 2009). An increase in end-expiratory lung volume can result in a reduction in the mechanical advantage of the diaphragm which is referred to as the mechanical disadvantage of the diaphragm (Troyer, 1988; Decramer, 1997).

The level of expiratory airflow obstruction in medium and severe airways obstruction might cause a change in respiratory pattern, as the expiratory will be driven by the active contraction of expiratory muscles rather than the elastic recoil of the lung and chest wall, causing an increased load on respiratory muscles (MacBean, 2014).

There are various methods to quantify respiratory muscles load. Conventional lung function techniques could be used to assess only a specific side of the load on the respiratory system caused by a respiratory condition. Spirometry, for instance, is used to quantify the degree of airflow obstruction using forced expiratory manoeuvres, whereas body plethysmography is used to measure functional residual capacity in lung hyperinflation. These measures do not provide a full perception of disease pathology (MacBean, 2014). Measuring pressures created by the respiratory system to initiate ventilation is used to quantify respiratory load. Intrathoracic and intra-abdominal pressures are quantified using invasive techniques such as catheterisation. Inter-abdominal pressure is then subtracted from Intrathoracic pressure to quantify the pressure produced by the diaphragm. Load on the respiratory system is then estimated by taking the peak or the mean value of the diaphragmatic pressure during breathing (Gaultier and Gallego, 2005). The work of breathing is the time integral of the diaphragmatic pressure and could be quantified to estimate respiratory load.

During tidal breathing in healthy people, changes in pressures produced by the respiratory muscles yield an efficient airflow (ventilation). In airways obstruction, this pressure - airflow relation is influenced because of gas trapping, which results in a positive resting intrathoracic pressure post-expiration. To account for this pressure changes are measured from the baseline when considering the peak value or the time integration of the pressure (MacBean, 2014).

2.6 Measures of the Lung Functions

An accurate diagnosis and monitoring of respiratory disease is required for optimal management of the respiratory condition; this requires an accurate evaluation of lung functions. Early diagnosis and treatment in childhood are linked to an improved outcome in later life (Grol et al., 1999; Rasmussen et al., 2002; Davies and Alton, 2009). Most of the pharmacological treatments used in lung diseases have side effects. Therefore, an inaccurate treatment or an overtreatment should be prevented (Douglas et al., 2008). Chronic respiratory diseases place a significant burden on patients and their families, which further support the importance of making accurate treatment decisions.

Conventional measures of pulmonary function such as spirometry require the patient to perform forced manoeuvres and are therefore unsuitable for use in younger age groups. Even in older age groups, a full understanding of the complex manoeuvres and cooperation are required. These tests also assess specific aspects of respiratory function and may, therefore, underestimate the full effect of the variety of pathophysiological changes. Distal airways collapse, airway narrowing and changes in respiratory pattern cause an increase in respiratory load and affect the capability of respiratory muscles to adapt to this increase (MacBean, 2014).

Clinical assessment by a physician plays a vital role in diagnosing lung disease, especially in younger age groups where objective measures are difficult to obtain. The clinical assessment could be used to detect airflow obstruction, but it cannot be used to measure its severity (Shim and Williams, 1980; Russell et al., 1986). Acute exacerbations resulted from an inaccurate assessment of the severity of the obstruction (Baker et al., 2000; Davenport and Kifle, 2001), which further emphasises the need of a comprehensive, objective measure in order to provide an optimal management of the condition.

2.6.1 Spirometry

A spirometer is a device which is used to measure timed exhaled and inhaled volumes, which is then used to calculate the effectiveness and the speed with which the lungs can be filled and emptied. Spirometry is considered the gold standard in pulmonary function assessment (Johns and Pierce, 2007).

Forced Vital Capacity (FVC), and the forced expired volume in one second (FEV1) are the main parameters looked at clinically (Figure 2-3). Some other parameters are looked at for research purposes but are not used clinically (MacBean, 2014). Measurement of flow can alternatively either be absolutely made or as a function of volume and, consequently, leading to Flow-volume curve as shown in Figure 2-4. The shape of Flow-volume loop is shown to be reproducible for subjects. However, the shape changes in the presence of a respiratory condition (Johns and Pierce, 2007).

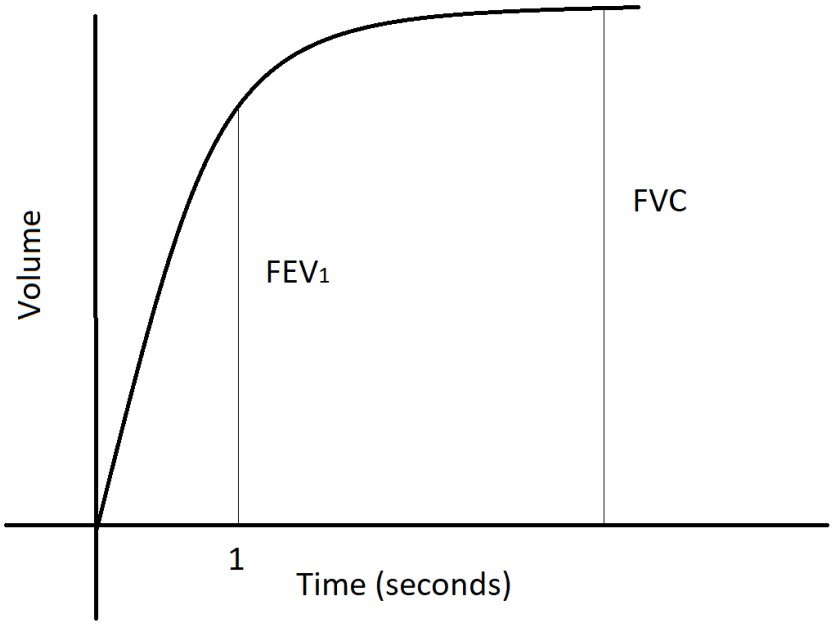

Figure 2-3. Forced expired volume in one second (FEV1) and forced vital capacity (FVC), displayed on a spirometry output.

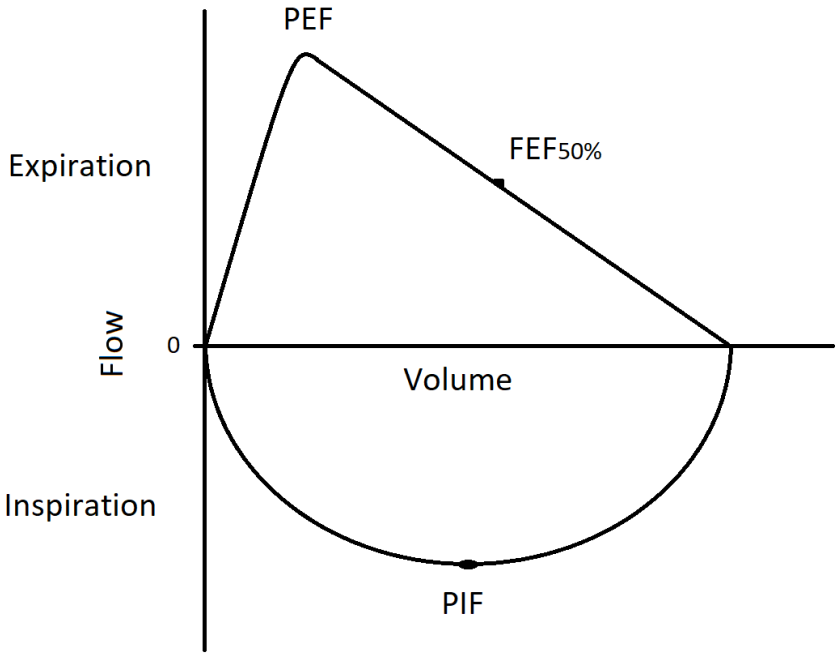

Figure 2-4. Maximal expiratory and inspiratory flow-volume loop

Although Spirometry is considered the gold standard to identify and evaluate the severity of various lung diseases, it has a few restrictions. One of the main limitations appears in the young paediatric population, who are not able to cooperate enough to perform the assessment procedure. Obtaining reliable outputs is usually not possible below the age of five years, although a few authors have shown the possibility to perform spirometry in younger children, through proper training and encouragement (Crenesse et al., 2001), this is not always possible in clinical settings (Bush and Davies, 2005).

For these reasons, national and international guidelines do not recommend spirometer as a tool to direct the treatment of children below five years of age (Flume et al., 2007; Douglas et al., 2008; Pedersen et al., 2011).

Respiratory conditions are usually accompanied by different symptoms such as breathlessness, cough and fatigue, which might influence patient's ability to perform the forced manoeuvres required for the test (Cooper *et al.*, 1990; Miller, Hankinson, *et al.*, 2005). Furthermore, the normal variability of spirometry-test outcomes could reach up to 20%, which might even increase in the presence of airway obstruction (Cooper et al., 1990), such variability can affect the accuracy of the outcomes and the diagnostic decisions (Cotes, Chinn and Miller, 2009).

Flow-Sensing Spirometers are among the range of new portable spirometers which have been developed over recent years due to advances in the electronics as well as the microprocessor technology Figure (2-5).

Figure 2-5. A flow-based spirometer

(Clinicalgate, 2015)

Generally, flow spirometers measure flow using a sensor as a primary signal, and then the volume is estimated by integrating the flow signal versus time (Johns and Pierce, 2007).

The advantages of flow spirometers, that have led to their popularity, are that they are portable, easy to use and maintain (in terms of cleaning as well as disinfection), and that a wide range of ventilatory indices can be calculated automatically. In addition, flow spirometers can provide instant readings, store patient results with feedback on the data quality and can provide reference ranges expected for the patents (Johns and Pierce, 2007).

Flow spirometers are associated with few limitations such as firstly, their regular calibration requirements, and appropriate correction to conditions of body temperature and pressure saturated (BTPS), which suggests that extra care should be taken when using them clinically. Secondly, their use is limited to adults who can understand the test procedure and be cooperative.

2.6.2 Whole-Body Plethysmography

The whole-body plethysmograph is made up of a rigid chamber, whose size and shape looks like an enclosed telephone booth, whereby the subject sits while breathing through a pneumotachograph. Pressure transducers, of different sensitivity, are arranged to measure the pressure across the pneumotachograph (flow). It also measures the difference in pressure across the wall of the plethysmograph as well as the pressure at the opening of the airway. Variations in alveolar pressure (PA) may be inferred from variations in plethysmograph pressure (Goldman, Smith and Ulmer, 2005), and this seems to be the main principle of the variable-pressure plethysmograph. In the plethysmograph, a shutter mechanism is placed close to the mouth. To gain transient airway occlusion, this shutter should be closed. Voluntary respiratory efforts are then carried out against the closed shutter, and at the same time, the estimation of the change in alveolar pressure (ΔPA) is made by recording the resulting change in mouth pressure (ΔPm). The mouth pressure Pm (PA) is then plotted against simultaneous plethysmographic pressure variations during respiratory efforts against the closed shutter to measure the absolute thoracic gas volume (TGV) and airway resistance (Raw)(Goldman, Smith and Ulmer, 2005).

Patients with obstructive lung diseases have a high airway resistance, which may cause air trapping in the lung at the end of expiration. Body plethysmograph is used to accurately quantify TGA and airways resistance, which can provide a precise description of the severity of the obstruction.

One of the main drawbacks of whole-body plethysmograph is that subjects have to be seated in the sealed chamber for several minutes, and they are asked to perform some complex manoeuvres, which make it challenging for use in younger children (Vilozni et al., 2009).

2.6.3 Measurements of Chest Wall Movement

Measurement of chest wall motion during tidal breathing may provide valuable information about respiratory function and mechanics (Adams et al., 1993). This includes many tradition and novel procedures and much research has gone into providing the pros and cons of these procedures. Furthermore, different techniques measure different parameters of the lungs, here I focus on chest wall movement, and give practitioners the required information for the patients. I will describe some of these techniques, concluding with the reasons behind my choice in using SLP for further investigation. For each of the techniques, a comparison with between the method and SLP is made, noting the advantages SLP has on each of these methods. This will provide a justification for choosing SLP in this thesis.

2.6.3.1 Introduction

Whether due to the pathology in the lungs, airways, chest wall or muscles, assessing chest wall motion is a basic and important constituent in managing the child with respiratory problems. Since the 1960s, clinical assessment has been supplemented with a plethora advanced and ever-growing technological options for measuring chest wall motion, each with its pros and cons. Measurements of chest wall motion has its many advantages (Seddon, 2015). These include:

1. Assess respiratory airflow and volume change, as a non-invasive alternative to measurement at the airway opening,

2. Monitor breathing over long periods of time, to help identify sleep-disordered breathing such as apnoea.

3. Identify and quantify patterns of abnormal chest wall movement and compare between certain breathing components or regions.

Measuring chest wall motion can provide practitioners with valuable information that cannot be obtained using ordinary respiratory function techniques such as spirometry: it allows respiratory airflow to be measured in cases when it is impossible, it also provides information about the movement of different chest wall parts to produce that airflow (Seddon, 2015).

The interest in measuring chest wall motion includes various and overlapping reasons. Firstly, it is to enable the measurement of tidal volume and respiratory airflow pattern. Secondly it is to monitor breathing and identify central and obstructive sleeping problems over long periods of time. Thirdly, it enables the quantification of the degree of asynchrony between chest and abdominal respiratory motion as a possible measure of upper or lower airway obstruction. Fourthly, it enables the characterization of patterns of pathological chest wall movement in chest wall or neuromuscular disease. Finally, it is to assess changes in end-expiratory lung volume (Seddon, 2015). The mathematical analysis of measuring chest wall motion was first achieved by Konno and Mead in which they demonstrated that it was possible to predict volume

changes (measured by spirometer) reasonably accurately in healthy adult subjects by measuring changes in the Anteroposterior (A-P) diameter of RC and AB (Konno and Mead, 1967). Since Konno and Mead's seminal article, a wide variety of measurement methods have been employed, classified in the following table.

Table 2-1 Methods Used for chest wall motion measurements

Methods use	Methods measure
Physical devices placed on the chest wall	a) linear displacement along the AP axis (eg using magnetometers or accelerometers) b) changes in chest wall circumference, either physically (strain gauges) or by its effect on thoracic impedance (impedance pneumography) c) changes in cross-sectional area (respiratory inductive plethysmography) d) changes in volume (electromagnetic inductive plethysmography)
External imaging devices	a) Radiological techniques b) Optical techniques

The basis of these techniques and their advantages and limitations will be reviewed and compared in this section.

2.6.3.2 Physical devices on the chest wall

a) Linear displacement along the AP axis

To measure an increase in AP diameter of RC and AB, linear displacement is quantified utilising a more sophisticated electronic versions in comparison to the Konno and Mead's method. Here, the advantages include its increasing miniaturisation, the cheapness of device, use in other devices such as mobile phone, simple and portable, and the fact that it has been used extensively in research with adults as well as early young patients. However, as with many devices, they have disadvantages with the biggest being that there is a continuous assumption that changes in one dimension, at two points along the chest wall (usually nipple and umbilicus level), are a precise reflection of changes in the volume of a complex 3D structure. The relationship between linear displacement and volume change varies across subjects, even if healthy adults, and the methods become less reliable when there is a greater the degree of chest wall distortion (Heldt, 1988; Reich and McHenry, 1990; Russell and Helms, 1994). Linear measurement techniques are insufficient for estimating respiratory volumes in children. However, they are adequate for estimating respiratory rate. An example of such a method, using three accelerometers has been shown in adults to precisely measure tPTEF/tE (Dehkordi et al., 2014). Other methods such as ultrasound signal transmission have been employed which are more sophisticated methods that measure the linear movement of different areas of the chest wall; this can be placed on the chest wall to an external receiver, and this has been used successfully to assess differential chest wall movement in scoliosis (Kotani et al., 2002). Laser displacement sensors have also been used to measure RC and AB movement (Hargrove, Zemper and Jannausch, 2009).

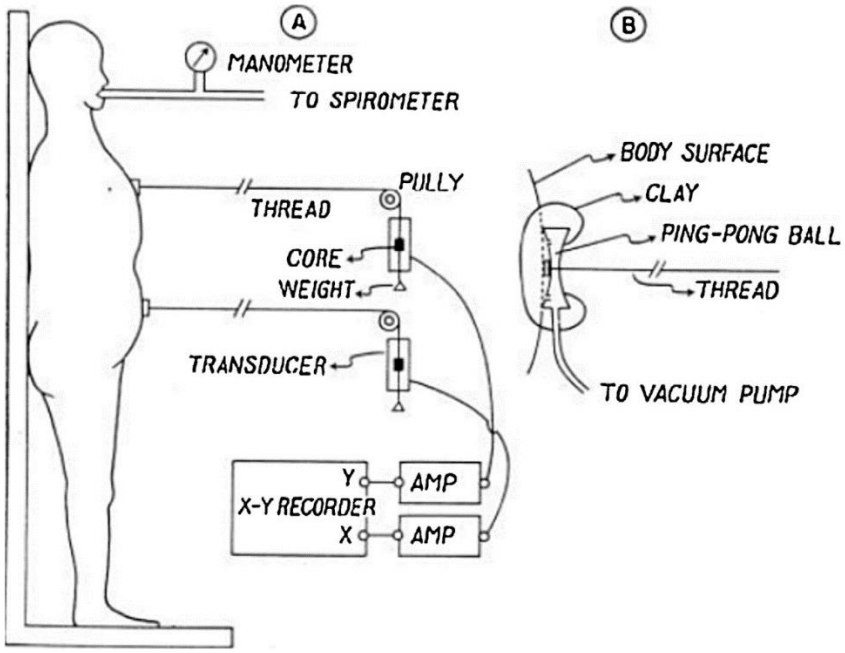

Figure 2-6 The device developed by Konno and Mead to measure chest and abdominal wall displacements
(Konno and Mead, 1967).

b) Measuring changes in chest wall circumference

Strain gauges utilise changes in electrical conductance of fine bands which encircle the RC and AB. The expansion of the chest wall increases the circumference, stretching the band and increasing the resistance to a low electrical voltage (Adams et al., 1993). There is a similar technique which measures the delay between ultrasound emission and reception at opposite ends of two rubber tubes encircling RC and AB (Lafortuna and Passerini, 1995). This technique has been effective in measuring and estimating tidal volumes during exercise in healthy adults but has yet to show its use in children. Fibre optic respiratory plethysmography is another approach that utilises light transmission through fibre-optic bands to measure changes in curvature (Davis et al., 1999). Both of these techniques are more effective methods in predicting volume change than linear measurements. However, their limitations remain in the assumptions that not only the cross-sectional shape remains constant but also that the measurements at one level for RC and one for AB represent changes at all levels. These limitations may be inaccurate in young infants, with either chest wall/neuromuscular disease or other severe respiratory disease. Although strain gauges have been used in some sleep monitoring systems, they have mainly been substituted by respiratory inductive plethysmography (RIP) (Figure). Through measuring the changes in electrical impedance, impedance pneumography examines changes in circumference of the chest wall to a very weak alternating current. This is often transmitted between ECG electrodes and is with respect to intensive care units; widely used to give a respiratory trace on multi-channel monitors. However, its main use is for respiratory rate and apnoea, as it only assesses changes in partial circumference. The other reason for this is because of the commonness in the random fluctuations in amplitude. Hence, It does not detect obstructive apnoea (Brouillette et al., 1987).

c) Measuring changes in cross-sectional area (respiratory inductive plethysmography)

Respiratory inductive plethysmography (RIP) uses sinusoidally-arranged wires. These wires, carrying a low-voltage oscillating current, are incorporated in cloth bands which encircle the chest and abdomen approximately at nipple and umbilicus level Figure 2-7. The current in each segment of the band affects the current in other segments, having a rippled effect, best known as self-inductance. When the cross-sectional area enclosed by the band is changed, there is a change in self-inductance, causing the frequency to change too. These are demodulated to yield a voltage change which is proportional to the change in the cross-sectional area (Stocks, 1996). RIP has the potentiality to accurately estimate tidal volumes, in comparison with linear and circumference chest wall measurements (Adams *et al.*, 1993). RIP advantages further include that it is able to calibrate fully using direct flow measurements at the airway opening, semi quantitaively using qualitative diagnostic calibration or uncalibrated (Sackner *et al.*, 1989). However, the theory of the matter is not accurate when looking at how practical it is; fully calibrated RIP can theoretically be used to measure tidal and minute volumes non-invasively, while the need for calibration using flow at the airway opening practically makes this less beneficial, and calibration carried out in different conditions vary. For example, the calibration

may be invalid when in quiet sleep in comparison to active sleep due to the changes in RC-AB relative contribution and chest wall distortion (Warren and Alderson, 1986). Nevertheless, both semi-calibrated and uncalibrated RIP has been extensively used in research and in clinical practice. Examples include:

- In polysomnography to detect and differentiate central and obstructive apnoeas (Brouillette *et al.*, 1987).

- In acute and chronic respiratory disease to estimate thoracoabdominal asynchrony (TAA).

To measure tidal flow timing parameters, uncalibrated RIP has also been used. An example is the time to peak tidal expiratory flow over total expiratory time (tPTEF/tE) (Stick *et al.*, 1992). However, questions about the accuracy of these parameters compared to direct flow measurement at the airway opening remain (Jackson *et al.*, 1995).

D) Measuring changes in volume

A relatively new technique, Electromagnetic inductive plethysmography (EIP) employs the following components:

1) Two helical coils, with each carrying a weak electrical current, sewn into a single elasticated fabric garment; each surrounding the entire RC and AB components of the chest wall.

2) A magnetic moment detector. This is suspended horizontally above the cot or bed, producing a weak homogeneous magnetic field around the two coils (Figure).

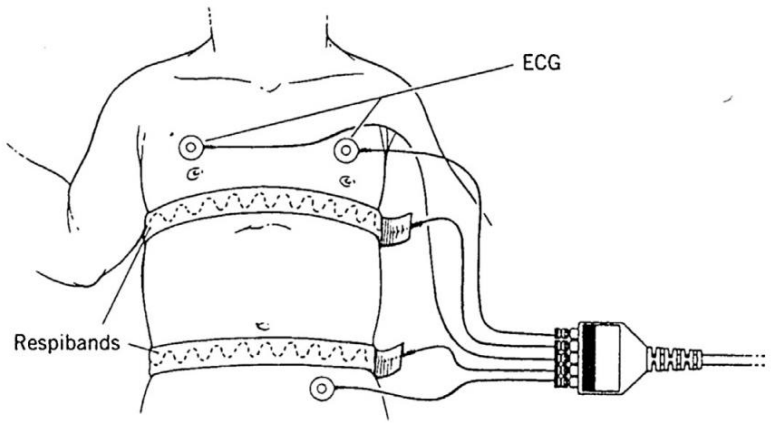

Figure 2-7 Respiratory inductance plethysmography, band are used to measure change in the cross-sectional area enclosed by the bands
(Stocks, 1996).

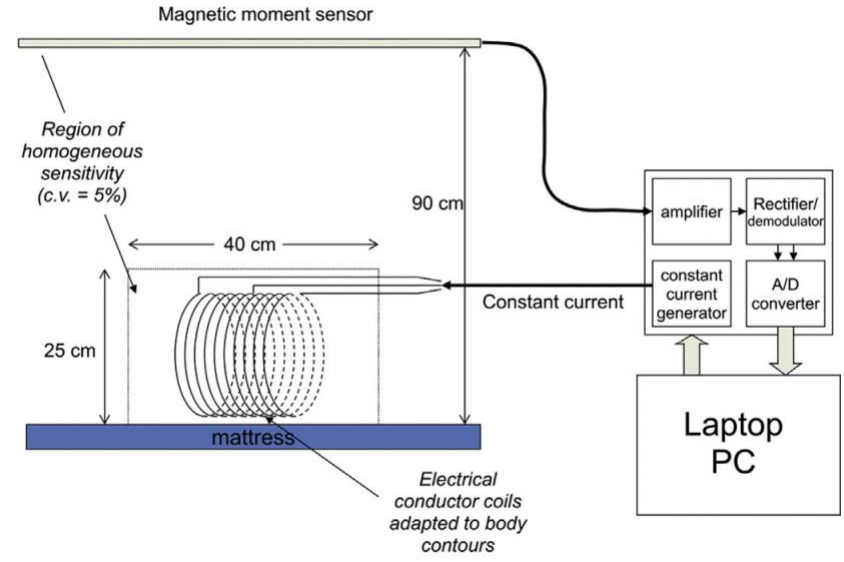

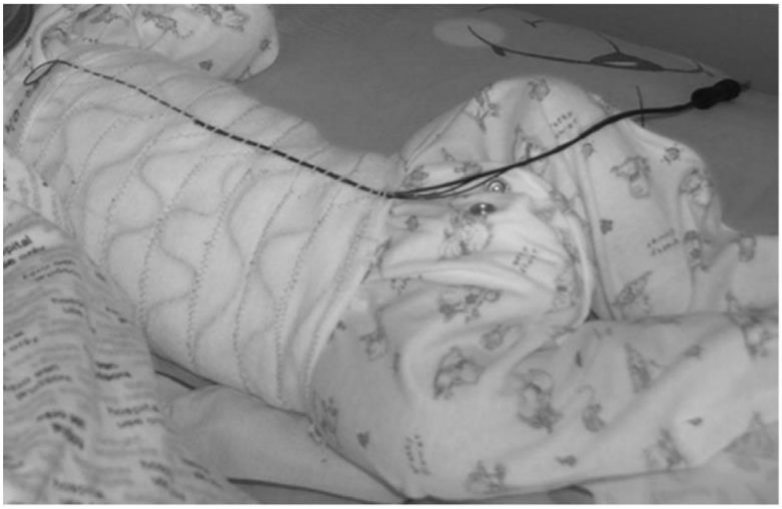

Figure 2-8 Electromagnetic inductive plethysmography. Upper shows a single coil representation of the device and lower shows a vest (containing the RC and B coils) placed on a new born infant (Seddon, 2015).

The volumes changes contained within the two coils yield proportional changes in electromagnetic inductance of the system (Sartene *et al.*, 1990). Using a calibration coil placed under the magnetic moment detector, the device can be calibrated off the patient. Mainly used for infants, EIP studies have involved healthy term newborns (Olden, Symes and Seddon, 2010; Petrus *et al.*, 2015; Drakatos *et al.*, 2016), preterm infants with lung disease (Williams *et al.*, 2011; Pickerd, Williams and Kotecha, 2013), and infants with lung disease (Olden, Symes and Seddon, 2010; Petrus *et al.*, 2015). These studies have shown that EIP can accurately be used to estimate tidal volume compared to flowmeter or pneumotach. With respect to tidal breathing parameters including t_{PTEF}/t_E, studies found a very close correspondence between EIP and airflow measurements . With respect to the measurment of TAA, RC and AB volume changes can be partitioned, and phase angle measurements have been reported in preterm infants. However, this technique has so far not been compared with TAA assessment using RIP. RIP

has the advantage over the other techniques that it allows a quantitative measurements of volume change without calibration on the child (e.g. with facemask and pneumotach). This is because the volume changes are measured over the whole chest wall, which makes this technique less susceptible to inaccuracy caused by the distortion of the chest wall, though this has not been practically proved. The need for a vest-type garment covering the whole torso remains a disadvantage, and this could be problematic in intensive care environments.

2.6.3.3 Methods using external imaging devices

a) Radiological techniques

Magnetic resonance imaging (MRI), a widely used effective technique, has been used to examine detailed aspects of chest wall motion in adults or adolescents. This has been used during:

1) Slow deep or tidal breathing (Kondo *et al.*, 2000; Kotani *et al.*, 2004; Herrmann *et al.*, 2006; Tokuda *et al.*, 2009). A study showed good correlation between changes in MRI cross-sectional area and in lung volume (Kondo *et al.*, 2000), but tidal breathing has been more problematic (Tokuda *et al.*, 2009).

2) During breath-holds in deep breathing (Raichura *et al.*, 2001; Chu *et al.*, 2006).

These techniques give comprehensive evidence about regional chest wall motion and have provided interesting data about the behaviour of the chest wall during breathing in pectus excavatum (Raichura *et al.*, 2001; Herrmann *et al.*, 2006) and scoliosis (Kotani *et al.*, 2004). However, this technique is limited; as it requires prolonged periods in which young and sick children need to be inside a scanner, and with the need of cooperative, controlled breathing, and the difficulty with rapid respiratory rates and small volumes, the disadvantages of MRI has been noted.

b) Optical techniques

By capturing a dynamic sequence of video images of the anterior surface of the chest and abdomen, Optoelectronic plethysmography (OEP) uses complex signal processing to calculate the changes in the volume of the chest wall (Morgan, Gourlay and Denison, 1984; Ferrigno *et al.*, 1994). To enable the signal processing, either a geometric pattern is projected onto the chest wall (Morgan, Gourlay and Denison, 1984), or markers are positioned on the chest wall (Ferrigno *et al.*, 1994) Figure 2-9. Reasonable correspondence has been shown in adults with spirometric measurement of lung volume changes (Morgan, Gourlay and Denison, 1984), and more recently OEP and pneumotach measurements of tidal volume in stable neonates have shown good agreement (Dellaca *et al.*, 2010). OEP has been used to investigate chest wall movement in tetraplegic adults (Morgan *et al.*, 1985). An advantage of OEP is that it is a non-invasive technique with considerable potential in young children. However, patients need to

remain still in order for measurements to be taken and this is at time problematic. Moreover, this technique is time-consuming and require equipped laboratories to perform the measurements.

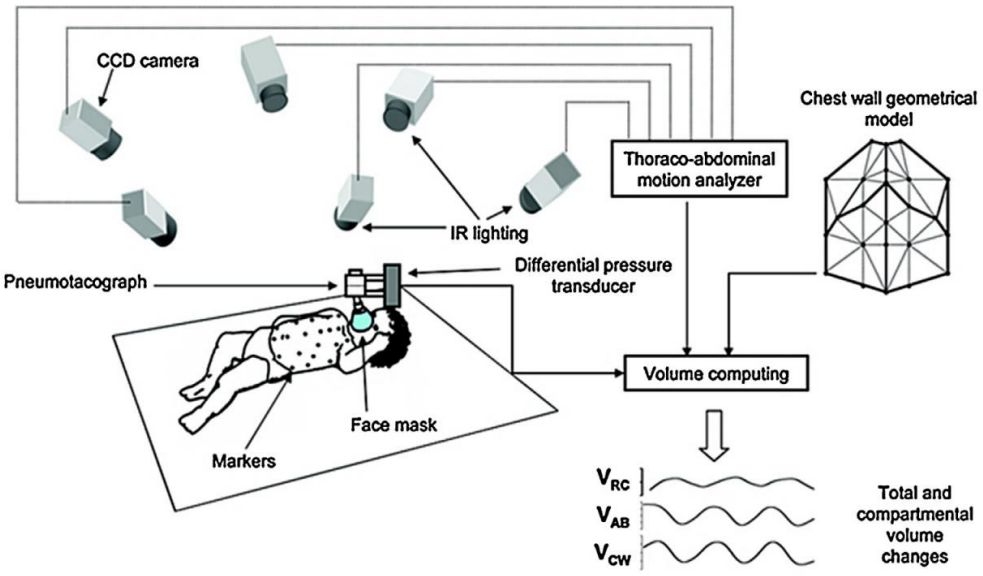

Figure 2-9 Optoelectronic plethysmography

(Dellaca *et al.*, 2010)

2.7 Summary

Childhood respiratory disorders place a significant burden on healthcare systems nationally and worldwide. Conventional objective measures of pulmonary functions allow accurate diagnosis and monitoring of respiratory disorders. Available techniques have some drawbacks such as inability to provide a complete image of the pathophysiological changes of lung disease, in addition to that, they are unsuitable for all ages and clinical conditions.

After reviewing these methods, how they work, their advantages and disadvantages, it is important to note that what SLP does to make it more feasible in chest wall measurement is that it does not require any physical contact in comparison to the methods mentioned here, making it more patient-friendlier and easier for the practitioner to use. As an external imagining device, it is rather simple and does not require or need markers; instead, it can be used on the bed side in the supine position. Thus it was worthy for further investigation in children for my research.

SLP is feasible in both healthy subjects and patients with COPD and was able to detect airway obstruction in the diseased group (Motamedi-Fakhr, Wilson and Iles, 2017). Further assessment

and validation of this technique in young children and infants is needed to assess its value and usefulness in paediatric patient groups. Although SLP requires the patient to be in a still position, which might be challenging in younger children, it could be, if feasible, used to provide an objective measure of pulmonary functions and valuable information about breathing mechanics.

3 Study Aims

The purpose of this study is to evaluate the use of SLP in Paediatric respiratory disorders. For this purpose, I have constructed two main aims, each with specific objectives in order to achieve these aims. These are:

Aim 1: To evaluate the use of SLP in clinical settings, demonstrating its feasibility and usefulness in various respiratory conditions at different ages.

The first objective here is to assess the use of SLP in (1) identifying the existence of airways obstruction, and (2) detecting changes, after bronchodilation administration, in airways obstruction in children with stable asthma (7-16 years). SLP readings were confirmed by using the gold-standard measure (Spirometry). The second objective consisted of comparing SLP-estimated parameters between (1) healthy and acute asthma/wheeze participants (2-12 years); (2) pre and post intervention for the Asthma group. Finally, the last objective aimed to assess the feasibility of utilising SLP with a younger population (< 2 years). This part consisted of comparing SLP-estimated parameters between: (1) healthy infants and infants with acute viral bronchiolitis (AVB); and (2) detecting changes, in the quantified parameters, between admission and discharge in the AVB group.

Aim 2: To evaluate the robustness of SLP outcomes against introduced artefacts (upper body movements and coughs) that might interfere with its reading.

The first objective here is to find the optimal SLP-recording period. The second objective is to assess the effects of upper-body movements and coughs on SLP-estimated parameters. Finally, the last objective aimed to investigate the use of various signal processing and statistical techniques to remove upper-body movements and coughs from SLP signals.

4 Structured Light Plethysmography (SLP)

4.1 Introduction

Structured light plethysmography is a novel, non-contact technique developed by a group of clinicians and engineers to measure tidal breathing (Boer *et al.*, 2010). SLP has shown potential clinical uses in various respiratory conditions, for example, it has been used to identify changes in chest wall motion in a group of patients with lung resection, a reduced chest wall contribution in the overall TA wall movement was observed on the operated side, with the amount of the reduction matching the size of the resection. Moreover, a higher thoraco-abdominal asynchrony (TAA) increase was identified in patients who had a lobectomy than in patients who had a resection (Elshafie *et al.*, 2016). In another feasibility study, SLP has been shown sensitive enough to detect differences in tidal breathing patterns between patients with COPD (with a range of severities) and healthy individuals (Motamedi-Fakhr, Wilson and Iles, 2017). It is believed that respiratory conditions like COPD have an effect on tidal breathing parameters (Williams, Madgwick and Morris, 1998; Kostianev, Hristova and Iluchev, 1999; Morris *et al.*, 2004; Wilkens *et al.*, 2010; Williams *et al.*, 2014), SLP has identified breathing patterns differences, which assert its sensitivity in obstructive lung conditions. No evidence has shown the feasibility of SLP in young children with obstructive respiratory conditions.

A study aimed to assess the agreement between tidal breathing parameters, measured simultaneously using PNT and SLP for 45 seconds, have shown that the fundamental parameters (will be explored later in the chapter) are in agreement. Moreover, the method has been proven to be repeatable, even though, SLP measures TA displacement and TA displacement-rate rather than flow or volume measurements in PNT (Motamedi-Fakhr *et al.*, 2017).

4.2 Tidal Breathing

Tidal breathing refers to the state of inhalation and exhalation during breathing at rest; its patterns can reveal crucial physiological information about both the respiratory control and pulmonary mechanical function (Bates *et al.*, 2000).

In healthy individuals, tidal breathing is maintained within a normal range. Respiratory diseases such as asthma and COPD not only change the character, but can also lead to changes in a series of patterns of breathing (Olden, Symes and Seddon, 2010) Thus, in patients with respiratory disorders, these alterations help clinicians to identify the underlying cause and establish care plans according to the disease.

By analysing tidal breathing parameters, clinicians can assess the respiratory health status of the patient (Seppa, 2013), all of this shines the light onto the importance of investigating tidal breathing, especially with little children, who cannot cooperate and perform forced respiratory manoeuvres needed for conventional lung function testing.

4.2.1 Flow-based tidal breathing parameters

Tidal breathing parameters are well explained by Stick *et al.* (1992) and Bates *et al.*(2000). Of flow-based parameters: peak tidal inspiratory flow (PTIF), peak tidal expiratory flow (PTEF), and times to reach those values (tPTIF and tPTEF). In addition, Parameters describing Flow-volume loop's shape such as: TEF50 (tidal expiratory flow at 50% of tidal volume), TIF50 (tidal inspiratory flow at 50% of tidal volume) and the ratio between them TIF50/TEF50 which is also referred to as IE50 (Black *et al.*, 2004).

4.3 Structured Light Plethysmography - Thora3Di^{TM}

Thora3Di^{TM} uses computer image and vision processing methodology to estimate tidal breathing parameters from the movement of the TA region; it does not require markers to be placed onto the body (Boer *et al.*, 2010). Tidal breathing parameters measured using SLP have shown good agreement with the parameters measured simultaneously by Pneumotachography (Motamedi-Fakhr *et al.*, 2017). SLP works by having a grid pattern projected onto the TA region of a subject, while in a supine or seated position.

Figure 4-1. A child undergoing an SLP assessment in a seated position

(PneumaCare, 2013)

Figure 4-2. A child undergoing an SLP assessment in a supine position

(PneumaCare, 2013).

4.3.1 Thora3Di™ Working Principle

4.3.1.1 Stereo Imaging

Two cameras which are separated spatially to image a 3-D object are used in stereo imaging as shown in Figure 4-3 below. The two cameras are separated by a distance S, with the two optical axes in parallel which is the simplest case for the stereo imaging (Hossack, 2006).

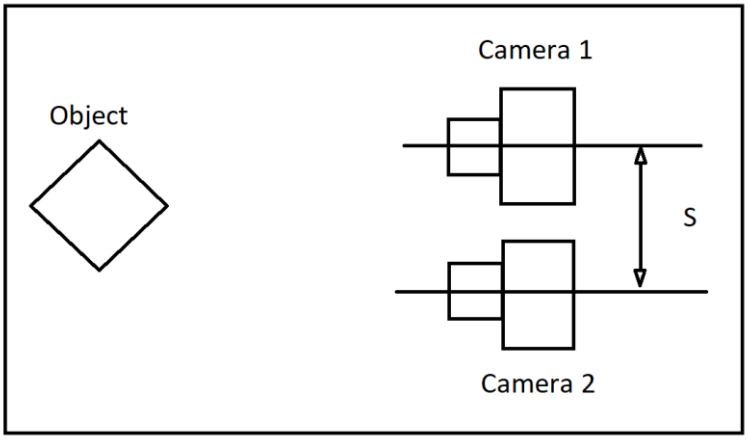

Figure 4-3. Basic Layout for a Parallel-optical axes Stereo Imaging system
(Faugeras, 1993).

A different view of the same object (a cube in this case) can be obtained from the two cameras as shown in Figure 4-4. This will involve shifts in the vertical lines only to extract depth information. The system is comparable to a human visual system which involves two eyes separated by between 60 to 70 mm so when someone views a 3-D object; each eye will be able to see two slightly different views (Faugeras *et al.*, 1993).

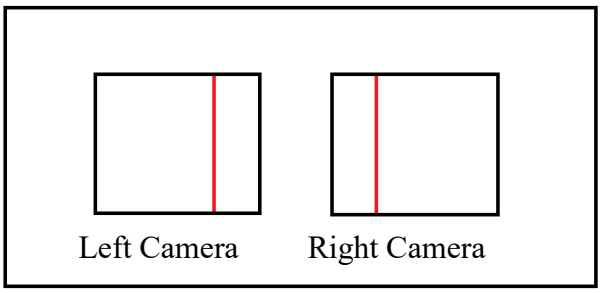

Figure 4-4. Two stereo Images of a Cube
(Faugeras et al.*, 1993)*

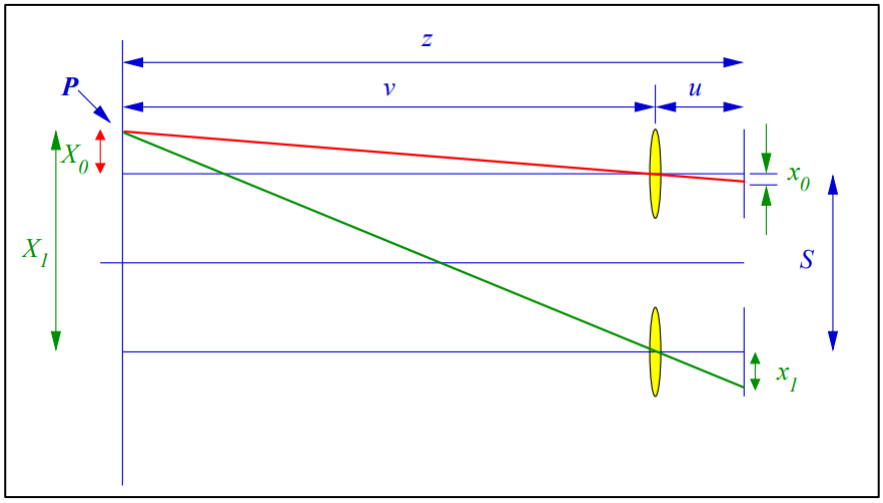

Figure 4-5. Parallel geometry system
(Hossack, 2006)

This figure shows a simple stereo imaging system where:

- The two cameras are aligned with respect to their optical axes so that they are parallel to each other.
- 'S' is the distance between both cameras' optical axes.
- x_0 and x_1 are the locations of the image of ***P*** on cameras 1 and 2 planes respectively.
- u is the distance from the lens to the detector plane, and it is assumed to be the same for both cameras.

Then from triangles similarities:

$$\frac{x_1}{u} = \frac{\mathrm{X}_1}{v} \qquad \text{Equation 4-1}$$

$$\frac{x_0}{u} = \frac{\mathrm{X}_0}{v} \qquad \text{Equation 4-2}$$

And from the locations of the two images of P:

$$X_1 = \frac{vx_1}{u} \qquad \text{Equation 4-3}$$

$$X_0 = \frac{vx_0}{u} \qquad \text{Equation 4-4}$$

Knowing that the optical axes of both cameras are parallel:

$$X_1 = X_0 + S \qquad \text{Equation 4-5}$$

by substitution we have:

$$x_1 = x_0 + \frac{uS}{v} \qquad \text{Equation 4-6}$$

Solving for v which is the length of the horizontal line from the point ***P*** to the two camera lenses:

$$v = \frac{uS}{(x_1 - x_0)} = \frac{uS}{\Delta x}$$ Equation 4-7

Δx : is the difference between the two images of ***P***, $(x_1 - x_0)$. From the Gaussian lens formula, which gives the relation between the focal length of a lens (***f***), and the position of the object and image plans as:

$$\frac{1}{f} = \frac{1}{u} + \frac{1}{v}$$ Equation 4-8

However, in most systems, there is a distant object so that for a short focal length lens, $v \gg u$ and we can assume that $u \approx f$, this means that the distance between the lens and detector is simply the focal length of the lens, then:

$$v \approx \frac{fS}{\Delta x}$$ Equation 4-9

And substituting $z = u + v$ from the figure above, we can get the equation representing the distance between the image plan and the object as:

$$z = f\left(1 + \frac{S}{\Delta x}\right)$$ Equation 4-10

So, knowing the focal lengths of both cameras and the separation distance between them, we can estimate the distance between the object and the image plane, by only calculating Δx, which is the difference between locations of the image of ***P*** in cameras 1 and 2.

Thora3Di uses the above principle to extract the corner features from the projected grid of light on the thoracoabdominal region to build a 3D- reconstruction of the projected area and track it over the recording period at a 30Hz frame rate.

The point of intersection of the grid is defined as the corner shared by four squares. The entire grid consists of $w_{grid} \times h_{grid}$ of these points.

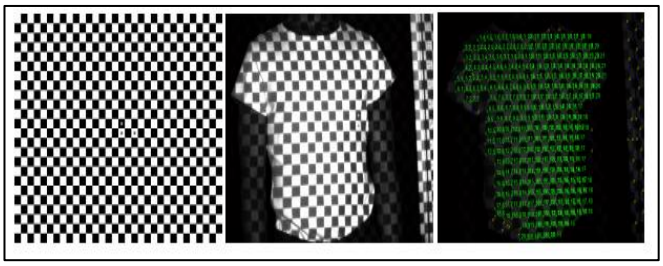

Figure 4-6. Grids identification on a patient's TA wall.

The grid pattern (left). The corners of the squares are 'grid intersection points', and there are $w_{grid} \times h_{grid}$ (23 × 28) of these. The grid pattern as projected onto a subject (centre), and after identifying grid intersection points (right) *(Boer* et al.*, 2010, p.3)*

The two cameras used to record the subject's chest area are placed at different and known positions and angles. The intersection points of the grid pattern are tracked and then brought into correspondence. External and internal parameters of the two cameras as well as the projector from the subset of point correspondences are inferred by a self-calibration algorithm. The 3D-reconstruction of the chest wall is then done by the use of camera calibration. Unwanted parts (such as limbs) are then removed as the missing parts are filled. The reconstruction is then tracked and used to calculate the breathing trace over the recording period (Boer *et al.*, 2010).

SLP technology was developed at Cambridge University; it attempts to solve most of the drawbacks of the previous methods by introducing a zero-contact and non-invasive method for monitoring tidal breathing and extracting lung functions.

4.3.2 Thora3Di™ tidal Breathing Parameters

PneumaCare's Thora3Di™ enables doctors and surgeons to understand the patient's pulmonary function and also to view the effort in the regional segments by measuring the movement of the TA wall. Images which are required can be taken even with the patient lying on their bed. The machine has the advantage of showing the data of lung function in 3D format. The machine builds the 3D reconstruction of the thoraco-abdominal region and allows the division of that region in order to see the movements of each part with respect to the other part.

Quantified tidal breathing parameters could be categorized into three different groups: parameters which describe the overall displacement of the thoraco-abdominal region, the ones which describe the displacement rate of it, and the parameters which describe the regional contribution and temporal movements of different thoraco-abdominal compartments.

4.3.2.1 SLP-estimated tidal breathing parameters derived from TA displacement with time signals

The tidal breathing trace is computed by quantifying the averaged axial displacement of each intersection of the grid of light projected onto the TA wall. Timing indices such as inspiratory time (tI), expiratory time (tE), total breath time (tTot), the ratios between them tI/tE and tI/tTot and respiratory rate (RR) are estimated from this trace. These timing indices have shown good correlation with those measured using a Pneumotachography (Motamedi-Fakhr *et al.*, 2017). Figure 4-7 (A) shows how the indices are calculated.

4.3.2.2 SLP-estimated tidal breathing parameters derived from TA displacement rate with time signals

Although SLP does not measure flow or volume, SLP tidal breathing flow parameters are calculated in the same way as PNT flow-based parameters, where TA displacement is considered analogous to volume, and TA displacement rate analogous to flow, and is calculated by taking the first time derivative of the TA displacement trace. By plotting TA displacement vs. time the following parameters can be derived: peak tidal inspiratory flow ($PTIF_{SLP}$), peak tidal expiratory flow ($PTEF_{SLP}$), and time taken to reach these points ($tPTIF_{SLP}$ and $tPTEF_{SLP}$) respectively Figure 4-7 (B). To correct for different respiratory rates, the latest parameters were normalised against total inspiratory and expiratory time ($tPTIF_{SLP}/tI$ and $tPTEF_{SLP}/tE$).

4.3.2.3 Parameters that describe the shape of the displacement loop

The loop produced by plotting TA displacement against TA displacement rate is considered comparable with a conventional Flow-Volume loop (H. Hmeidi *et al.*, 2017).

Many parameters were used to describe the shape of both the inspiratory and the expiratory parts of this loop: tidal inspiratory TA displacement rate at 50% of inspiratory displacement ($TIF50_{SLP}$), and tidal expiratory TA displacement rate at 50% of expiratory displacement ($TEF50_{SLP}$) respectively Figure 4-7 (C).

$IE50_{SLP}$ (inspiratory to expiratory TA displacement rate ratio), which is the ratio between $TIF50_{SLP}$ and $TEF50_{SLP}$ could also be calculated (Black *et al.*, 2004). SLP validation study has shown a good agreement between $IE50_{SLP}$ and IE50 measured simultaneously by Pneumotachography (Motamedi-Fakhr *et al.*, 2017).

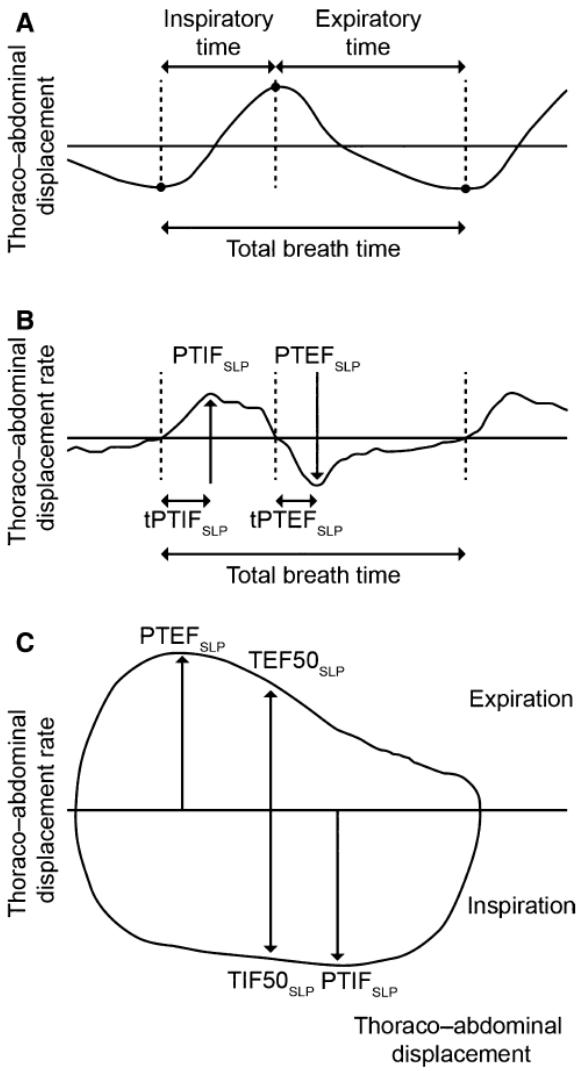

Figure 4-7. SLP-traces of tidal breathing and the derived parameters.

(A)Timing indices. (B) TA displacement rate-derived parameters. (C) TA displacement rate with TA displacement-derived parameters (Hmeidi *et al.*, 2017, p.3)

4.3.2.4 SLP assessment of regional tidal breathing parameters

The TA region could be split into different compartments such as Thorax/Abdomen, Left/Right or even quadrants: Upper Left (UL), Upper Right (UR), Lower Left (LL) and Lower Right (LR).

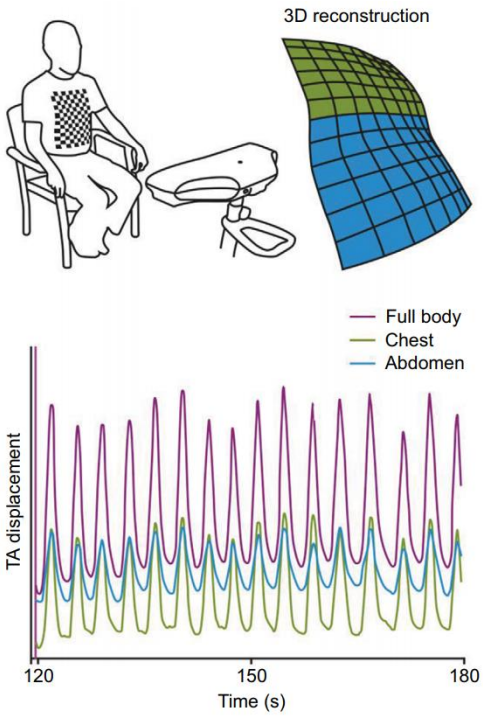

Figure 4-8. The anterior TA wall split into two sections,

One representing the thorax and the other the abdomen. The axial displacements of the thorax and abdomen are averaged to produce the overall TA wall displacement (Motamedi-Fakhr, Wilson and Iles, 2017, p.3).(Motamedi-Fakhr, Wilson and Iles, 2017)(Motamedi-Fakhr, Wilson and Iles, 2017)(Motamedi-Fakhr, Wilson and Iles, 2017)(Motamedi-Fakhr, Wilson and Iles, 2017)(Motamedi-Fakhr, Wilson and Iles, 2017)(Motamedi-Fakhr, Wilson and Iles, 2017)(Motamedi-Fakhr, Wilson and Iles, 2017)

The relative contributions of any compartment are calculated as a percentage of the total displacement. Figure 14 below shows total TA displacement and its thoracic and abdominal components for a single breath. To obtain the relative thoracic contribution for the shown breath, the peak of ribcage displacement (the dashed line b) is divided by the peak of TA displacement (dashed line a), similarly dividing peak abdominal displacement (dashed line c) by the peak of TA displacement (dashed line a) provide the relative abdominal contribution.

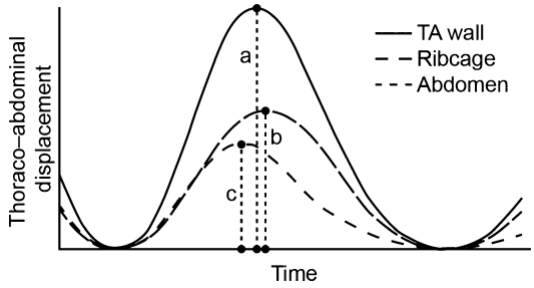

Figure 4-9. Thoracic and abdominal components of one breath as calculated using SLP

(Hmeidi *et al.*, 2017, p.3).

Konno-Mead Loop

Konno-Mead loop shows the relationship between Chest and Abdominal contributions in the overall movement. It shows the percentage of chest movements versus percentage abdomen movements or the percentage left movements versus percentage right movements (Warren, Horan and Robertson, 1997).

Phase Angle

The phase describes the time lag in movement between one TA region with respect to another. A phase lag of zero degrees means a full unison or synchrony between both the regions. If the movement of one region lags behind the movement of the other, then those regions are considered asynchronous.

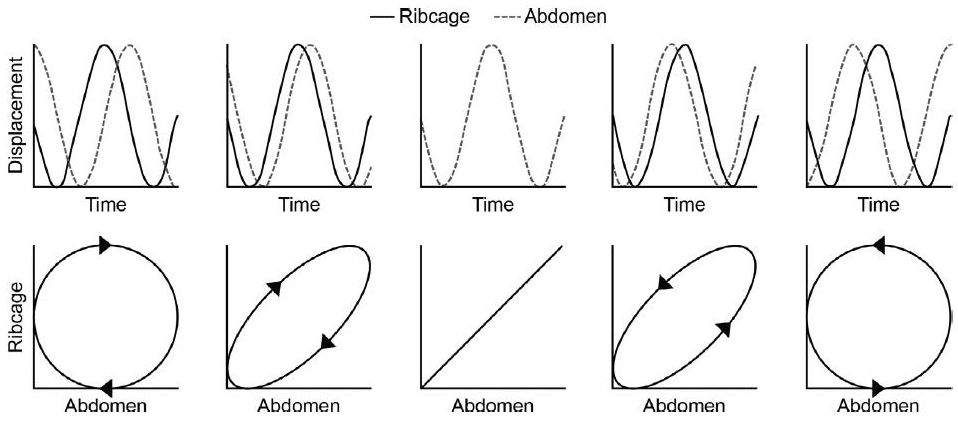

Figure 4-10. A representation of Konno and Mead method of quantifying thoracoabdominal asynchrony for a single breath.

An example. From left to right the figures show -90°,-45°, 0°, 45°, and 90° phase shifts between the ribcage and abdomen signals. The direction of the Konno–Mead loop determines which signal is lagging behind or leading the other (Hmeidi *et al.*, 2017, p.4).

Phase is quantified by plotting the displacement of both regions against each other (Konno-Mead Loop) and then calculating the magnitude of asynchrony using the shape of this plot (Konno and Mead, 1967). Phase usually represent only thoracoabdominal asynchrony (TAA). However, the asynchrony between left and right compartments could be assessed with SLP. Phase is quantified in degrees using the following equation:

$$\text{phase} = \text{TAA} = \sin^{-1}\left(\frac{\text{m}}{\text{s}}\right) \qquad \text{Equation 4-11}$$

where: m is the width of the Konno-Mead loop at 50% of ribcage displacement, and s is the range of abdominal displacement Figure 4-11.

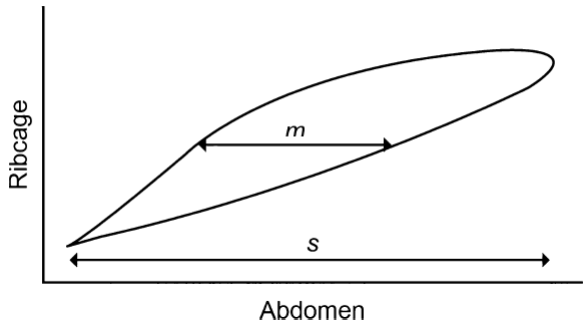

Figure 4-11. A single breath representation using Konno-Mead approach.

m is the width of the loop at 50% of ribcage displacement, and s is the range of the abdominal displacement (Hmeidi *et al.*, 2017, p.4).

SLP data is usually acquired for up to five minutes which allows the acquisition of many breaths. Previously mentioned parameters are calculated for every single breath, median value is calculated for each parameter to estimate its magnitude. Median is preferred over the mean because of its stability in the presence of outliers.

4.3.2.5 Variability in SLP tidal breathing parameter

Each tidal breathing parameter shows an amount of within-subject variability. SLP allows the quantification of this variability, as data is acquired for many successive breaths, each parameter is quantified for every single breath, then the variability is obtained over the recorded period. The interquartile range (IQR) was used for this purpose, because of its robustness in the presence of outliers unlike the standard deviation (H. Hmeidi *et al.*, 2017).

4.3.3 Thora3Di™ Software and Data Analysis

PneumaView-3D™ software (PneumaCare, Ltd.) allows the movement of the reconstructed TA surface to be viewed as a video. The assessment of the movement of this surface is an important step as it may identify subtle tracking errors that are not obvious in the TA displacement-time trace.

These tracking errors can be due to excessive wrinkling of the white T-shirt or by a lack of contrast in the projected grid (which could be caused by unsuitable lighting in the room). This can cause either flickering or missing of some points in the reconstructed surface.

Subject movement or coughing is another kind of artefact which might occur during the recording. A sudden movement of the reconstructed surface from its trajectory can be used to identify these artefacts and exclude them later from the analysis.

Datasets are excluded from the analysis if >50% of their respiratory cycles were affected by one or more of the above artefacts. Accepted datasets are exported by the PneumaView3D software. The exported data included information on the overall TA wall movement, as well as regional movements. A breath detection algorithm was used, which was developed, based on the work explained by Bates et al. (2000) and Schmidt et al. (1998), by identifying the peaks and troughs of the signal using a zero-crossing of the first-time derivative of the overall displacement signal. Finally, for the cycle to be considered as a breath, its peak-to-peak amplitude should be > 25% of the median peak-to-peak amplitude of the entire breaths in the signal.

5 Tidal breathing parameters in healthy children and those with stable asthma

The work reported in this chapter has been published in Physiological Reports ISSN 2051-817X, with the title "Tidal breathing parameters measured using structured light plethysmography in healthy children and those with asthma before and after bronchodilator" by (Hmeidi *et al.*, 2017). Permission was obtained from the publisher to reuse relevant aspects of this work in this thesis (i.e. figures, plots and tables).

5.1 Introduction

Asthma is the most common chronic disease in childhood, and one of the main causes of morbidity among other chronic diseases in children (Pedersen *et al.*, 2011). According to Asthma UK, one in every 11 children is diagnosed with asthma, and 185 people are hospitalised daily because of asthma attacks (most of those admissions are for children). Asthma causes a significant burden on the healthcare systems in the UK and worldwide (Bateman *et al.*, 2008; Nunes, Pereira and Morais, 2017). Lung function assessment is required in order to diagnose asthma accurately and provide optimal management of the condition (Brusasco, Crapo and Viegi, 2005; Miller, Crapo, *et al.*, 2005; National Heart Lung, Institute and others, 2007; Wijngaart, Roukema and Merkus, 2015). Spirometry is the technique used clinically to assess lung functions, but it is not suitable for all ages due to the nature of the test (Beydon *et al.*, 2007). In young children obtaining objective measures of airways obstruction might improve their care, thus investigating the use of new simpler techniques is essential.

Tidal breathing measurements can provide valuable information about respiratory function and mechanics (Bates *et al.*, 2000). On their own, many tidal breathing parameters have been shown the ability to diagnose several lung conditions (Bates *et al.*, 2000). Tidal breathing reveals some important physiological indications relating to pulmonary mechanics and respiration control mechanism in healthy adults and infants. Moreover, airflow limitation and its degree have shown to affect tidal breathing patterns in both children and adults (Williams *et al.*, 2014).

Tidal breathing measurements are relatively simpler than other methods of assessing lung function in infants, which highlights the importance of analysing tidal breathing patterns (Stick, 1996). Traditional techniques include the measurement of airflow signals using a mouthpiece or a facemask (i.e. Pneumotachography) or measurements of thoracoabdominal (TA) wall movement using bands placed around thorax and abdomen (i.e. respiratory inductive plethysmography [RIP-bands]) (Stick *et al.*, 1992; Adams *et al.*, 1993). Those techniques require direct contact with the patient, and the placement of the mouthpiece or the facemask in Pneumotachography can result in changing of tidal breathing pattern (Weissman *et al.*, 1984; Laveneziana *et al.*, 2015a), whereas in RIP slippage of the elastic band that contains the elastic coil during data collection could provide an erroneous reading (Caretti *et al.*, 1994).

Structured light plethysmography (SLP) allows a detailed assessment of tidal breathing patterns using a light-based technique in a zero-contact environment. Two digital cameras record the movement of a pattern of light projected onto the anterior TA wall. The average axial displacement of the grid over time is used to estimate tidal breathing parameters (Boer *et al.*, 2010). SLP recording requires the subject to sit still and breath, without the need to perform any forced breathing manoeuvres. Minimal patient cooperation was required to obtain an SLP scan in adults (Motamedi-Fakhr, Wilson and Iles, 2017), which make it suitable even for young children.

Furthermore, using some distraction methods to reduce excessive patient movement, SLP scans could be successfully obtained from younger children down to 3 years of age (Hmeidi *et al.*, 2015). As a result, SLP might be a useful technique for children who cannot perform

conventional tests of respiratory function assessment such as spirometry. School-age children were investigated in this study because of their ability to perform spirometry, which is used as a reference to confirm the obstruction and the response to bronchodilator treatment.

5.2 Study Aims

In this study the use of SLP in assessing tidal breathing was evaluated in two groups: school-age children with asthma and age-matched healthy children, then the findings were compared. The effect of bronchodilation on both tidal breathing parameters and spirometry was also assessed in the asthmatic group.

5.3 Methods

5.3.1 Study participants and design

For this study, children visiting an outpatient clinic for a routine check who were found to have an airway obstruction were recruited. Airway obstruction was determined by abnormal spirometry, such that the forced expiratory volume in 1 second (FEV1) was less than 80% of the predicted value. Bronchodilator reversibility assessment was performed as a part of the clinical procedure in the outpatient clinic. Spirometry was repeated after the administration of bronchodilation (four puffs of 100 mg salbutamol using a metered dose inhaler via a large volume spacer) to assess the response to bronchodilation. Asthmatic children aged 7-16 were recruited, to ensure their ability to perform spirometry. A group of healthy children of matched ages and genders were recruited. Health is defined as no current or previous diagnosis of respiratory disease.

Children with significant comorbidity or chest wall abnormality, obstructive sleep apnea or any other condition which could affect the study were excluded from the study. Furthermore, the body mass index was restricted to 40kg/m^2.

After consenting, asthmatic children were assessed twice using SLP; the first time once the obstruction was confirmed with the abnormal spirometry, and the second time after the administration of salbutamol and just before repeating spirometry. Healthy children were assessed only once using SLP.

The study was approved by the UK Health Research Authority National Research Ethics Service (reference number 11/EE/00/37) and was performed at the Royal Stoke University Hospital (Stoke-on-Trent, UK) according to International Council for Harmonisation Guidelines for Good Clinical Practice. It is registered on ClinicalTrials.gov as part of a larger evaluation of SLP in individuals aged 2–80 years (NCT02543333). All children were enrolled between March 2014 and June 2015 (Hmeidi *et al.*, 2017).

5.3.2 Study devices and procedures

Tidal breathing trace was recorded using an SLP device for five minutes, and tidal breathing parameters were derived. The following procedure is followed:

- Children were seated in a high-backed chair as far back in the seat as possible and were instructed to be as still as possible.
- A close-fitting white T-shirt was provided by the study sponsor for them to wear during the procedure. Also a research nurse provided a distraction for the children during the scan so that they remained still, breathing as naturally as possible.
- For each subject, the scanner head of the device was positioned at 1 - 1.2 meters from the chest wall, then its height and angle were adjusted by the researcher. These adjustments included fixing the optical axis perpendicularly to the chest wall and the midpoint of the grid located at the base of the child's xiphisternum.
- The grid pattern projected by SLP was altered to accommodate the size of each TA area and to cover an equidistant area above and below the xiphisternum from the clavicles to the anterior iliac crests.
- The size of the grid was chosen to fit the chest size of the child among three different sizes with various numbers of squares (14x10, 12x8 or 10x6) contributing equally to the signal.
- 30 Hz sampling rate was adequate to capture the dynamics of TA wall displacement.

5.3.3 Parameters

Tidal breathing parameters derived from both: TA displacement with time, as well as its derivative, displacement rate with time, were quantified. Other parameters that describe the shape of the displacement loop and regional the parameters were also calculated. Magnitudes and the within-subject variabilities of all these parameters were quantified, for more details about the parameters and the selection criteria see chapter 4.

5.3.4 Statistical Analysis

Power calculations were not carried out prior to the study because this study began as a pilot and no data regarding variability of SLP parameters were known beforehand.

The median value (***m***) and the inter-quartile range IQR (***v***) were calculated for each parameter in each 5 min SLP assessment. To compare the data between healthy children and those with asthma (before administration of a bronchodilator), a Mann-Whitney U test was used, comparing the SLP parameters and their variability. In addition, a Wilcoxon signed-rank test was used to evaluate the effect of a bronchodilator in children with asthma. Differences between the groups and the response to treatment in the asthma group were further assessed using the nonparametric common language effect size (CLES) for the parameters which showed a significant difference. CLES was used to assess the ability of the significant parameters to differentiate between health and asthma or to detect response to treatment. Finally, the correlation between $\boldsymbol{IE50_{SLP}}$ and lung functions measured using a Spearman´s rank correlation Figure 5-3.

5.4 Results

5.4.1 Study population

The children who met the selection criteria and provided evaluable data were 30 asthmatics and 41 healthy children. There were no differences between the asthmatic and the healthy groups in their age (10.7 ± 2.4 and 11.2 ± 3.2 years) respectively, height (145.0 ± 17.4 and 148.0 ± 17.6 cm), or weight (41.4 ± 15.1 and 43.9 ± 17.5 Kg). Males in both groups were 17 (57%) and 21 (51%), respectively. At baseline, there was a clear airway obstruction in the children with asthma (FEV1[% predicted] 68.4±12.5; FEV1/ forced vital capacity [FVC] 69.1±10%).

For the SLP procedure, the success rate is defined as the number of subjects who provided valuable data divided by the total number of eligible subjects, for more details about the main criteria for this decision see chapter four. The success rate for each group was high: asthma 30/32 [93.8%]; healthy: 41/48 [85.4%].

5.4.2 Spirometry

Significant increases in spirometry measures were observed after the administration of bronchodilation, including FEV1, FVC and FEV1 (% predicted). FEV1/FVC (%) also increased significantly after bronchodilator but stayed abnormal (mean=76.1%), showing that airway obstruction was still present (Table 5-1).

Table 5-1. Comparison of spirometry measures in children with asthma (N=41) before and after bronchodilator administration.

	FEV1 (L) mean ± SD	FVC (L) mean ± SD	FEV1/FVC (%) mean ± SD	FEV1(% predicted) mean ± SD
Prebronchodilator	1.62 ± 0.64	2.36 ± 0.89	69.1 ± 10	68.4 ± 12.5
Postbronchodilator	1.93 ± 0.67	2.58 ± 0.94	76.1 ± 9.7	81.2 ± 11.2
Significance*	P < 0.0001	P < 0.01	P < 0.0001	P < 0.0001

(FEV1, forced expiratory volume in 1sec; FVC, forced vital capacity; SD, standard deviation. Significance* tested using a paired t-test.

5.4.3 Tidal breathing parameters' magnitudes and within-subject variabilities

Table 5-2 shows the differences between tidal breathing parameters measured with SLP between healthy children and children with asthma (Prebronchodilator). (*Significant *with P<0.05, ** Significant with P<0.001).*

Table 5-3 shows the differences in the parameters between pre and post-bronchodilator in the asthmatic group.

Those tables show all median SLP-obtained parameters and their within-subject variability. In each SLP assessment, the median number of detected breaths in each SLP scan was 82-86 and did not change significantly in any of the performed comparisons.

A significantly higher inspiratory to expiratory TA displacement-rate ratio (i.e. IE50) and its variability were observed in children with asthma (prebronchodilator) than in healthy children ($mIE50_{SLP}$: 1.53 vs. 1.22, P< 0.001; $vIE50_{SLP}$: 0.63 vs. 0.47, P<0.001) (Hmeidi *et al.*, 2017) (Table 5-2, Figure 5-1). In asthmatic children after bronchodilation, both $mIE50_{SLP}$ and $vIE50_{SLP}$ decreased from 1.53 to 1.45 (P = 0.001) and 0.63 to 0.60 (P = 0.04) respectively (Comparison of tidal breathing parameters measured with SLP between healthy children and children with asthma (prebronchodilator) Figure 5-1). Esven though both values decreased after bronchodilation, they stayed higher than in the healthy group (1.45 vs. 1.22, P <0.001; 0.60 vs. 0.47, P < 0.01) (*Significant *with P<0.05, ** Significant with P<0.001).*

Table 5-3**,** Figure 5-1**,** showing that the obstruction was still present.

Asthmatic children were divided into two subgroups; children who responded to bronchodilation (with a response defined as ≥ 12% increase in FEV1 predicted, n=16 (Papadopoulos *et al.*, 2012)), and children who did not respond to bronchodilation. In the responder subgroup, there was a significant difference in $mIE50_{SLP}$ before and after bronchodilation (P=0.038), while no significant change was observed in the non-responder group (P=0.24).

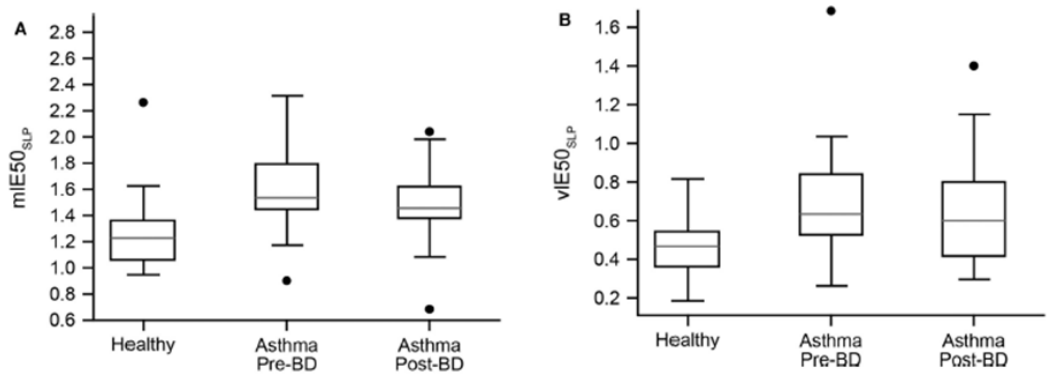

Figure 5-1. Box plots showing $mIE50_{SLP}$(A) and $vIE50_{SLP}$(B) in healthy children and those with asthma (pre- and postbronchodilator).

The grey line indicates the median value, the rectangle spans the IQR, and the black whiskers indicate the minimum and maximum values (excluding the outliners indicated by the black circles). BD, bronchodilator; $IE50_{SLP}$, thoracoabdominal (TA) inspiratory displacement rate at 50% of inspiratory displacement divided by TA expiratory displacement rate at 50% of expiratory displacement; IQR, interquartile range; m, median; v, variability (Hmeidi *et al.*, 2016, p.7) .

Table 5-2. Comparison of tidal breathing parameters measured with SLP between healthy children and children with asthma (prebronchodilator).

	Healthy children (N = 41)		**Children with asthma (Prebronchodilator) (N = 30)**			
	Median	IQR	Median	IQR	z-stat	Significance (*MWU* test)
Timing indices and ratios						
mRR (brpm)	19.89	7.58	20.34	5.73	0.5	0.62
vRR (brpm)	3.32	2.2	3.93	2.57	1.48	0.14
mtI (sec)	1.33	0.46	1.18	0.2	-1.9	0.06
vtI (sec)	0.27	0.17	0.24	0.14	-1.61	0.11
mtE (sec)	1.63	0.64	1.7	0.47	0.43	0.67
vtE (sec)	0.39	0.21	0.44	0.35	1.53	0.13
mtTot (sec)	3.02	1.13	2.95	0.83	-0.49	0.62
vtTot (sec)	0.53	0.32	0.56	0.44	0.72	0.47
mtI/tE	**0.82**	**0.16**	**0.69**	**0.1**	**-3.6**	**<0.001****
vtI/tE	0.22	0.1	0.2	0.11	-0.36	0.72
mtI/tTot	**0.45**	**0.05**	**0.41**	**0.04**	**-3.61**	**<0.001****
vtI/tTot	0.06	0.03	0.07	0.03	0.95	0.34
Displacement with time-derived parameters						
$mtPTEF_{SLP}/tE$	0.35	0.09	0.31	0.09	-1.81	0.07
$vtPTEF_{SLP}/tE$	**0.18**	**0.1**	**0.21**	**0.11**	**2.22**	**0.03***
$mtPTIF_{SLP}/tI$	0.5	0.09	0.54	0.09	1.58	0.11
$vtPTIF_{SLP}/tI$	0.21	0.07	0.21	0.05	-0.08	0.94
$mIE50_{SLP}$	**1.22**	**0.29**	**1.53**	**0.35**	**4.71**	**<0.001****
$vIE50_{SLP}$	**0.47**	**0.18**	**0.63**	**0.32**	**4.45**	**<0.001****
Regional Parameters (Phase and relative contribution)						
mrCT(%)	41.96	20.04	39.18	11.3	-1.16	0.25
vrCT(%)	7.62	6.52	9.53	8.03	1.01	0.31
mHTA (deg.)	3.21	1.7	3.29	1.54	0.3	0.77
vHTA (deg.)	3.76	2.55	3.96	2.28	0.79	0.43
mTAA (deg.)	11.19	9.92	11.89	8.71	0.29	0.78
vTAA (deg.)	10.55	9.67	12.67	9.48	0.77	0.44
No. of Breaths	82	26.25	84	22	0.45	0.65

(*Significant with P<0.05, ** Significant with P<0.001).

Table 5-3. Comparison of tidal breathing parameters measured with SLP in children with asthma before and after bronchodilator administration.

	Children with asthma (Prebronchodilator) (N = 30)		**Children with asthma (Postbronchodilator) (N = 30)**			
	Median	IQR	Median	IQR	z-stat	Significance (Signed-rank test)
Timing indices and ratios						
mRR (brpm)	20.34	5.73	22.16	5.91	-0.93	0.35
vRR (brpm)	3.93	2.57	4.62	2.34	-1.12	0.26
mtI (sec)	1.18	0.2	1.13	0.3	-0.85	0.40
vtI (sec)	0.24	0.14	0.23	0.1	-0.46	0.65
mtE (sec)	1.7	0.47	1.6	0.43	-1.31	0.19
vtE (sec)	0.44	0.35	0.43	0.21	-0.52	0.60
mtTot (sec)	2.95	0.83	2.71	0.77	-1.2	0.23
vtTot (sec)	0.56	0.44	0.6	0.28	-0.18	0.85
mtI/tE	0.69	0.1	0.69	0.12	-0.92	0.36
vtI/tE	0.2	0.11	0.21	0.09	-0.03	0.98
mtI/tTot	0.41	0.04	0.41	0.04	-0.89	0.37
vtI/tTot	0.07	0.03	0.07	0.03	-0.48	0.63
Displacement with time-derived parameters						
$mtPTEF_{SLP}/tE$	0.31	0.09	0.29	0.14	-0.57	0.57
$vtPTEF_{SLP}/tE$	0.21	0.11	0.19	0.12	-1.39	0.16
$mtPTIF_{SLP}/tI$	0.54	0.09	0.54	0.09	-0.66	0.51
$vtPTIF_{SLP}/tI$	0.21	0.05	0.19	0.09	-0.75	0.45
$mIE50_{SLP}$	**1.53**	**0.35**	**1.45**	**0.24**	**-2.44**	**0.01***
$vIE50_{SLP}$	**0.63**	**0.32**	**0.6**	**0.38**	**-2.05**	**0.04***
Regional Parameters (Phase and relative contribution)						
mrCT(%)	39.18	11.3	39.11	12.8	-0.34	0.73
vrCT(%)	9.53	8.03	8.02	7.66	-1.61	0.11
mHTA (deg.)	3.29	1.54	3.05	1.26	-1.8	0.07
vHTA (deg.)	3.96	2.28	3.79	1.39	-1.24	0.21
mTAA (deg.)	11.89	8.71	11.73	11.44	-0.05	0.96
vTAA (deg.)	12.67	9.48	11.9	9.92	-1	0.32
No. of Breaths	84	22	86	32	-0.34	0.73

(*Significant with $P<0.05$).

There are other parameters which were different between children with asthma and healthy children, but they do not show a significant change after bronchodilation. Before bronchodilation, the ratios of inspiratory to expiratory time and inspiratory to total breath time were significantly lower in children with asthma (mtI/tE, P<0.001, mtI/tTot, P<0.001). The variability in the normalised time taken to reach peak tidal expiratory TA displacement rate was significantly higher ($vtPTEF_{SLP}/tE$, P=0.03) (Table 5-2, Figure 5-2). After the administration of bronchodilation, both mtI/tE and mtI/tTot stayed significantly lower in the asthmatic group, whereas the difference in $vtPTEF_{SLP}/tE$ between both groups was no longer present (P=0.51) (Table 5-4).

Table 5-4. Comparison of tidal parameters measured with SLP between healthy children and children with asthma (postbronchodilator).

	Healthy children (N = 41)		**Children with asthma (Postbronchodilator) (N = 30)**			
	Median	IQR	Median	IQR	z-stat	Significance (MWU test)
$mIE50_{SLP}$	**1.22**	**0.29**	**1.45**	**0.24**	**4.02**	**<0.001*** **
$vIE50_{SLP}$	**0.47**	**0.18**	**0.6**	**0.38**	**2.96**	**<0.01** **
mtI/tE	**0.82**	**0.16**	**0.69**	**0.12**	**-3.09**	**<0.01** **
mtI/tTot	**0.45**	**0.05**	**0.41**	**0.04**	**-3.09**	**<0.01** **
$vtPTEF_{SLP}/tE$	0.18	0.1	0.19	0.12	0.65	0.51
No. of Breaths	82	26.25	86	32	0.68	0.50

(**Significant with P<0.01,*** Significant with P<0.001).

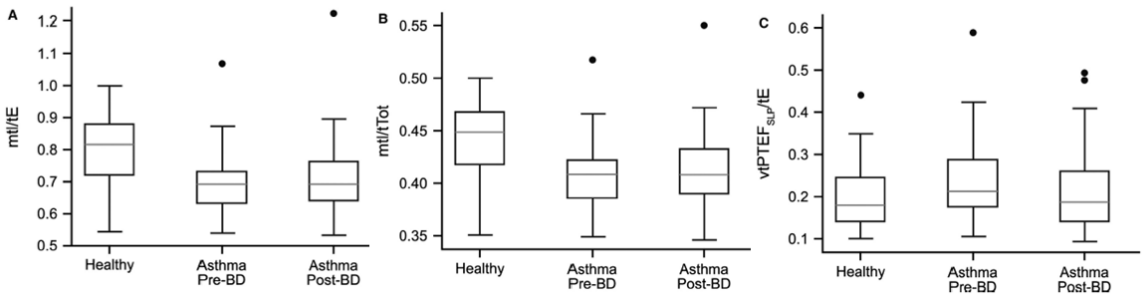

Figure 5-2 Box plots showing mtI/tE(A), mtI/tTot(B), $vtPTEF_{SLP}/tE$(C) in healthy children and in those with asthma (pre- and postbronchodilator).

The grey line indicates the median value, the rectangle spans the IQR, and the black whiskers indicate the minimum and maximum values (excluding the outliners indicated by the black circles). BD, bronchodilator; IQR, interquartile range; m, median; tE, expiratory time; tI, inspiratory time; $tPTEF_{SLP}$, time to reach peak tidal expiratory thoraco-abdominal displacement rate; tTot, total breath time; v, variability (Hmeidi *et al.*, 2017, p.9).

Also, as it is shown in Table 5-5, CLES evaluation showed that SLP parameters which were significantly different between healthy children and children with asthma could differentiate between both groups with high sensitivity, particularly IE50 and its variability (CLES: 82.9% and 81.1%, respectively). In the same way, bronchodilator effects could be detected in children with asthma in most of the cases but not as accurate as the spirometry-obtained outcomes (FEV1 and FEV1/FVC)

Table 5-5. CLES evaluation of SLP and spirometry-obtained breathing parameters.

Hypothesis	CLES (%)	Interpretation
Healthy versus children with asthma[1]		
mtI/tE: lower in asthma group	75.2	In 75.2% of cases, mtI/tE was lower in asthma group
mtI/tTot: lower in asthma group	75.3	In 75.3% of cases, mtI/tTot was lower in asthma group
VtPTEF/tE: higher in asthma group	65.5	In 65.5% of cases, vtPTEF/tE was higher in asthma group
$mIE50_{SLP}$: higher in asthma group	82.9	In 82.9% of cases, $mIE50_{SLP}$ was higher in asthma group
$vIE50_{SLP}$: higher in asthma group	81.1	In 81.1% of cases, $vIE50_{SLP}$ was higher in asthma group
Pre- versus post-BD[2] (children with asthma)		
FEV1: increases after BD	100.0	FEV1 was increased in all patients after BD
FEV1/FVC: increases after BD	86.7	In 86.7% of casas, FEV1/FVC increased after BD
$mIE50_{SLP}$: reduced after BD	70.0	In 70.0% of casas, $mIE50_{SLP}$ reduced after BD
$vIE50_{SLP}$: reduced after BD	73.3	In 73.3% of casas, $vIE50_{SLP}$ reduced after BD

Median and IQR values for parameters are denoted by the prefix m and v respectively.
BD: bronchodilator; CLES: common language effect size; FEV1: forced expiratory volume in 1 sec; FVC: forced vital capacity; $IE50_{SLP}$: TA inspiratory displacement rate at 50% of inspiratory displacement divided by TA expiratory displacement rate at 50% of expiratory displacement; IQR: interquartile range; tE: expiratory time; tI: inspiratory time; tTot: total breath time; $tPTEF_{SLP}$: time to reach peak tidal expiratory TA displacement rate.
[1]Data are shown for parameters that significantly differed between healthy children and children with asthma (prebronchodilator) only (see Table 5-2). Note spirometry data were not available for healthy subjects and hence only effect sizes for SLP parameters are given.

[2]Data are shown for parameters that significantly differed following bronchodilator administration in children with asthma only (See Table 5-3) (*Significant with *P<0.05,* ** *Significant with P<0.001).*

Furthermore, a Spearman's rank correlation was carried out between $mIE50_{SLP}$ and spirometry parameters in children with asthma (prebronchodilator). The correlations between ***$mIE50_{SLP}$*** and both ***FEV1*** (% predicted) and FEV1/FVC were (-0.49, P=0.0054) (Figure 5-3) and (-0.38, P=0.034), respectively. No correlation in these parameters was found after bronchodilation. The correlation between $mIE50_{SLP}$ and FEV1 (% predicted) stayed significant after bronchodilation in the responded asthmatic subgroup (i.e. exhibited ≥ 12% increase in FEV1%; P=0.016), but for those who did not respond was not significant (P=0.25). Finally, the correlation between $mIE50_{SLP}$ and FEV1/FVC was not significant post bronchodilation in any of the subgroups, responder (P=0.08) or non-responder (P=0.11).

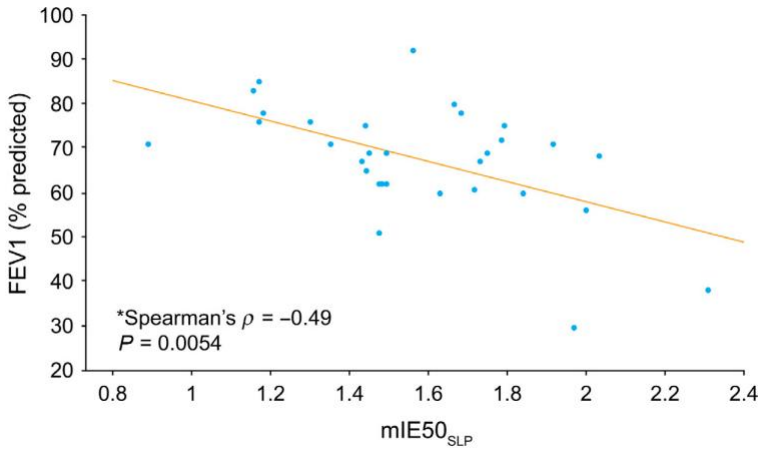

Figure 5-3. Correlation between $mIE50_{SLP}$ and FEV1 (% predicted) in children with asthma (prebronchodilator)
(Hmeidi *et al.*, 2017, p.10)

5.5 Discussion

As noted by Weissman *et al.*, 1984; Caretti *et al.*, 1994; Laveneziana *et al.*, 2015a, measuring tidal breathing has some restrictions which limit its use. This study aimed to investigate the use of SLP, as a non-invasive, non-contact technique for measuring tidal breathing, to differentiate children with asthma from healthy children, and to assess its sensitivity in detecting response to bronchodilation in the asthmatic group.

From the results, it is shown that some SLP parameters can differentiate between healthy participants and children with asthma, particularly the inspiratory to expiratory TA displacement rate ratio ($mIE50_{SLP}$) and its within-subject variability ($vIE50_{SLP}$) which have distinguished healthy children from those with asthma and indicated a response to bronchodilation. This parameter is comparable to IE50 which defines the ratio of inspiratory to expiratory flow at 50% of tidal volume (H. Hmeidi *et al.*, 2017). These two SLP parameters have shown promising results, being sensitive enough to detect a response to bronchodilation in a non-invasive assessment, however not as sensitive as spirometry measure (FEV1).

Previous studies have shown that during an acute asthma attack, there is an increase in airway resistance and indices of expiratory flow, such as FEV1, FEV1/FVC, peak expiratory flow and TEF50 decreases (Papiris *et al.*, 2001). The reduction in TEF50 was shown in various studies with patients similar to the asthmatics in this study.

For example, Tauber *et al.* (2003) in his study using a negative expiratory pressure technique, has shown that TEF50 is lower in asthmatic children visiting outpatient clinic for a routine check than healthy children. As $IE50_{SLP}$ is the ratio between $TIF50_{SLP}/TEF50_{SLP}$, an obstruction-related reduction in $TEF50_{SLP}$ will cause an increase in $IE50_{SLP}$. Tauber in his study showed that the decrease in airway resistance post bronchodilation improved expiratory flow (Tauber *et al.*, 2003). In our study, the increase in $TEF50_{SLP}$ after bronchodilation did not return it to normal. As a result, the drop in $mIE50_{SLP}$ did not bring it to the level found in healthy children. This might indicate incomplete airway obstruction reversibility. In addition, $mIE50_{SLP}$ was found to be higher in chronic obstructive pulmonary disease (COPD) patients compared to healthy subjects (Motamedi-Fakhr, Wilson and Iles, 2017).

It is known that breathing patterns are not constant, allowing speech and tasks unrelated to gas exchanged to occur (Brack, Jubran and Tobin, 2002). In this study, IQR for all parameters was calculated for each SLP assessment, as a measure of within-subject variability, and showed that $vIE50_{SLP}$ was significantly higher in children with asthma than healthy children. It has been reported previously that obstructive lung disease such as asthma can affect the variability of tidal breathing. In a study by (Kuratomi *et al.*, 1985), tidal volume variability was measured using electrical impedance pneumography in healthy adults and adults experiencing an exacerbation of asthma, and it was shown that the asthmatic group have a significantly higher tidal volume variability than the healthy group and that the variability was reduced to normal after treatment. However, in this study, $vIE50_{SLP}$ decreased after bronchodilation but did not come back to normal. Within-subject variability in $vtPTEF_{SLP}/tE$ was also higher in children with asthma before treatment than in controls. Even though $vtPTEF_{SLP}/tE$ did not change significantly after bronchodilation, there was no longer a significant difference between the asthmatics after bronchodilation and controls, indicating some decrease in within-subject variability.

Furthermore, regional parameters did not show significant differences in this study. The relative contribution of the thorax to each breath (rCT) was similar in healthy children and patients with asthma, and no effect after bronchodilation was observed. This was also demonstrated by (Motamedi-Fakhr, Wilson and Iles, 2017), where no difference on rCT was detected between COPD patients and healthy subjects using SLP. However, in a previous study on patients with COPD, a reduction in rCT after bronchodilation was reported (Laveneziana *et al.*, 2015a).

Different TA regions' movement with respect to each other, is described by phase parameters. The synchronization between the abdomen and thorax during tidal breathing is often disturbed in children with acute asthma, when the movement of the abdomen supersedes the movement of the thorax. In this study, patients attended a routine outpatient clinic, and were not in an acute condition, and thus, they were not likely to show asynchrony.

In the next chapter, the effect of acute asthma exacerbation and treatment on SLP parameters is investigated, which include regional and temporal parameters such as rCT, TAA and left-right hemithoracic asynchrony.

The use of SLP in the measurement of tidal breathing has several advantages over current methods for assessing tidal breathing (i.e. Pneumotachography and RIP), mainly the non-invasive and the contactless nature of the test. The participant should remain as still as possible during the test to avoid any interference being introduced to the signal, even though previous work has shown that children as young as three years of age could be measured (Hmeidi *et al.*, 2015). Also, it should be known that some slight tracking errors which are non-breathing related, could be detected and excluded from the data.

In this study, because many statistical comparisons were made, and there is a risk of some statistically significant result to appear by chance, the Bonferroni correction method was used. Dividing the P-Value by the number of comparisons results in $P<0.002$ (0.05/24). This method, however, assumes that all the parameters are independent, which is not the case in many SLP-measured parameters and may, therefore, be very conservative. Some differences between these parameters have a physiological basis and supported by previous researches. CLES calculation further supported those findings.

The use of spirometry was a prerequisite for recruitment in this study to confirm the existence of airway obstruction and its changes after treatment. Hence, younger subjects who might benefit the most from SLP were not included, because they are not able to perform spirometry. This cohort of children is considered in the next chapter.

5.6 Conclusions

This study has demonstrated that SLP which is a non-contact and non-invasive technique to measure tidal breathing, can (1) be successfully utilized in children as young as 7 years of age, and (2) distinguish between children with and without airway obstruction and detect responses to bronchodilator.

6 Tidal breathing parameters in Children recovering from acute asthma

The work reported in this chapter has been published in Physiological Reports ISSN 2051-817X, with the title “Tidal breathing parameters measured by structured light plethysmography in children aged 2-12 years recovering from acute asthma/wheeze compared with healthy children” by (Hmeidi *et al.*, 2018). Permission was obtained from the publisher to reuse relevant aspects of this work in this thesis (i.e. figures, plots and tables).

6.1 Introduction

An accurate assessment of lung function is crucial to effectively manage respiratory conditions such as asthma (Beydon *et al.*, 2007; Wijngaart, Roukema and Merkus, 2015).

Even though spirometry is considered the gold standard, it is often inappropriate to use in younger children because the test involves forced breathing manoeuvres which children might be unable to perform (Wijngaart, Roukema and Merkus, 2015). Measuring tidal breathing patterns is a different approach to assess breathing. Pneumotachography (PNT) and respiratory inductive plethysmography (RIP) are used for this purpose, and both can be utilized in children (J. H. Bates *et al.*, 2000; Stick *et al.*, 1992). The clinical use of those techniques is limited due to some practical drawbacks, such as individuals tending to change their breathing patterns due to the use of a mouthpiece in PNT, and the movement of the transducer bands in RIP can result in erroneous readings (Stick *et al.*, 1992; Caretti *et al.*, 1994; Laveneziana *et al.*, 2015a). In literature, the quantified tidal breathing parameters were not consistent. Thus, there is a lack of agreement in identifying which are the important parameter(s) to be investigated in the presence of respiratory disease (Kuratomi *et al.*, 1985; Brack, Jubran and Tobin, 2002; Schmalisch, Wilitzki and Wauer, 2005).

This is an observational cohort study, which aimed to compare SLP-estimated parameters between: (1) healthy and acute asthma/wheeze participants (2-12 years); (2) pre and post intervention for the Asthma group; (3) younger children (aged 2–5 years), who cannot perform spirometry with older children (aged 6–12 years).

6.2 Materials and Methods

6.2.1 Participants

Children (2–12 years) recovering from an acute exacerbation of asthma (wheezes in those without a formal asthma diagnosis) were recruited for this study. Children with this condition receive regularly inhaled bronchodilators with the repetition depending on the severity of the condition as a part of standard care. Within the first three days of admission, children were recruited as they were in the recovery phase of an attack, on a treatment frequency of 3-hourly or longer regular salbutamol. All children were considered clinically stable, based on the on-duty clinician's opinion, before taking part in the study.

SLP-parameters from the asthma group were compared with those from a group of age-matched healthy children without a diagnosis of any respiratory condition.

Children were excluded from the study if they had significant co-morbidity or chest wall abnormality, obstructive sleep apnea, a body mass index >40 kg/m^2, any acute or chronic condition that restricted his/her ability to take part. Children were also excluded if they were not able to comply with the protocol.

6.2.2 Study design

Once well enough, asthma/wheeze children underwent two five-minute SLP assessments. The first one was performed 5-10 minutes before the administration of bronchodilation, which was given routinely once clinicians determined its need. Children had received different numbers of bronchodilator treatments before this according to their condition. The second SLP assessment was performed 10-15 minutes post bronchodilation. Healthy children underwent one SLP assessment. A research nurse provided a distraction method (cartoon played on a tablet computer) in order to keep the subjects as still as possible.

The study (ClinicalTrials.gov identifier: NCT02543333) was conducted in line with International Conference on Harmonisation Good Clinical Practice guidelines and was approved by the UK Health Research Authority National Research Ethics Service (reference number 11/EE/00/37). Parents or guardians provided written informed consent.

6.2.3 SLP procedure and data analysis

Tidal breathing was measured using an SLP device on the bedside. To ensure data were as artefact-free as possible, the criteria presented in chapter four were used to define and exclude artefacts.

6.2.4 Statistical Analysis

This study was conducted parallel to the stable asthma study. Thus, no power calculations were performed before this study because these are the first data reported using SLP in young children. prefix ‘m’ represents parameter’s magnitude and ‘v’ its within-subject variability. For each group parameter’s magnitude and variability are represented using median and IQR.

A Mann-Whitney-U test was used to compare each ‘m’ and ‘v’ parameter in healthy children and those with acute asthma/wheeze (both before and after bronchodilator administration). A robust two-way ANOVA was utilised to test for significant interactions between these effects and age (Kloke and Mckean, 2012).

To assess the effect of bronchodilator in asthma/wheeze group, a paired Wilcoxon signed-rank (WSR) was utilised. Mann-Whitney-U test of the differences (post – pre-bronchodilator) was used to compare these effects in younger and older children. Common Language Effect Size (CLES) was used to assess the ability of SLP parameters to differentiate between children with asthma/wheeze and healthy children. It was also used to evaluate the effect of bronchodilator for the parameters that have shown significant differences. “CLES is the probability that a score sampled from one distribution will be higher than a score from another distribution” (Björgvinsson and Kerr, 1995, p. 151). CLES is easily interpreted, and it is robust against the deviation from normality assumption. Thus, an important measure in clinical research (Björgvinsson and Kerr, 1995).

No corrections were made to p-values for the multiple tests done because this was an exploratory study.

6.3 Results

Thirty-nine children with acute asthma/wheeze (26 with a formal diagnosis of asthma, 13 with no formal diagnosis) in addition to 54 age-matched healthy controls were eligible for this study and provided valuable data for the analysis.

Figure 6-1 and Table 6-1 show the similarity in demographics between the study groups. The success rate of SLP procedure was 87.8% which is defined as the number of measurements which have provided evaluable data divided by the total number of measurement done (137/156).

The success rate according to age differed such that: in older participants (aged 6–12 years inclusive) was 93.7% (59/63), and in the younger pre-school participants (aged 2–5 years inclusive) was 83.9% (78/93). The excluded data was because of their poor quality resulted from either excessive movement, light or creases in the t-shirt (See 4.3.3).

Numerous parameters have shown significant differences between healthy controls and children recovering from an acute exacerbation of asthma/wheeze (before bronchodilator administration) Table 6-5.

Table 6-2. Of the timing parameters, mRR was significantly higher in children with asthma (30 vs. 23 brpm; $p<0.001$), while mtI (0.83 vs. 1.13 seconds), mtE (1.14 vs.1.48 seconds), and mtTot (2.00 vs. 2.60 seconds) were significantly lower (all $p<0.001$). Apart from vRR, the within-subject variability in all timing indices and ratios were significantly lower in children with asthma/wheeze than in healthy controls.

Of the flow-based parameters, $vtPTIF_{SLP}/tI$ was significantly lower (0.16 vs. 0.21, $p<0.001$), whereas $mIE50_{SLP}$ was significantly higher in children with asthma/wheeze compared with healthy children (1.47 vs. 1.31, $p=0.002$) Figure 6-2. Both asynchrony parameters (mTAA and mHTA) were significantly higher in children with asthma/wheeze (mTAA: 40.16 vs. 11.88 degrees; mHTA: 5.53 vs. 3.43 degrees; both $p<0.001$), as well as their variabilities (vTAA: 24.08 vs. 13.53 degrees; vHTA, 6.82 vs. 4.58 degrees; both $p<0.001$) Figure 6-3.

mTAA differed significantly between younger and older children with asthma/wheeze (2–5 vs 6-12 years) (interaction $p<0.001$) Table 6-2 showing the age-related effect of asthma. In healthy children, there was a slight decrease in mTAA with age (12.6 to 11.4 degrees for younger and older children, respectively), while in children with asthma/wheeze, mTAA has shown more than 50% reduction from 52.2 in the younger children to 25.1 degrees in the older ones (Figure 6-4).

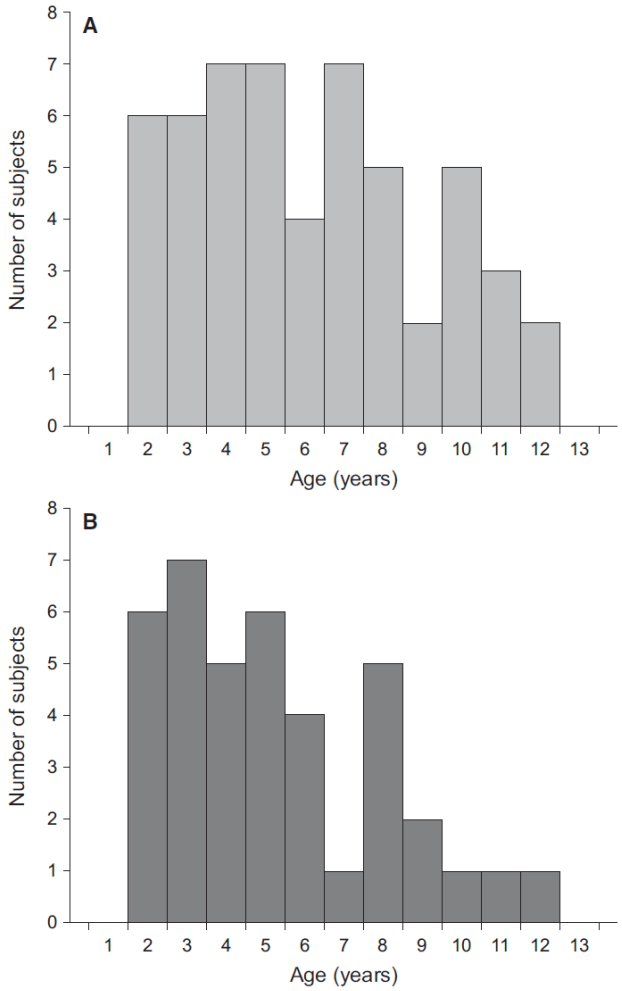

Figure 6-1. Distribution of ages in both groups: (A) Healthy and (B) Acute asthma/wheeze (Hmeidi *et al.*, 2018, p.4).

Table 6-1. Participants demographics from both groups. Data are mean (standard deviation) unless otherwise specified.

	Healthy children (N = 54)	**Children with Acute asthma/wheeze (N = 39)**
Gender (male: female), n	33:21	26:13
Age, years	6.1(2.9)	5.2(2.7)
Age groups (2-5: 6-12 years), n	26:28	24:15
Height, cm	116.5(21.0)	114.1(18.3)

None of the parameters' magnitudes changed significantly after bronchodilation administration for overall asthma/wheeze group (Table 6-3). The within-subject variability of $tPTEF_{SLP}/tE$ was

the only parameter that has shown a change from 0.21 to 0.15 ($p<0.001$) Figure 6-2 (C). When assessed based on age, the effect of bronchodilation varied between the older and the younger cohorts for mrCT, mTAA and vTAA (interaction $p <0.05$). After bronchodilation, mrCT dropped significantly in the younger cohort (interaction $p<0.05$ and WSR $p<0.05$), but increased for most of the individuals in the older cohort (Figure 6-5 A).

Bronchodilation effect was significantly different between the two cohorts for mTAA, such that it decreased in the younger children and increased in the older cohort, although the effects in both cohorts were not significantly different from zero (Figure 6-5 B). Likewise, vTAA has shown a significant decrease after bronchodilation in the younger cohort ($p <0.05$) but did not show any difference in the older children (Figure 6-5 C).

Table 6-4 shows that all the parameters that were significantly different between healthy children and those with asthma/wheeze pre bronchodilation stayed so post bronchodilation. Based on CLES calculations, mtI and mTAA have shown the largest effect in differentiating between healthy children from those with acute asthma/wheeze Table 6-5. The same parameters have also shown the largest effect size in differentiating between both groups post bronchodilation (mtI: 83.4%; mTAA: 81.8%), as well as mRR and mtTot (both 80.2%). Furthermore, bronchodilation effect in children with acute asthma could be detected using within-subject variability of $tPTEF_{SLP}/tE$ (74.4% of cases) Table 6-5.

Table 6-2. SLP-estimated tidal breathing parameters in healthy children versus children with acute asthma/wheeze (before bronchodilator administration).

	Healthy children (N = 54)		**Children with acute asthma/wheeze (before bronchodilator) (N = 39)**				
	Median	IQR	Median	IQR	z-stat	(*MWU* test) P-value	Robust ANOVA) P-value
Timing indices and ratios							
mRR (brpm)	**23.00**	**5.35**	**30.00**	**7.71**	**-4.74**	**<0.001****	0.369
vRR (brpm)	4.52	2.95	4.45	3.16	0.11	0.913	0.761
mtI (sec)	**1.13**	**0.30**	**0.83**	**0.19**	**5.44**	**<0.001****	0.569
vtI (sec)	**0.22**	**0.20**	**0.13**	**0.12**	**3.99**	**<0.001****	0.476
mtE (sec)	**1.48**	**0.40**	**1.14**	**0.43**	**4.10**	**<0.001****	0.888
vtE (sec)	**0.43**	**0.25**	**0.23**	**0.15**	**4.87**	**<0.001****	0.385
mtTot (sec)	**2.60**	**0.64**	**2.00**	**0.57**	**4.74**	**<0.001****	0.727
vtTot (sec)	**0.53**	**0.31**	**0.33**	**0.11**	**4.86**	**<0.001****	1.000
mtI/tE	0.73	0.13	0.70	0.15	1.20	0.229	0.653
vtI/tE	**0.23**	**0.12**	**0.16**	**0.08**	**3.55**	**<0.001****	0.397
mtI/tTot	0.42	0.04	0.41	0.05	1.20	0.229	0.652
vtI/tTot	**0.07**	**0.03**	**0.05**	**0.03**	**3.37**	**0.001***	0.248
Flow-based parameters							
$mtPTEF_{SLP}/tE$	0.34	0.11	0.38	0.18	-1.76	0.079	0.987
$vtPTEF_{SLP}/tE$	0.22	0.10	0.21	0.20	0.14	0.885	0.102
$mtPTIF_{SLP}/tI$	0.55	0.10	0.53	0.06	1.18	0.236	0.248
$vtPTIF_{SLP}/tI$	**0.21**	**0.09**	**0.16**	**0.06**	**4.65**	**<0.001****	0.113
$mIE50_{SLP}$	**1.31**	**0.30**	**1.47**	**0.40**	**-3.13**	**0.002***	0.335
$vIE50_{SLP}$	0.60	0.33	0.56	0.41	1.01	0.313	0.130
Regional Parameters (Phase and relative contribution)							
mrCT(%)	41.01	14.48	42.86	20.69	-0.77	0.439	0.876
vrCT(%)	9.22	6.83	10.13	7.40	-0.60	0.551	0.271
mHTA (deg.)	3.43	2.09	5.53	5.79	-4.47	<0.001**	0.566
vHTA (deg.)	**4.58**	**2.19**	**6.82**	**4.67**	**-3.64**	**<0.001****	0.550
mTAA (deg.)	**11.88**	**9.84**	**40.16**	**43.55**	**-5.41**	**<0.001****	**<0.001****
vTAA (deg.)	**13.53**	**12.97**	**24.08**	**14.71**	**-4.21**	**<0.001****	0.170
No. of Breaths	**81**	**27**	**103**	**35.5**	**-4.11**	**<0.001****	0.269

Significantly different parameters are shown in bold italic (*Significant with P<0.01, ** Significant with P<0.001).

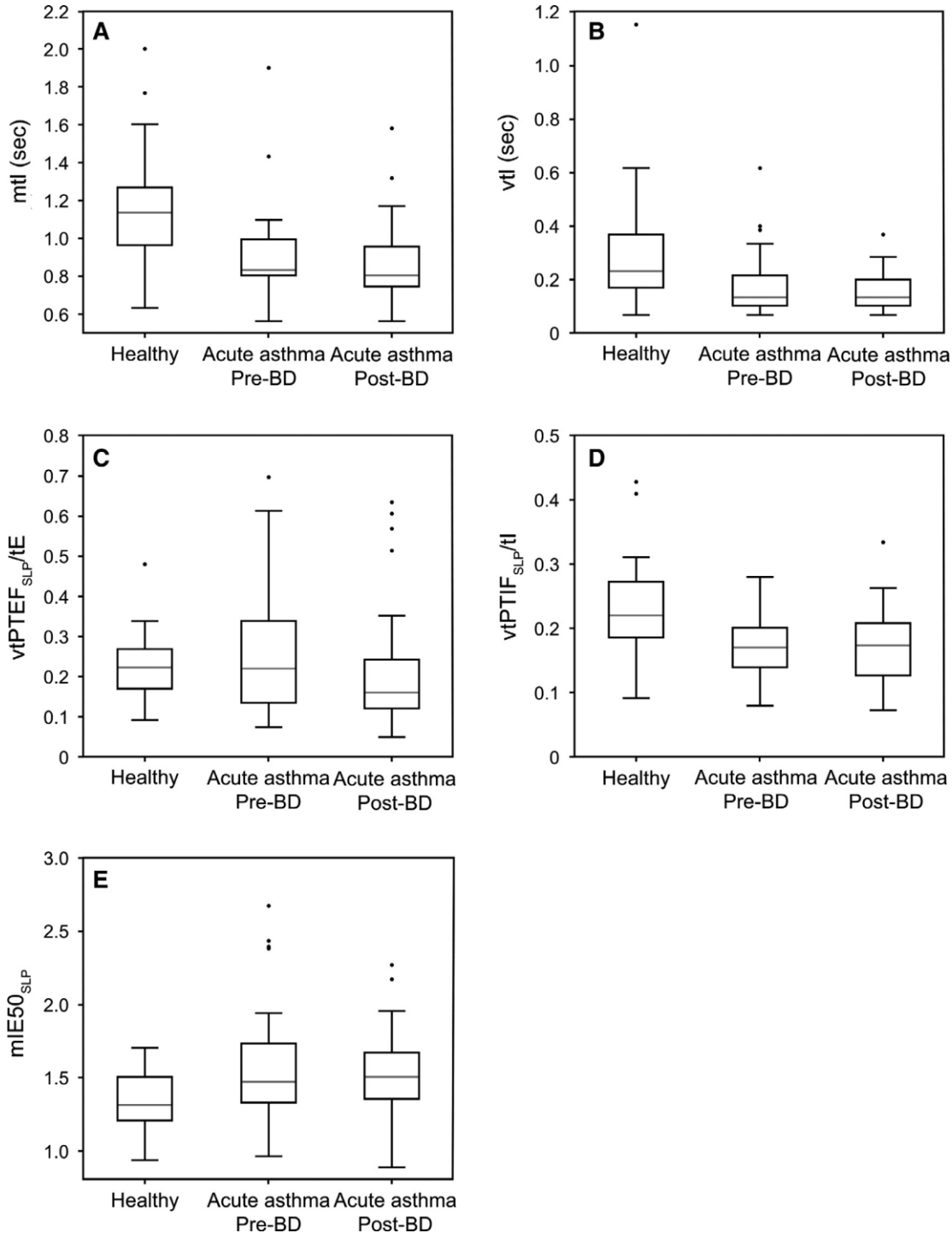

Figure 6-2. Comparison between SLP-estimated parameters in health and acute asthma pre and post-bronchodilation administration.

Two of the timing-based parameters [mtI (A), vtI (B)], and three flow-based parameters [vtPTEF$_{SLP}$/tE (C), vtPTIF$_{SLP}$/tI (D), and mIE50$_{SLP}$ (E)] differed between healthy children and those with asthma/wheeze both pre- and post-bronchodilator administration. The reduction in vtPTEF$_{SLP}$/tE in the children with asthma following bronchodilator administration is also illustrated (C) (Hmeidi et al., 2018, p.6).

6.4 Discussion

In this study, SLP-estimated tidal breathing parameters in children recovering from acute asthma/wheeze (2-12 years) were compared with healthy children of the same age. The effect of bronchodilator administration in the acute asthma group was also investigated, then a secondary analysis was carried out to investigate whether the effect of asthma/wheeze or the effect of bronchodilation varied between younger (aged 2–5 years) and older (aged 6–12 years) children.

In the whole asthma group, median values of seven parameters, and the within-subject variability of eight parameters showed significant differences from healthy children. None of the median values changed after the administration of bronchodilation. However, a reduction in the within-subject variability of one flow-based parameter was observed. The response to bronchodilation in younger children was different than in the older children, with greater changes observed in regional parameters (TAA and rCT).

In the whole group, median $IE50_{SLP}$ was higher in children with acute asthma/wheeze than those in the healthy group. Conventionally, the tidal breathing parameter IE50 is defined as the ratio of inspiratory to expiratory flow at 50% of tidal volume (TIF50/TEF50) (Stick, 1996). Previous studies have shown a reduction in tidal expiratory flow at 50% tidal volume (TEF50) in obstructive airways disorders such as asthma (Totapally et al., 1996; Papiris et al., 2002; Tauber et al., 2003). A drop in TEF50, without a change in TIF50, would increase the ratio between them (IE50) and could justify the higher median $IE50_{SLP}$ observed in this study.

Higher IE50 has been reported in the previous study in children aged 7–16 years with stable asthma (H. Hmeidi *et al.*, 2017) and in adults with COPD (Motamedi-Fakhr, Wilson and Iles, 2017). $IE50_{SLP}$ did not change as a response to bronchodilation administration and stayed higher than in normal although they were in the recovery phase of their disease (considered clinically stable). Contrary to the findings in the previous study in children with stable asthma where $IE50_{SLP}$ dropped significantly following bronchodilation administration. In the previous study, children included were known to have abnormal forced expiratory volume in one second (FEV_1), and that the reduction in $IE50_{SLP}$ after bronchodilation administration was linked with an increase in % predicted FEV_1, showing a bronchodilator response. In this study, however, spirometry was not performed, and thus it was not known if FEV_1 was low prior to bronchodilator treatment. Therefore, it could be that the observed increase in $IE50_{SLP}$ is indicative of the components of airflow obstruction which was not sensitive to bronchodilation, or simply no detectable bronchodilator response occurred.

In the previous study, $IE50_{SLP}$ stayed significantly higher than normal after bronchodilation. The observation in this study might suggest that these children were still experiencing the effect of respiratory exacerbation even though they were considered in the recovery phase of there illness.

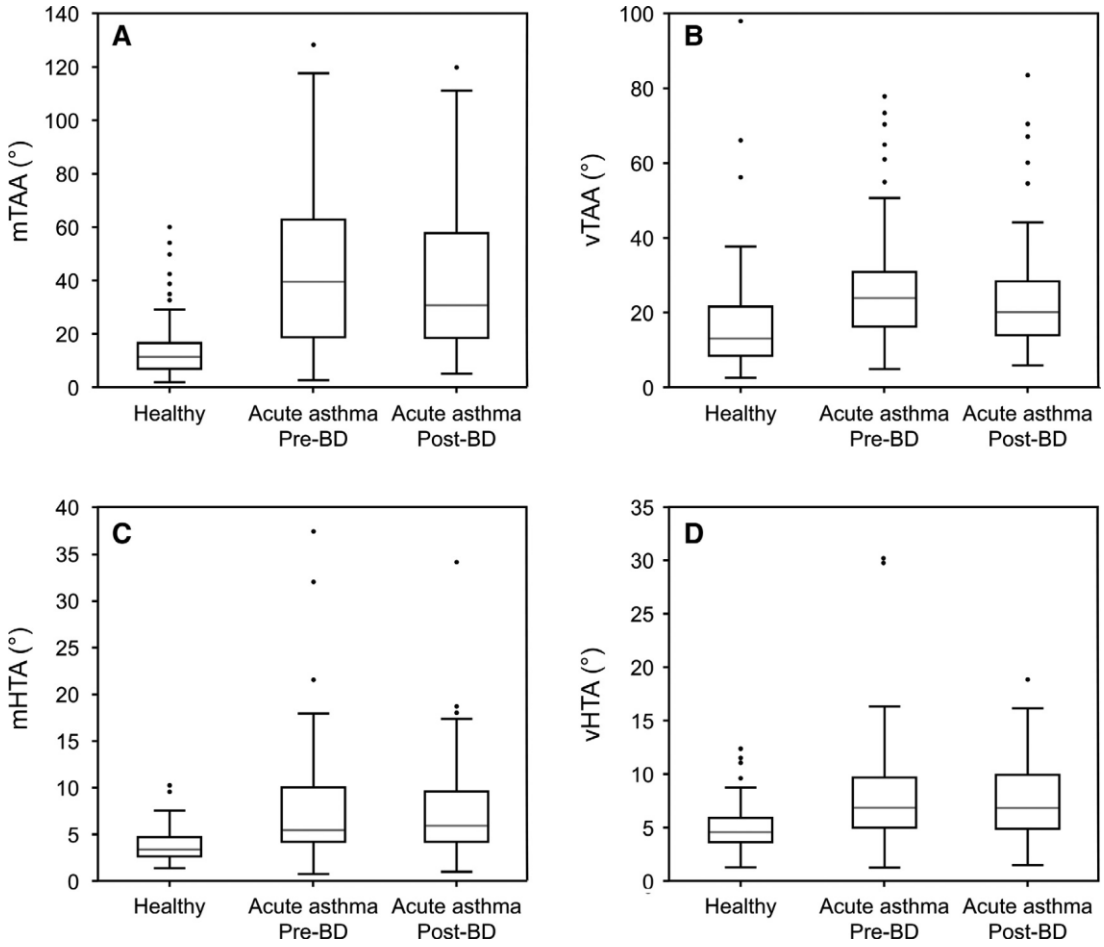

Figure 6-3. Asynchrony parameters mTAA (A), vTAA (B), mHTA (C), and vHTA (D) differences in healthy children compared with those with asthma/wheeze which remained after bronchodilator administration (Hmeidi et al., 2018, p.6).

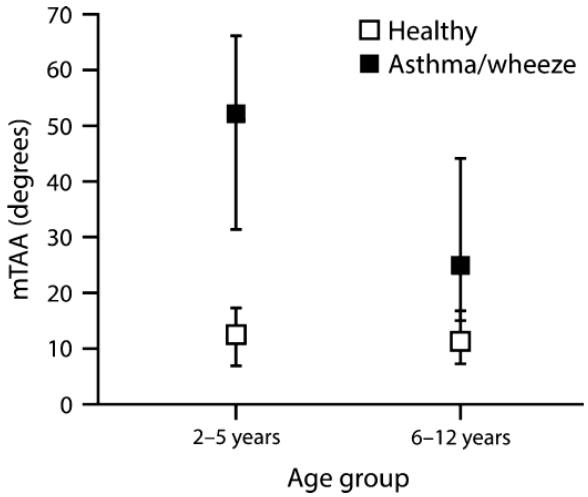

Figure 6-4. mTAA in healthy children and with those with asthma/ wheeze, classified by age groups (Hmeidi *et al.*, 2018)

In other studies, tidal breathing parameters in asthmatic children were returned towards normal after bronchodilation (Kuratomi et al., 1985; van der Ent et al., 1996). Comparing $IE50_{SLP}$ in

the same asthmatic children with and without an exacerbation and during recovery from an exacerbation would be of interest, in order to see whether this variable is sensitive enough to monitor disease activity.

Asynchrony parameters' magnitudes and their within-subject variability for TAA and rCT were significantly higher in the acute asthma/wheeze group than in healthy children. Even though some asynchrony was observed in healthy children (Sivan and Newth, 1990; Newth and Hammer, 2005), generally the thorax and abdomen move in synchrony when no obstructive disease exists. Conversely, the movement of the abdomen precedes that of the thorax with the increase in work of breathing that happens in children with acute asthma, causing a loss of this synchrony (Giordano *et al.*, 2012). Within-subject variability in asynchrony parameters is higher in children with acute asthma (for thorax-abdomen and left-right hemi-thorax), which might suggest a compensatory mechanism such that spatial variability is presented into the system once temporal variability is decreased.

In the stable asthma study, the within-subject variability of asynchrony was not observed when compared with healthy children (Hmeidi *et al.*, 2017) ; however, children in that study were older, therefore, were likely to have reduced chest wall compliance, and thus, less tendency for regional variation. The observation in this study that the effect of asthma/wheeze on TAA was higher in younger children than in older cohort has further supported this effect of age. Asthma effect on HTA or on the within-subject variability in asynchrony parameters has not been previously reported.

Unexpectedly, the variability observed in $tPTIF_{SLP}/tI$ was lower in the asthma group than in normal children, which contradicts with previously reported results. For instance, studies have found that children with asthma have greater variability in airway resistance (Lall *et al.*, 2007). This observation could be attributed to the frequent bronchodilator treatment given to asthmatic children in this study before the test intervention. The reduced variability in $tPTEF_{SLP}/tE$ as a response to bronchodilator treatment, which is in line with the reported airways resistance variations following bronchodilation in both asthmatics and controls (Lall et al., 2007). Similarly, a non-significant decrease in the variation of $tPTEF_{SLP}/tE$ was observed in the stable asthma study as a response to bronchodilation. Furthermore, the difference was seen between healthy and asthmatics (pre-bronchodilator) was no longer noticeable post-bronchodilator, indicating that a drop has happened (H. Hmeidi *et al.*, 2017). No such drop was observed in the variability of $IE50_{SLP}$ following bronchodilation in children with acute asthma/wheeze. A reduction in the variability of airways resistance was higher than that of FEV1 as reported by (Lall et al., 2007). The variability of tPTEF/tE could similarly, be more sensitive to the effects of bronchodilator treatment than the variability of IE50 based on this study's observations, which need to be further investigated.

The effect of bronchodilator treatment was higher on mTAA and vTAA in younger children, who have shown a reduced and less variable asynchrony. Additionally, their breathing became more abdominal as shown by the reduction of mrCT. In the stable asthma study, these

observations were not evident in older children with stable asthma, indicating that it is an age-related effect because of the differences in chest wall compliance.

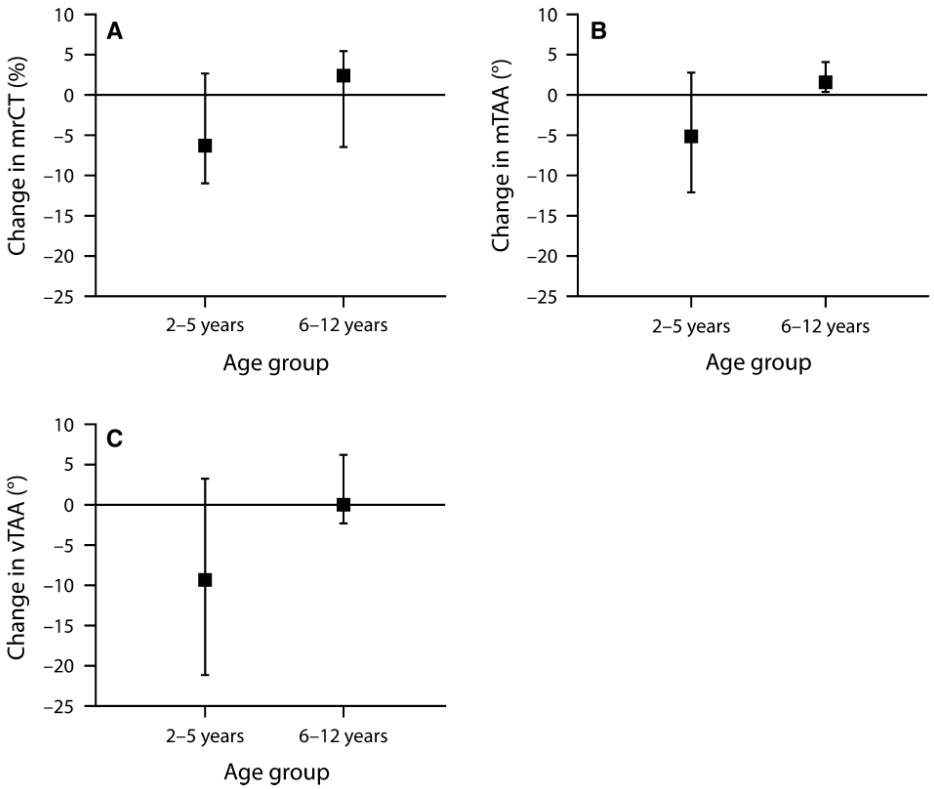

Figure 6-5. Changes in mrCT (A), mTAA (B) and vTAA (C) after bronchodilator administration in children with asthma/wheeze, classified by age group.
Error bars indicate the 25th and 75th percentiles
(Hmeidi et al., 2018, p.9).

Table 6-3. SLP-estimated tidal breathing parameters in children with acute asthma/wheeze before and after bronchodilator administration.

	Children with acute asthma/wheeze (before bronchodilator) (N = 39)		**Children with acute asthma/wheeze (After bronchodilator) (N = 39)**				
	Median	IQR	Median	IQR	z-stat	(*WRS* test) P-value	(MWU test) P-value
Timing indices and ratios							
mRR (brpm)	30.00	7.71	31.03	8.25	-1.56	0.118	0.305
vRR (brpm)	4.45	3.16	4.36	2.85	-0.47	0.635	0.146
mtI (sec)	0.83	0.19	0.80	0.21	1.61	0.108	0.612
vtI (sec)	0.13	0.12	0.13	0.11	0.50	0.619	0.828
mtE (sec)	1.14	0.43	1.13	0.40	1.06	0.290	0.175
vtE (sec)	0.23	0.15	0.25	0.15	-0.82	0.410	0.603
mtTot (sec)	2.00	0.57	1.93	0.59	1.61	0.107	0.363
vtTot (sec)	0.33	0.11	0.32	0.20	-0.30	0.763	0.419
mtI/tE	0.70	0.15	0.70	0.14	1.03	0.301	0.665
vtI/tE	0.16	0.08	0.14	0.06	1.35	0.176	0.283
mtI/tTot	0.41	0.05	0.41	0.05	0.97	0.331	0.707
vtI/tTot	0.05	0.03	0.05	0.02	1.3`	0.190	0.246
Flow-based parameters							
$mtPTEF_{SLP}/tE$	0.38	0.18	0.37	0.14	0.85	0.395	0.679
$vtPTEF_{SLP}/tE$	**0.21**	**0.20**	**0.15**	**0.12**	**3.87**	**<0.001****	0.352
$mtPTIF_{SLP}/tI$	0.53	0.06	0.53	0.06	-1.24	0.213	0.564
$vtPTIF_{SLP}/tI$	0.16	0.06	0.17	0.08	0.10	0.922	0.658
$mIE50_{SLP}$	1.47	0.40	1.50	0.32	0.71	0.477	0.598
$vIE50_{SLP}$	0.56	0.41	0.52	0.37	1.84	0.065	0.309
Regional Parameters (Phase and relative contribution)							
mrCT(%)	42.86	20.69	39.47	19.85	1.95	0.051	**0.041***
vrCT(%)	10.13	7.40	8.98	4.58	1.45	0.147	0.051
mHTA (deg.)	5.53	5.79	5.98	5.33	0.82	0.41	0.338
vHTA (deg.)	6.82	4.67	6.82	5.09	0.03	0.978	0.449
mTAA (deg.)	40.16	43.55	31.08	39.26	0.89	0.372	**0.030***
vTAA (deg.)	24.08	14.71	20.31	14.57	1.41	0.159	**0.020***
No. of Breaths	103	35.5	107	22.8	-1.68	0.094	0.862

Significantly changed parameters are shown in bold italics italic (*Significant with P<0.05, ** Significant with P<0.001).

Patients with acute asthma/wheeze have higher RR than in healthy children in order to compensate for the decreased amount of air inhaled in each breath caused by the airway obstruction (Kesten *et al.*, 1990). In this study, RR was higher in asthmatic children, tTot and its components tI and tE were shorter compared with those of healthy children. Except for RR, all timing indices and ratios have shown a reduced within-subject variability in children with acute asthma/wheeze, which is attributed to the faster RR, restricting variation. Healthy subjects naturally show some variability in tidal breathing parameters (Tobin *et al.*, 1988), which was confirmed in this study. The tendency of normal breathing patterns to change permits the participation of respiratory system in other tasks besides gas exchange, such as speech and coughing (Brack, Jubran and Tobin, 2002). SLP measures a large number of consecutive breaths (mean ≥ 80 breaths per assessment in this study). Thus it is suitable to measure within-subject variability.

SLP is a contactless technique which does not require the use of equipment such as nose clips and face masks, which might affect tidal breathing (Gilbert *et al.*, 1972), and requires minimal cooperation from the subject. This method requires individuals to stay still for five minutes, which is one of the limitations of this method. Consequently, in this study children with acute asthma were not assessed until they were clinically stable. It is possible, therefore, that the study might have missed changes in tidal breathing parameters happening during the exacerbation.

Moreover, as these participants were in the NICU, they were exposed to high or more frequent dosages of bronchdialators. These treatments could have created a carry-over effect, which was sustained during SLP assessment. Consequently, after exposing participants to this study's treatment, SLP's ability to detect response may have been violated.

The risk of some statistically significant results happening by chance, due to the multiple comparisons made in this study was taken into account (Hmeidi *et al.*, 2018). The Bonferroni correction was not applied in this study as it assumes the independence between the comparisons, which is not the case here. Though CLES calculations have supported the initial statistical comparisons, and many of the observed changes in SLP parameters had a firm physiological origin or are confirmed by other studies (Laveneziana *et al.*, 2015b; Motamedi-Fakhr, Wilson and Iles, 2017).

In this study, it is shown that SLP can be successfully utilized in children as young as two years recovering from acute asthma/wheeze. Furthermore, several SLP parameters, specifically $IE50_{SLP}$, RR and asynchrony (both hemi-thoracic and thoraco-abdominal), with the within-subject variability of multiple parameters were different in the acute asthma group. Thus, SLP could offer the clinician ways of distinguishing asthmatic children from their healthy counterparts, and also ways of monitoring recovery.

Table 6-4. SLP-estimated tidal breathing parameters in children with acute asthma/wheeze (after bronchodilator administration) versus healthy children.

	Healthy children (N = 54)		**Children with acute asthma/wheeze (After bronchodilator) (N = 39)**				
	Median	IQR	Median	IQR	*z*-stat	*MWU* test P-value	Robust ANOVA P-value
Timing indices and ratios							
mRR (brpm)	**23.00**	**5.35**	**31.03**	**8.25**	**-5.01**	**<0.001****	0.642
mtI (sec)	**1.13**	**0.30**	**0.8**	**0.21**	**5.67**	**<0.001****	1.000
vtI (sec)	**0.22**	**0.20**	**0.13**	**0.11**	**4.57**	**<0.001****	0.782
mtE (sec)	**1.48**	**0.40**	**1.13**	**0.40**	**4.17**	**<0.001****	0.814
vtE (sec)	**0.43**	**0.25**	**0.25**	**0.15**	**4.72**	**<0.001****	0.195
mtTot (sec)	**2.60**	**0.64**	**1.93**	**0.59**	**5.02**	**<0.001****	0.924
vtTot (sec)	**0.53**	**0.31**	**0.32**	**0.20**	**4.66**	**<0.001****	0.508
vtI/tE	**0.23**	**0.12**	**0.14**	**0.06**	**4.18**	**<0.001****	0.663
vtI/tTot	**0.07**	**0.03**	**0.05**	**0.02**	**4.09**	**<0.001****	0.321
Flow-based parameters							
vtPTIF$_{SLP}$/tI	**0.21**	**0.09**	**0.17**	**0.08**	**4.26**	**<0.001****	0.083
mIE50$_{SLP}$	**1.31**	**0.30**	**1.50**	**0.32**	**-3.26**	**0.001***	0.350
Regional Parameters (Phase and relative contribution)							
mHTA (deg.)	**3.43**	**2.09**	**5.98**	**5.33**	**-4.11**	**<0.001****	0.796
vHTA (deg.)	**4.58**	**2.19**	**6.82**	**5.09**	**-3.29**	**0.001****	0.767
mTAA (deg.)	**11.88**	**9.84**	**31.08**	**39.26**	**-5.21**	**<0.001****	0.054
vTAA (deg.)	**13.53**	**12.97**	**20.31**	**14.57**	**-3.34**	**0.001****	0.682
No. of Breaths	**81**	**27**	**107**	**22.8**	**-5.33**	**<0.001****	0.271

Significantly different parameters are shown in bold italics italic (*Significant with P<0.01, ** Significant with P<0.001).

Table 6-5. CLES evaluation of SLP-estimated tidal breathing parameters.

Hypothesis	CLES (%)	Interpretation
Healthy versus children with asthma (before BD administration)		
mRR: High in asthma group	78.5	In 78.5% of cases, mRR was higher in asthma group
mtI: lower in asthma group	82.1	In 82.1% of cases, mtI was lower in asthma group
vtI: lower in asthma group	73.2	In 73.2% of cases, vtI was lower in asthma group
mtE: lower in asthma group	74.2	In 74.2% of cases, mtE was lower in asthma group
vtE: lower in asthma group	79.2	In 79.2% of cases, vtE was lower in asthma group
mtTot: lower in asthma group	78.5	In 78.5% of cases, mtTot was lower in asthma group
vtTot: lower in asthma group	79.1	In 79.1% of cases, vtTot was lower in asthma group
vtI/tE: lower in asthma group	71.7	In 71.7% of cases, vtI/tE was lower in asthma group
vtI/tTot: lower in asthma group	70.6	In 70.6% of cases, vtI/tTot was lower in asthma group
$vtPTIF_{SLP}$/tI: lower in asthma group	78.4	In 78.4% of cases, $vtPTIF_{SLP}$/tI was lower in asthma group
$mIE50_{SLP}$: higher in asthma group	69.1	In 69.1% of cases, $mIE50_{SLP}$ was higher in asthma group
mHTA: higher in asthma group	77.3	In 77.3% of cases, mHTA was higher in asthma group
vHTA: higher in asthma group	72.2	In 72.2% of cases, vHTA was higher in asthma group
mTAA: higher in asthma group	83.0	In 83.0% of cases, mTAA was higher in asthma group
vTAA: higher in asthma group	75.7	In 75.7% of cases, vTAA was higher in asthma group
Healthy versus children with asthma (after BD administration)		
mRR: High in asthma group	80.2	In 80.2% of cases, mRR was higher in asthma group
mtI: lower in asthma group	83.4	In 83.4% of cases, mtI was lower in asthma group
vtI: lower in asthma group	76.5	In 76.5% of cases, vtI was lower in asthma group
mtE: lower in asthma group	74.9	In 74.9% of cases, mtE was lower in asthma group

vtE: lower in asthma group	78.1	In 78.1% of cases, vtE was lower in asthma group
mtTot: lower in asthma group	80.2	In 80.2% of cases, mtTot was lower in asthma group
vtTot: lower in asthma group	77.9	In 77.9% of cases, vtTot was lower in asthma group
vtI/tE: lower in asthma group	75.5	In 75.5% of cases, vtI/tE was lower in asthma group
vtI/tTot: lower in asthma group	75.0	In 75.0% of cases, vtI/tTot was lower in asthma group
$VtPTEF_{SLP}$/tE: lower in asthma group	64.9	In 64.9% of cases, $VtPTEF_{SLP}$/tE was lower in asthma group
$VtPTIF_{SLP}$/tI: lower in asthma group	76.0	In 76.0% of cases, $VtPTIF_{SLP}$/tI was lower in asthma group
$mIE50_{SLP}$: higher in asthma group	69.9	In 69.9% of cases, $mIE50_{SLP}$ was higher in asthma group
mHTA: higher in asthma group	75.1	In 75.1% of cases, mHTA was higher in asthma group
vHTA: higher in asthma group	70.1	In 70.1% of cases, vHTA was higher in asthma group
mTAA: higher in asthma group	81.8	In 81.8% of cases, mTAA was higher in asthma group
vTAA: higher in asthma group	70.4	In 70.4% of cases, vTAA was higher in asthma group
Before vs. after BD administration (Children with asthma)		
$vtPTEF_{SLP}$/tE: reduced after BD	74.4	In 74.4% of cases, $vtPTEF_{SLP}$/tE decreased after BD

SLP is a useful technique especially for pre-school children, due to the difficulties in assessing airflow obstruction (hence, provide an accurate asthma diagnosis) in this age group. The preliminary results in this study are promising and could support further investigation and improvements in this technique in order to introduce it into routine clinical practice. The effect of age on breathing patterns needs to be further investigated, SLP might introduce a method for assessing lung function in patients who cannot use traditional techniques such as spirometry.

7 Acute Viral Bronchiolitis (AVB) Study

7.1 Introduction

Bronchiolitis is a lower respiratory tract infection, which affects infants usually in their first year of life (Ralston *et al.*, 2014). In most cases, bronchiolitis results from a respiratory syncytial virus (RSV), and symptoms clear up without any treatment. However, some infants develop severe symptoms which make hospitalisation essential (Gajdos *et al.*, 2010). In some cases, bronchiolitis can cause respiratory failure, and the assessment of respiratory muscle function might be clinically useful in these cases even though it has some limitations (Gaultier, 1995). Since existing methods are designed to be used in adults, its use in infants is deemed to be inconvenient.

Most advanced pulmonary function techniques for neonates and infants require sedation and highly trained technicians to perform the tests, which restricts their use to specialised research centres. Thus, the measurements of tidal breathing parameters have been proposed to be an alternative approach to simplify lung function testing in this group (Banovcin, Seidenberg and Von Der Hardt, 1995; Bates *et al.*, 2000).

Many studies have shown the usefulness of the analysis of tidal breathing (such as flow-volume loops) in assessing lung functions in infancy (Lodrup-Carlsen and Carlsen, 1993; Banovcin, Seidenberg and der Hardt, 1995; Carlsen *et al.*, 1995; Frey and Merkus, 2010). In infants, tidal breathing yields more information than in adults, due to the small geometric dimensions of the tracheal tree. Therefore, tidal breathing in infancy is closer to maximal work of breathing, and any additive load during respiratory disease can bring the infant to a forced expiration breathing state (Seddon, Davis and Coates, 1996). Hence, tidal breathing can be very informative for diagnosing different pathologies (Lødrup, 2000).

Gas exchange is usually used to assess the severity of AVB and the effectiveness of different treatments in children who develop respiratory failure and increased work of breathing (WOB) (Greenough, 2009). Remarkably, Limited research has been done investigating respiratory mechanics in infants with severe bronchiolitis under mechanical ventilation (Øymar, Skjerven and Mikalsen, 2014; Ralston *et al.*, 2014).

This study aims to investigate the use of SLP in the assessment of tidal breathing in infants with AVB. Tidal breathing parameters were examined whether they can differentiate between infants with AVB and healthy controls. In addition, changes in tidal breathing parameters between the day of admission and discharge were investigated in the AVB group.

7.2 Materials and methods

7.2.1 Participants

Thirty-four infants diagnosed with AVB (12 female), aged 0-1 year were recruited on admission to the children's assessment unit (CAU) or children's intensive care unit. In the clinician's opinion, all infants were clinically stable, without any immediate danger, to take part in the study. SLP-parameters from the AVB group on admission were compared with those from a

group of 22 healthy infants (16 female) recruited from the maternity department. In this context, healthy is defined as not having any signs of respiratory disease or need for extra oxygen. Four AVB infants were discharged on the same day, and the rest stayed in the hospital for at least two days for observation and were re-assessed using SLP on discharge.

Infants were excluded from the study if they had significant co-morbidity or chest wall abnormality, obstructive sleep apnoea, a body mass index >40 kg/m2, any acute or chronic condition that restricted his/her ability to participate, or they were unable to comply with the protocol.

The study was approved by the UK Health Research Authority National Research Ethics Service (reference number 11/EE/00/37) and was performed at the Royal Stoke University Hospital (Stoke-on-Trent, UK), according to International Council for Harmonisation Guidelines for Good Clinical Practice. Parents or guardian provided written informed consent.

7.2.2 Study design

Infants with AVB underwent two SLP assessments; the first was performed on admission and the last on discharge. Healthy infants underwent one SLP assessment. Each assessment was planned to be for five minutes, but for practicality reasons it was not possible to record the full duration in all infants, as some infants moved or cried during the assessment. A distraction method (sleeping music) was used to keep the subjects as still as possible.

7.2.3 SLP procedure and data analysis

Tidal breathing was measured using an SLP device on the bedside, as previously described in chapter three. The 3D-reconstruction was played and checked to ensure that data were as artefact-free as possible. Visual assessment of the 3D surface is an important step to identify tracking errors such as errors caused by a lack of contrast in the projected grid for more details see 4.3.3.

7.2.4 Statistical Analysis

Power calculations were not performed before this study since this is the first data reported using SLP in infants and data on expected variability were not available. A Mann-Whitney-U test was used to compare each ‘m’ and ‘v’ parameter (4.3.2 for more details) in healthy infant and those with AVB. To assess the differences in clinical measures and tidal breathing parameters between admission and discharge a paired Wilcoxon signed-rank (WSR) was utilised. Common language effect size (CLES) was used to further assess the ability of SLP parameters, which have shown a significant difference to differentiate between the two groups and to detect recovery. No corrections were made to P-values for the multiple tests performed, as this was an exploratory study.

Figure 7-1. SLP assessment on an infant with AVB during sleeping.

7.3 Results

Thirty-four infants with AVB, in addition to 22 healthy controls were eligible for this study and provided valuable data for the analysis. Table 7-1 shows the demographics of both studied groups. The success rate of SLP procedure was 96.6% and was defined as the number of measurements which have provided usable data divided by the total number of measurements performed (86/89). The excluded measurement was because of its poor quality caused by either excessive movement or light.

Many parameters have shown significant differences between healthy controls and infants with AVB (on the admission day) (Table 7-3). Of the timing parameters, none of the parameters' magnitudes has shown a significant difference between infants with AVB and healthy controls. Apart from vtI/tE, the within-subject variability in all timing indices and ratios were significantly lower in infants with AVB than in healthy controls; vRR (9.97 vs. 17.33 brpm; $p<0.001$), vtI (0.13 vs. 0.22 sec; $p<0.01$), vtE (0.17 vs. 0.33 sec; $p<0.001$) and vtI/tTot (0.07 vs. 0.11 sec; $p=0.03$).

Of the flow-based parameters, $vtPTEF_{SLP}/tE$, $mIE50_{SLP}$ and $vIE50_{SLP}$ were significantly lower in the AVB group compared with healthy infants (0.16 vs. 0.27, $p = 0.02$), (1.00 vs. 1.19, $p=0.03$) and (0.48 vs. 0.97, $p<0.001$), respectively. Finally, of the regional parameters, Thoraco-

abdominal asynchrony (TAA) was significantly higher in infants with AVB than in healthy controls (mTAA: 62.13 vs. 16.17 degrees, $p<0.01$).

Thirty infants with AVB were compared between admission and discharge as they were kept in hospital for observation, and four were discharged on the same day. None of the parameters' magnitudes differed significantly between admission and discharge (Table 7-4). The within-subject variability of $IE50_{SLP}$ was the only parameter that has increased as a result of the natural recovery of the condition from 0.48 to 0.62 ($p=0.047$). The increase that occurred was toward the normal value seen in healthy controls (0.97).

Table 7-1. Participants demographics from both groups.

	Healthy infants (N = 22)	**Children with AVB (N=34)**
Gender (male: female), n	6:16	22:12
Age, weeks	8.60 (6.99)	19.29 (14.06)
Length, cm	56.75 (1.20)	62.75 (8.99)

Data are mean (standard deviation).

Table 7-2. Comparison of clinical measures in infants with AVB (N=30) on admission and discharge. Heart Rate; Respiratory Rate; Oxygen saturation.

	Heart Rate (bpm) Median (IQR)	**Respiratory Rate (brpm) Median (IQR)**	**SaO2 (%) Median (IQR)**
Admission day	146.5 (22)	44 (8)	96 (5)
Discharge day	137.5 (18)	40 (6)	96 (2)
p-value*	0.108	<0.01	0.753

Significance* tested using Wilcoxon Signed rank-test.

Table 7-3. Comparison of tidal breathing parameters measured with SLP between healthy children and infants with AVB (Admission).

	Healthy Infants (N = 22)		**Infants with AVB (Admission) (N = 34)**			
	Median	IQR	Median	IQR	z-stat	Significance *(MWU* test*)*
Timing indices and ratios						
mRR (brpm)	50.04	19.45	48.01	19.10	-0.48	0.63
vRR (brpm)	**17.33**	**10.24**	**9.97**	**5.87**	**4.47**	**<0.001****
mtI (sec)	0.55	0.20	0.58	0.27	-0.64	0.52
vtI (sec)	**0.22**	**0.33**	**0.13**	**0.13**	**3.09**	**<0.01***
mtE (sec)	0.62	0.27	0.62	0.30	0.65	0.52
vtE (sec)	**0.33**	**0.35**	**0.17**	**0.11**	**3.41**	**<0.001****
mtTot (sec)	1.20	0.57	1.25	0.47	0.48	0.63
vtTot (sec)	**0.54**	**0.57**	**0.20**	**0.17**	**3.73**	**<0.01****
mtI/tE	0.88	0.09	0.93	0.19	-1.89	0.06
vtI/tE	0.43	0.45	0.29	0.31	1.48	0.14
mtI/tTot	0.47	0.02	0.48	0.05	-1.89	0.06
vtI/tTot	**0.11**	**0.11**	**0.07**	**0.07**	**2.30**	**0.03***
Flow-based parameters						
$mtPTEF_{SLP}/tE$	0.41	0.08	0.45	0.35	-0.84	0.40
$vtPTEF_{SLP}/tE$	**0.27**	**0.14**	**0.16**	**0.13**	**2.27**	**0.02***
$mtPTIF_{SLP}/tI$	0.47	0.10	0.47	0.16	-0.65	0.52
$vtPTIF_{SLP}/tI$	0.24	0.17	0.14	0.21	1.05	0.29
$mIE50_{SLP}$	**1.19**	**0.25**	**1.00**	**0.48**	**2.17**	**0.03***
$vIE50_{SLP}$	**0.97**	**0.64**	**0.48**	**0.38**	**3.70**	**<0.001****
Regional Parameters (Phase and relative contribution)						
mrCT(%)	62.59	18.74	57.39	37.24	-0.16	0.87
vrCT(%)	17.06	9.00	17.49	13.26	-0.39	0.69
mTAA (deg.)	**16.17**	**30.87**	**62.13**	**97.54**	**-3.08**	**<0.01***
vTAA (deg.)	29.44	26.87	27.13	29.31	0.60	0.55
No. of Breaths	75	63	79	72	0.63	0.53

(*Significant with P<0.05, ** Significant with P<0.001).

Table 7-4. Comparison of tidal breathing parameters measured with SLP in infants with AVB on admission and discharge.

	Infants with AVB (Admission) (N = 30)		**Infants with AVB (Discharge) (N = 30)**			
	Median	IQR	Median	IQR	z-stat	WSR test P-value
Timing indices and ratios						
mRR (brpm)	48.01	19.10	48.65	15.21	-0.47	0.64
vRR (brpm)	9.93	5.72	9.80	7.94	-0.52	0.60
mtI (sec)	0.57	0.27	0.53	0.17	-1.708	0.09
vtI (sec)	0.13	0.09	0.10	0.13	-0.05	0.96
mtE (sec)	0.62	0.27	0.62	0.27	-0.42	0.67
vtE (sec)	0.17	0.09	0.16	0.13	-0.62	0.54
mtTot (sec)	1.25	0.47	1.23	0.37	-0.62	0.54
vtTot (sec)	0.20	0.17	0.22	0.17	-0.54	0.59
mtI/tE	0.93	0.19	0.89	0.24	-1.870	0.06
vtI/tE	0.29	0.27	0.29	0.30	-0.05	0.96
mtI/tTot	0.48	0.05	0.47	0.07	-1.85	0.06
vtI/tTot	0.07	0.07	0.09	0.08	-0.55	0.59
Flow-based parameters						
$mtPTEF_{SLP}/tE$	0.45	0.37	0.41	0.23	-1.08	0.28
$vtPTEF_{SLP}/tE$	0.16	0.12	0.25	0.18	-1.80	-0.07
$mtPTIF_{SLP}/tI$	0.47	0.18	0.45	0.10	-0.94	0.35
$vtPTIF_{SLP}/tI$	0.14	0.21	0.15	0.19	-0.30	0.77
$mIE50_{SLP}$	0.96	0.45	1.06	0.30	-0.59	0.56
$vIE50_{SLP}$	**0.48**	**0.38**	**0.62**	**0.49**	**-1.96**	**0.047***
Regional Parameters (Phase and relative contribution)						
mrCT(%)	56.21	37.24	61.00	25.34	-0.50	0.61
vrCT(%)	17.49	13.75	17.55	11.76	-0.44	0.66
mTAA (deg.)	62.13	104.43	53.15	103.77	-0.52	0.60
vTAA (deg.)	28.76	29.46	24.48	26.91	-0.40	0.69
No. of Breaths	79	72	61.50	68	-0.23	0.82

(*Significant with $P<0.05$).

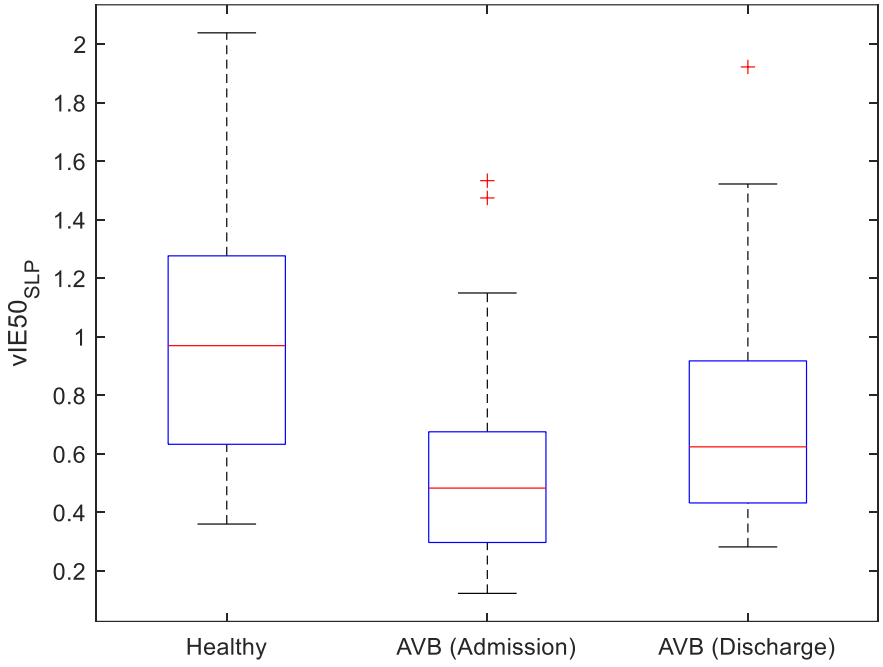

Figure 7-2. $vIE50_{SLP}$ differed in healthy infants compared with those with AVB at admission and discharge.

7.4 Discussion

In this study, SLP-estimated tidal breathing parameters in infants recovering from acute viral bronchiolitis were compared with healthy infants. Differences in the parameters between admission and discharge were studied in the AVB group.

Median values of two parameters and the within-subject variability of seven parameters have shown significant differences from healthy infants. As a part of the normal regulatory mechanism of breathing, the within-subject variability is expected to be higher in healthy infants. Because of the load on the respiratory system caused by airways obstruction in the AVB group, the system becomes more rigid resulting in a drop in the within-subject variability. This is in line with the findings of this study that the within-subject variability of $IE50_{SLP}$ has shown a significant increase on discharge.

In our previous study comparing asthmatic children (7-16 years) with healthy controls, $IE50_{SLP}$ was significantly higher in the asthmatic group. Similarly, $IE50_{SLP}$ was higher in children with asthma/wheeze (2-12 years) compared to healthy controls. The increase in $IE50_{SLP}$ was attributed to the drop in $TEF50_{SLP}$ caused by airways obstruction. The physiology of bronchiolitis suggests lower airways obstruction caused by the secretion of mucus in the airways, and as such, its value was expected to be higher in infants with AVB. Median $IE50_{SLP}$

was lower in infants with AVB than in the healthy infants, and the reduction is caused by a reduced $TIF50_{SLP}$ compared to $TEF50_{SLP}$. This could be attributed to either (1) the higher effect of AVB on the inspiratory part than on the expiratory part of breathing or (2) the natural age-related differences in $IE50_{SLP}$ components, knowing that patients with AVB were relatively older than their healthy counterparts 19.29 (14.06) vs. 8.60 (6.99). This contradiction with what was previously reported about $IE50_{SLP}$ changes in airways obstruction needs to be further investigated.

TAA was significantly higher in the AVB group than in healthy infants. Some degree of thoraco-abdominal asynchrony was observed in healthy infants (Sivan and Newth, 1990; Newth and Hammer, 2005), but generally, thorax and abdomen move in synchrony in the absence of an airways obstruction. In AVB infants, the increased work of breathing caused by airways obstruction could disturb this synchronization (Giordano *et al.*, 2012).

The variability observed in tPTEF/tE was lower in infants with AVB than in healthy infants, which is in line with the results reported in previous studies on infants and children with airways obstruction (Morris and Lane, 1981; Lødrup, 2000; Latzin *et al.*, 2009).

In this study, $vIE50_{SLP}$ was the only parameter that was sensitive to recovery, but contrary to the finding in the stable asthma group, $vIE50_{SLP}$ has significantly increased toward normal value on discharge compared to admission. Even though, the value did not reach the normal level. CLES have shown that $vIE50_{SLP}$ have increased in 70.0 % of the cases on discharge. The recovery was confirmed by the drop of both heart rate and respiratory rate (**P=0.01**), and the stabilized SaO2 level.

Although the Bonferroni correction was not applied in this study, CLES have supported the multiple comparisons performed. Furthermore, many of the observed differences and changes in SLP parameters were confirmed by previous studies.

In this study, it is shown that SLP can be successfully utilised in infants (< 1 year), recovering from AVB. Numerous SLP parameters, specifically thoraco-abdominal asynchrony (TAA), with the within-subject variability of timing indices and ratios, were different in the AVB group and hence, could offer the clinicians ways of differentiating infants with AVB from their healthy counterparts, and also ways to monitor recovery.

The preliminary results and the success rate in this study are promising and could support further investigations in infants with AVB prior the administration of Oxygen (and pre/post different interventions).

Table 7-5. CLES evaluation of SLP-estimated tidal breathing parameters which have shown significant differences.

Hypothesis	CLES (%)	Interpretation
Healthy versus infants with AVB (Admission)		
vRR: Higher in AVB group	85.7	85.7% of cases, mRR was higher in AVB group
vtI: lower in AVB group	74.6	74.6% of cases, vtI was lower in AVB group
vtE: lower in AVB group	77.1	77.1% of cases, vtE was lower in AVB group
vtTot: lower in AVBgroup	79.8	79.8% of cases, vtTot was lower in AVB group
vtI/tTot: lower in AVB group	67.9	67.9% of cases, vtI/tTot was lower in AVB group
$vtPTEF_{SLP}$/tE: lower in AVB group	67.4	67.4% of cases, $vtPTEF_{SLP}$/tE was lower in AVB group
$mIE50_{SLP}$: lower in AVB group	79.6	79.6% of cases, $mIE50_{SLP}$ was lower in AVB group
$vIE50_{SLP}$: lower in AVB group	68.2	68.2% of cases, $vIE50_{SLP}$ was lower in AVB group
mTAA: higher in AVB group	74.6	74.6% of cases, mTAA was higher in AVB group
Admission vs. discharge (infants with AVB)		
$vIE50_{SLP}$: increased on discharge	70.0	In 70.0% of cases, $vIE50_{SLP}$ increased on discharge

7.5 Conclusion

SLP procedure can be successfully conducted in infants as young as one week of age, and that SLP-estimated tidal breathing parameters can differentiate between infants with AVB and healthy infants and can also identify recovery. Further research to confirm these observations needs to be conducted. It would be very interesting to demonstrate the use of SLP with AVB infants who are not clinically stable. However, upon arrival to the hospital, infants with AVB are in a critical medical condition that requires an immediate medical intervention to stabilise their condition. A study of this nature must be carefully designed to overcome this major ethical issue.

8 Investigating the effect of upper-body movements and coughs on SLP quantified parameters

8.1 Introduction

Any signal produced from a medical or biological source is called a bio-signal, those signals could be at different levels from the molecular to the systemic or organ levels (Muthuswamy, 2003).

Bio-signals are considered as combinations of noise and signal of interest, one of the main goals of signal processing is to remove noise components and preserve the components of the signal of interest, a step called signal filtering (Blinowska and Zygierewicz, 2012).

For example, an electroencephalogram (EEG) is the electrical activity in the human brain and is usually recorded from the scalp. The EEG signal may be contaminated by the electrical activity of muscles such as those around the eye or the heart (ECG) and the powerline interference (50-60 Hz). The main goal of signal processing is to selectively remove irrelevant information from the signals in order to make the information of interest more easily available and usable by a human or computer (Delgutte, 2007). More specifically, SLP uses reflected light to track the movement of TA region of patients, which requires them to be in a still position throughout the assessment. However, this is not always achievable due to either the duration of the assessment or the ability of a child to follow instructions. Thus, upper-body movements and coughs were commonly observed during an SLP assessment.

In a typical biomedical application, signal processing consists of four steps: data acquisition, signal conditioning, feature extraction, and decision making.

The goal of data acquisition is to record the signal in a form suitable for computer processing; the second step is signal conditioning, which aims mainly to remove extraneous components from the recorded signal. In the feature extraction stage, a number of parameters are quantified which describe the signal of interest. Finally, the hypothesis testing and decision making stage is of great importance in clinical applications as it may involve diagnosis decisions and medical interventions (Kayvan and Splinter, 2012).

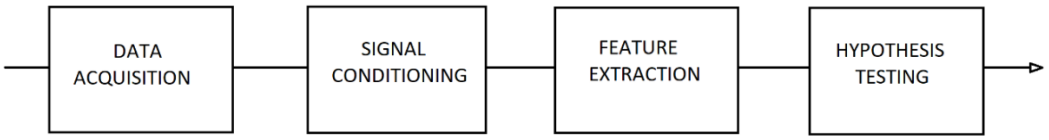

Figure 8-1. Biomedical signal processing steps:
Data Acquisition, signal conditioning (filtering), feature extraction and finally hypothesis testing.

Biomedical signals are used clinically for monitoring specific pathological or physiological states, which could be used for diagnosis or the assessment of a clinical intervention.

Digital Signal Processing (DSP) offers numerous powerful tools which could be applicable for each specific type of noise. Therefore, the purpose of this chapter is to investigate the SLP

signal and the interferences that might be introduced to it, mainly upper-body movements and coughs. Some fundamental signal processing concepts are introduced, that can be utilised to understand the nature of the SLP signal and noise. This study aimed to propose an algorithm that can identify and remove those artefacts and improve SLP-parameters estimation.

Prior to choosing the appropriate DSP method, we need to understand the frequency spectrum in relation to the signal-of-interest and noise. Such that, if the frequency spectra of signal-of-interest and noise do not overlap, with enough frequency-separation between them, then filtering could be used to reduce the noise. Another condition is the use of specific features, of either signal-of-interest or noise, to differentiate between them if their spectra overlap (Davis, 2002).

The most commonly observed artefacts during SLP signal data acquisition is upper-body movements. SLP cameras capture TA-wall movements, and patients are instructed to sit as still as possible during the data acquisition, but even a small upper-body movements might be detected by SLP and could affect SLP parameters estimation, this problem is more likely to happen in younger children who are the subjects of our studies. In addition, one of the main symptoms of asthma is a chronic cough, which might also occur during SLP data acquisition.

In this study, one type of upper-body movement (forward-backwards from the camera) is studied. This type of movements was studied due to its direct impact on the SLP recording, in where the forward-backwards TA wall movement is the signal of interest during breathing. The limited duration of this study and the diversity of movements restricted further investigations of more complex movements. The chosen movement is not a comprehensive representation of the effect of upper-body movement on SLP signal, but it provides an idea about the specific features of this artefact and allows us to investigate possible methods to remove it.

Different filtering techniques used in filtering biomedical signals are discussed in this chapter, and an experiment was designed to assess the effect of those two types of artefact on SLP outcomes. The effect was assessed by quantifying the agreement between tidal breathing parameters measured using a simultaneous SLP and Pneumotachograph (PNT) recordings, considering PNT signal as the gold standard in measuring tidal breathing parameters.

Frequency components of breathing and artefacts were investigated using continuous wavelet transformation (CWT). CWT has shown a clear overlap in frequency spectra between breathing and upper-body movements. Thus, spectral subtraction method was used in an attempt to remove upper-body movements without affecting the breathing signal. However, as coughs are considered rejected breaths, they were removed from the time series. The removal was done using a statistical approach (which will be discussed later in this chapter), whilst taking into considerations coughs' specific features, such as a high amplitude or short duration. In addition, removal of both coughs and upper-body movements was assessed to test the removal's effect on the estimated parameters.

By viewing the video of the 3D-reconstructed surface, movements or coughs could usually be identified as sudden deviations. This approach cannot be used in clinical settings, where quick diagnostic or therapeutic decisions are needed.

This study aimed to: (1) identify the optimal SLP recording time in an ideal SLP session-still position, (2) investigate the effect of upper-body movements and coughs on SLP-estimated tidal breathing parameters, and (3) assess the effect of using different techniques in removing these artefacts on the estimated parameters.

8.2 Digital Filters

Digital filters are widely used in the studies of major systems of the body such as electrograms of hearing, blood pressure and flow, and nerve action potentials (Challis and Kitney, 1982)

Digital filters are used to achieve two main goals: either separating combined signals or restoring distorted signals (Smith, 1997). The properties of these filters and their uses are described briefly in this section.

Signal separation is required when the signal is combined with another signal or artefact, such as the signal acquired from a device measuring ECG of an infant in the mother's uterus, the signal will be contaminated with the heartbeat of the mother, filtering is used in this case to separate the two signals. Whereas signal restoration is used when the captured signal is distorted, such as the deblurring of an ultrasound image acquired with an unstable probe.

Filter characteristics for every linear filter are shown in Figure 8-2; those parameters can best describe its properties; impulse response, step response and frequency response. The most straightforward way to apply a digital filter is by using the convolution between the input signal and the digital filter's impulse response (Smith, 1997).

The step response shows how the information characterised in the time domain is being changed by the system, while the frequency response shows how information characterised in the frequency domain is being changed. There is a trade-off between the time domain and frequency domain performances, where if a good performance in the time domain is required, a poor performance in the frequency domain will be obtained, and vice versa. Hence, designing a digital filter is an application dependent (Smith, 1997).

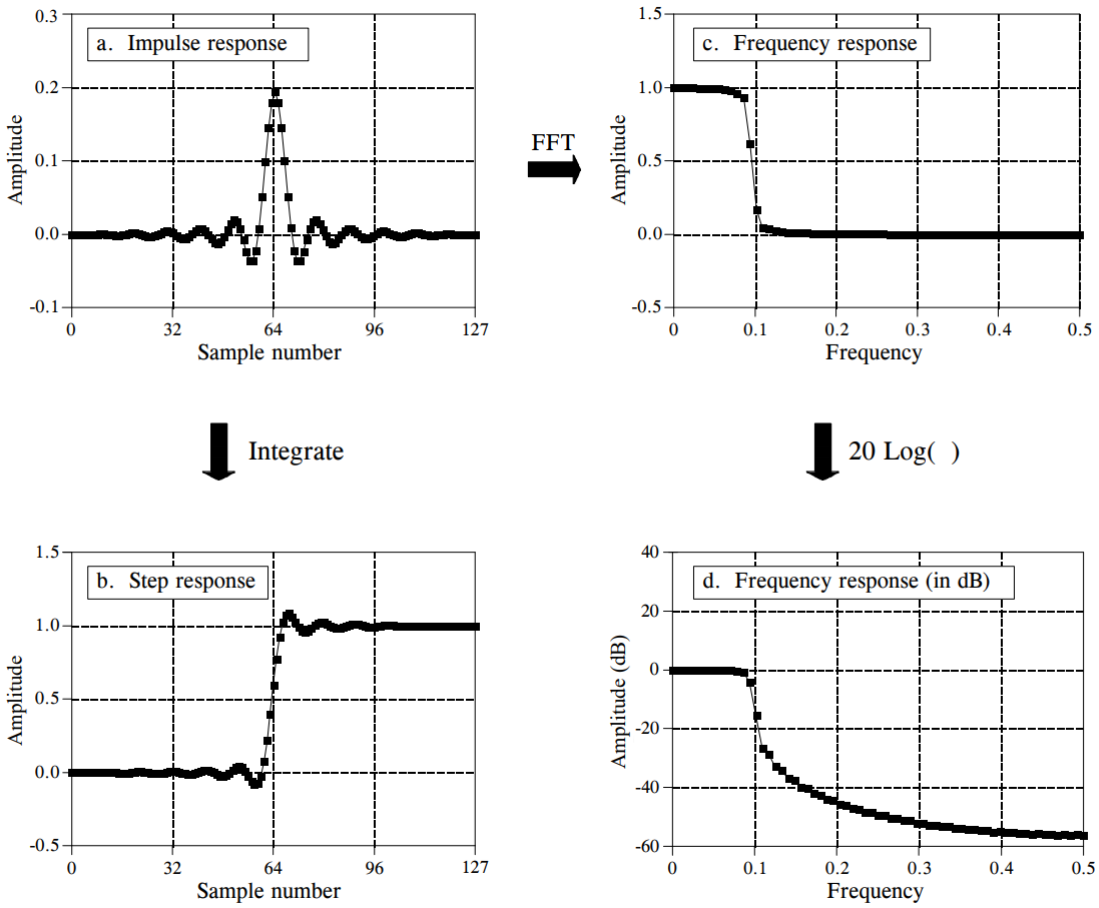

Figure 8-2. Filter characteristics.
(a) Linear filter's impulse response, (b) step response which is the discrete integration of the impulse response, (c) Linear frequency response which is the Fast Fourier Transform (FFT) of the impulse response, (d) Frequency response in decibels. The linear scale is best at showing the passband ripple and roll-off, while the decibel scale is best for showing the stopband attenuation (Smith, 1997).

8.2.1 Frequency Domain Parameters

In frequency-domain filters, the main goal is to let some frequencies pass through unchanged while stopping other frequencies (Smith, 1997). Figure 8-3 shows the four commonly used frequency responses with the main parameters which determine the performance of the filter in the frequency domain. Firstly, the passband denotes the frequencies which are accepted, the stopband refers to the frequencies which are rejected, and the transition band is the band that connects them. The cut-off frequency is the frequency between the passband and the transition band, it is usually defined as the frequency where the amplitude is reduced to 70.7%, and finally, the roll-off describes the width of the transition band (Smith, 1997).

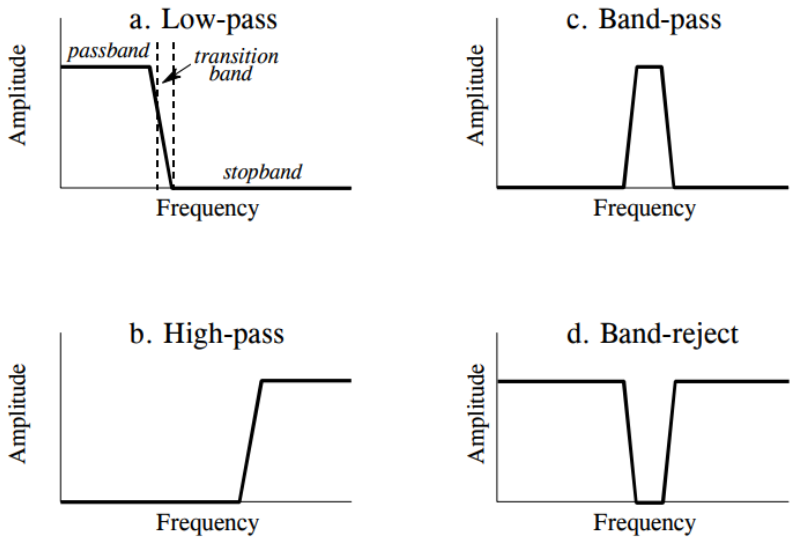

Figure 8-3. The Four common filter types (frequency responses).
(a) low-pass,(b) high-pass, (c) band-pass, and (d) band-reject (Smith, 1997) (permission obtained from the author).

To obtain good filter performance, the passband should be free of ripples to pass the frequencies in that band unchanged. Moreover, the stopband should have a good attenuation, to sufficiently stop the frequencies in that band. Furthermore, if the passed and the stopped frequencies are close, a fast roll-off is needed or in other words a narrow transition band (Smith, 1997).

8.3 Discrete Fourier Transform (DFT)

Discrete Fourier transform is the transform which is used to transform a discrete input signal into its sinusoidal components. Usually, input signals which enter DFT are in the time domain as they are sampled at even periods of time, it can also refer to any discrete signal to be analysed. There are mainly two types of DFT transforms, real and complex transforms. Numerous ways to calculate the DFT exist, with the Fast Fourier Transform (FFT) algorithm being the most effective for calculating the complex DFT (Smith, 1997).

In real DFT, an N point input signal is decomposed into two N/2+1 point signals in the frequency domain, N is any positive integer of power 2, i.e., 128, 256, 512, etc. The two signals in the frequency domain are the real and the imaginary parts, which represent the amplitudes of the cosine and sine waves, respectively (Smith, 1997). In the complex DFT, two N point time domain signals are transformed into two N point frequency domain signals. Each domain contains a real and an imaginary part.

In order to calculate the real DFT for an N point signal using the complex transform (e.g. FFT algorithm), first, the N point signal is filled into the time domain's real part of the Complex DFT, and the imaginary part samples are set to zero. The output of the complex DFT is real and

imaginary signals in the frequency domain, each containing N points. The real DFT is the samples from 0 to N/2 of those signals.

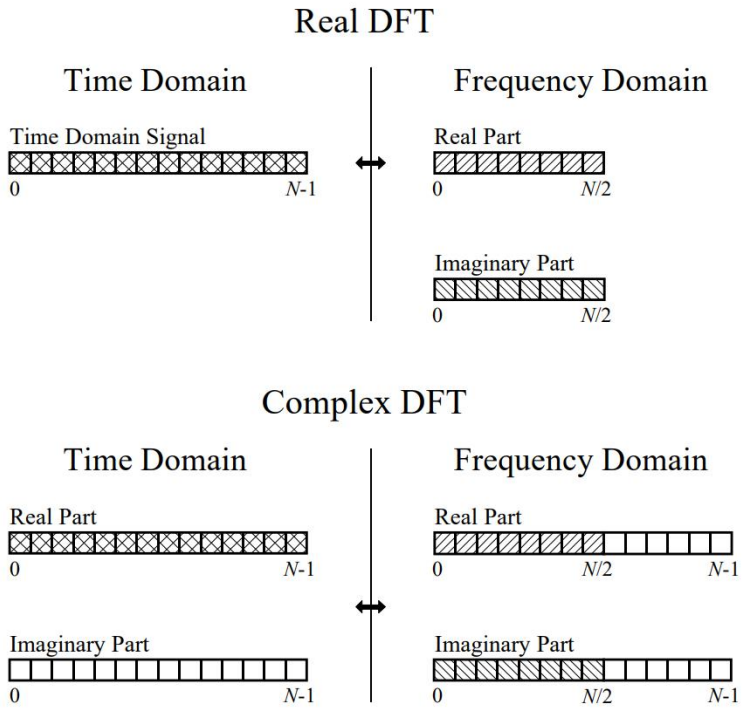

Figure 8-4. Real and complex DFT.
In Real DFT an N point time domain signal is transformed into N/2+1 point signals in the frequency domain, whereas the complex DFT creates two N point signals in the frequency domain from two N point time domain signals. Changing from time-Domain to frequency-Domain is referred to as Forward DFT, while the transformation from Frequency-Domain to time-Domain is called Inverse DFT (Smith, 1997).

The information in both time and the frequency domains are identical but represented in different forms, so that the data can be looked at in different ways. This has the advantage that some signal-related information which is not revealed in the time domain, could be easily discovered in the frequency domain.

Fourier transform is the conventional analytical tool used for frequency domain analysis. However, Fourier transform assumes the stationarity of the signal (which means that its frequency content is not changing with time); thus, it is not an adequate method to analyse non-stationary physiological signals, as FFT does not provide any time resolution. To overcome this shortcoming in Fourier transform, Short-Time Fourier transform (STFT), was introduced wherein a time series is windowed into smaller parts of fixed length, then the Fourier transform is calculated for each smaller part, this allows the reveal of time information about the spectral content of the signal (Polikar, 1994).

STFT allowed for the analysis of signals with time-varying spectra. However, it cannot be used to determine activities at different time scales because of the fixed window size in its definition. Wavelet transformation is a multi-scaled signal analysis tool, which was developed to overcome this deficiency in STFT. SLP signals, like most biomedical signals, are non-stationary. Moreover, transient changes which may interfere with SLP signals such as upper-body movements and coughing can happen at any time during data acquisition; this requires a solid tool to be able to represent those changes and reveal time-amplitude information. Thus, wavelet transformation was employed here to analyse SLP signals, for a better understanding of the signal and the artefacts.

8.4 Wavelet Transformation

8.4.1 Introduction

Wavelet transformation is a linear process in which a signal is analysed into a different resolution components (Sahambi, Tandon and Bhatt, 1997). Wavelet analysis has been developed in the past decades as a robust tool for the multiscale representation of signals. This technique has the advantage over the traditional Fourier techniques by the way it represent the information content of signals (Unser and Aldroubi, 1996).

Wavelet transformation possesses the capability of providing information on both the time and frequency simultaneously, hence portraying the time-frequency representation of the signal, which make it a convenient tool for analysing non-stationary signals (Polikar, 1994). Physiological signals contain non-stationary features such as drifting, abrupt changes, and starting and ending of events, those features are sometimes of big importance to understand (Shoeb and Clifford, 2006; Sorkhabi, 2014); hence, wavelet could give information on a specific spectral component occurring at any interval. This can be of particular interest in biomedical applications, for instance, EEG measures the time lapse between a stimulus to the brain and the response to it. Hence, the knowledge on time intervals of occurrence of a specific frequency can help in acquiring more information from the EEG. Wavelet transforms help in gaining this knowledge.

Wavelet analysis incorporates a multi-resolution analysis of the signal (Liu, 2010). This concept analyses different frequencies with different resolutions. The multi-resolution analysis is formulated to yield good time resolution and poor frequency resolution in the case of high frequencies and provide good frequency resolution and poor time resolution in the event of low frequencies. This concept is highly appropriate in practical scenarios which are characterized by the occurrence of high frequencies for short durations and the existence of low frequencies for long time periods.

In this chapter, a brief explanation of wavelets and the main equations to clarify the concept are given. More about the mathematics behind the concept can be found in (Burrus, Gopinath and Guo, 1998).

8.4.2 Continuous-time Wavelet Transformation (CWT)

Similar to STFT, continuous wavelet transform uses a window function to obtain signal segments. In CWT the window is called a wavelet function but rather than being only translated over the input signal, it is also scaled (dilated and contracted), which allows capturing different time scale events (Polikar, 1994; Shoeb and Clifford, 2006). Equation 8-1 shows the continuous-time wavelet transform of signal $x(t)$:

$$C(s,\tau) = \int_{-\infty}^{\infty} x(t)\psi_{s,\tau}\, dt \qquad \text{Equation 8-1}$$

Where:

$$\psi_{s,\tau}(t) = \frac{1}{\sqrt{s}}\psi\left(\frac{t-\tau}{s}\right) \qquad \text{Equation 8-2}$$

The analysis function ψ , also called the mother wavelet is moved in time by τ, and scaled by s , then correlated with the input signal $x(t)$. A scalogram is created which describes the strength of correlations between $x(t)$ and s scaled ψ at a specific time τ, this correlation quantifies the degree of similarity between $x(t)$ and ψ over time.

τ is related to the location of the window, as it is shifted throughout the signal, while s is a scale parameter and is related to frequency. The multiplication of $\frac{1}{\sqrt{s}}$ is for energy normalization purposes.

Wavelet transformation has solved the resolution problem encountered in STFT, by changing the time and frequency resolutions at different scales. This is achieved by contracting and dilating the mother wavelet which reveals short and long time-scale events Figure 8-5 shows that short time-scale events such as spikes are emphasised in the upper end of the plot, whereas the long time-scale events such as a baseline oscillation are emphasised in the bottom end of the plot (Shoeb and Clifford, 2006). This offers the potential of time-localizing the prompt changes in the SLP signal caused by the artefacts.

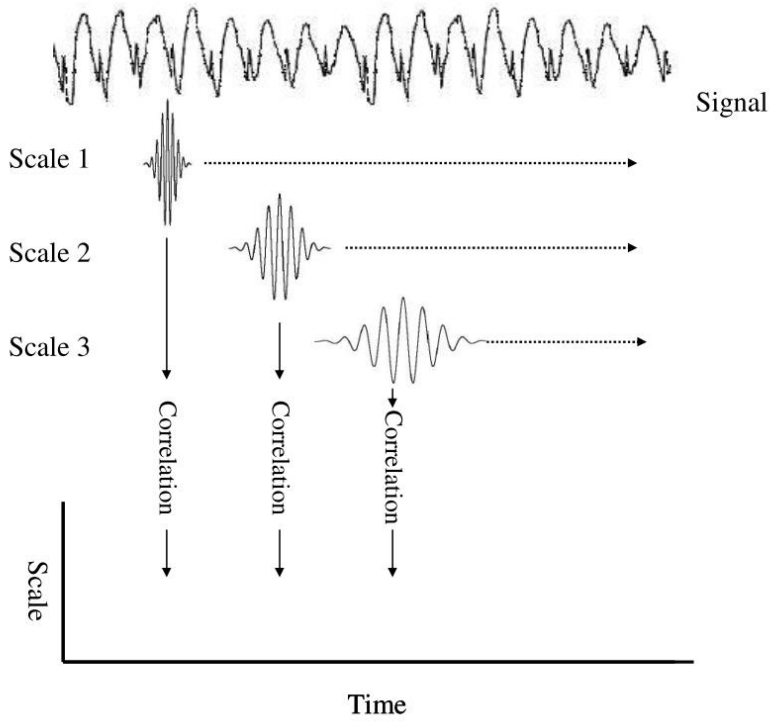

Figure 8-5. Constructing a Scalogram in CWT.
Signal's activities can be revealed at different times and scales, by plotting the correlation-change between the input signal and the mother wavelet over time (Shoeb and Clifford, 2006, p.10).

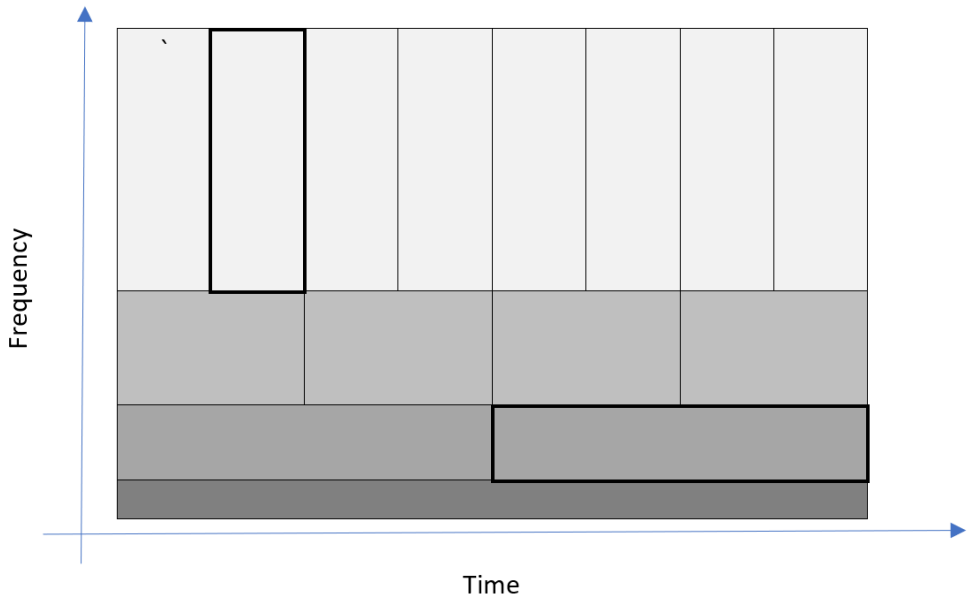

Figure 8-6. Time-Frequency plane of the Continuous Wavelet transform.
There is a trade-off between time and frequency resolutions in cwt; x and y-axes refer to the time and frequency resolutions, respectively. It is to be noted that though the rectangles differ in the dimensions, they have the same area. This denotes that if the time resolution is high, the frequency resolution is proportionally low and vice versa.

8.5 Spectral Subtraction

Spectral subtraction is one of the oldest algorithms that has been used for the enhancement of speech signals (Upadhyay and Karmakar, 2015). In this method, the spectrum of noise is estimated from the noisy signal during the intervals where speech is absent and only noise exists and then is subtracted from the spectrum of the noisy signal (Upadhyay and Karmakar, 2015). Spectral subtraction algorithms have been commonly used for reducing additive noise in speech signals, with the assumption that the noise is stationary, such that its spectrum does not change significantly with time (Boll, 1979; Vaseghi, 2000).

Additive noise causes an increase in the mean and the variance of the magnitude spectrum of the signal; spectral subtraction can eliminate the increase in the mean but not the increase in the variance (Vaseghi, 2000).

8.5.1 Spectral Subtraction Principle

If a noisy signal $y(m)$ is made up of a clean speech $x(m)$ and statistically independent additive noise $n(m)$:

$$y(m) = x(m) + n(m) \qquad \text{Equation 8-3}$$

The main two assumptions here are that the additive noise has a zero mean and does not correlate with the clean signal. The speech signal is non-stationary as it changes its spectral content with time. Therefore it is usually processed on a frame basis.

The short-time Fourier transform (STFT) of the previous equation is:

$$Y(f,k) = X(f,k) + N(f,k) \qquad \text{Equation 8-4}$$

Where k is the number of frames. By dropping k for simplicity and finding the power spectrum of $y(m)$:

$$|Y(f)|^2 = |X(f)|^2 + |N(f)|^2 \qquad \text{Equation 8-5}$$

Thus, the clean speech power spectrum could be estimated by subtracting the power spectrum of the estimated noise from the power spectrum of the noisy signal.

$$|X(f)|^2 = |Y(f)|^2 - |N(f)|^2 \qquad \text{Equation 8-6}$$

Where the power spectrum of noise is estimated by averaging the periods of the noisy signal when the speech was absent. In order to reconstruct the clean signal, phase information is required, and the phase information of the noisy signal is usually used for this purpose (Upadhyay and Karmakar, 2015). Finally, the inverse Fourier transform is applied to estimate the clean waveform in the time domain, by using the addition and overlapping of $|X(f)|^2$ (Boll, 1979; Vaseghi, 2000).

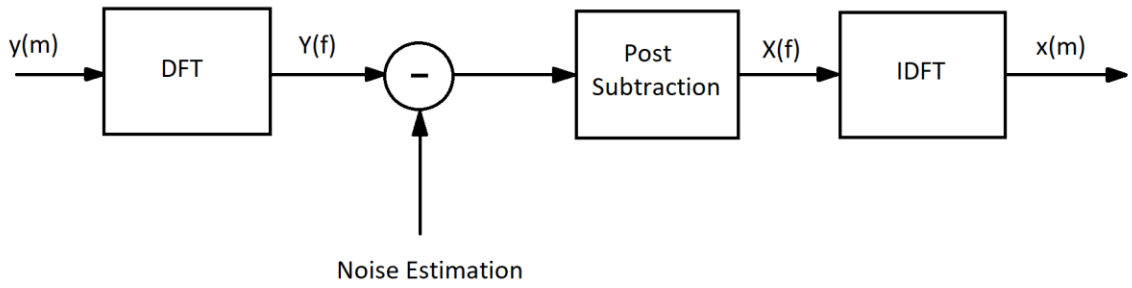

Figure 8-7. A block diagram representation of spectral subtraction

One of the limitations in spectral subtraction is that its performance highly depends on the estimation of noise, such that an inaccurate estimation of noise may distort the speech signal (Upadhyay and Karmakar, 2015).

In this study, the noise spectrum is available and derived from upper-body movement signal recorded by Vicon. Assuming that body movement is statistically independent and additive to the SLP signal, spectral subtraction could be a suitable technique to remove the upper-body movement from breathing in an SLP recording.

8.6 Abnormalities-Removal Algorithm

This section will discuss the statistical approach implemented to remove upper-body movements and coughs from SLP signals. An algorithm has been developed to identify abnormal breaths using a statistical approach. After identifying breath-cycles as trough-peak-trough, the algorithm quantifies the rising and the falling edges' amplitudes and durations for each cycle. Any cycle with a rising or a falling edge of less than 0.2 is excluded from the median

calculation. 0.2 was chosen as a threshold for two reasons: firstly, it has been observed that the level of breathing peak-to-peak amplitude is almost five times higher than this value. Hence, this small peak is likely to represent a ripple. Secondly, this step was done to make sure that the median calculation is not influenced by peak-to-peak amplitudes of the ripples before using the median value as a reference for breath selection.

The whole breath-cycle will be considered as rejected if either the rising or the falling edge is above a max-amplitude threshold, or below a min-amplitude threshold. Similarly, the cycle will also be rejected if the duration of either the rising or the falling edge is above a max_duration threshold or below a min_duration threshold.

Duration threshold values as:

min_duration = 0.5* Median value of rising/falling edges' durations.

max_duration= 1.5 * Median value of rising/falling edges' durations.

Amplitude threshold values:

min_amplitude = 0.5 * Median value of rising/falling edges' amplitudes.

max_amplitude = 1.5 * Median value of rising/falling edges' amplitudes.

If the duration of the rising or the falling edge is below the min_duration threshold, it is unlikely to represent a breath and might represent a fast event instead such as a ripple or a cough. Moreover, if duration exceeded a max_duration, it represents slow events such as a slow body-movements or a very slow breath, in all the previous cases the cycle is unlikely to represent a tidal breath.

If the amplitude of the rising or the falling edge is also below the min_amplitude threshold, it is unlikely to represent a breath and might represent a ripple instead. Moreover, if it exceeds max_amplitude, it might represent a body-movements or a deep breath.

If any of the previous conditions is met, the cycle is unlikely to represent a tidal breathing cycle. Therefore, the complete cycle will be removed from the time series. The signal will then be attached to the next cycle by placing the troughs on each other accounting for the difference in the y-amplitude between the two breaths.

The abnormalities-removal algorithm was applied on SLP_{Mov}, and the sensitivity of the algorithm in detecting and removing upper-body movements was calculated. The agreement between Tidal breathing parameters measured by SLP and PNT was assessed before and after applying the algorithm. Movements, if detected, are removed because they do not represent a pure tidal breath.

The algorithm was also applied on SLP_{Cough}, and the sensitivity of the algorithm in detecting and removing coughs was evaluated. Differences between tidal breathing parameters estimated from SLP_{Still} and SLP_{Cough} were calculated before and after applying the algorithm. Coughs, if detected, are removed because they do not represent a tidal breath.

8.7 Methodology

8.7.1 Study Participants and design

In this study, 14 participants (7M:7F) aged 18- 60 with no history of respiratory diseases were recruited. Participants were excluded if they had a cold or any other viral infection, chest surgery within the past month or an acute disease-process likely to interfere with data acquisition.

The study was approved by the Keele University Ethical Review Panel (ERP), (Ref number: ERP1303), and was performed in the Turing lab/Colin Reeves at Keele University.

8.7.2 Study Devices and Procedures

8.7.2.1 Pneumotachometer (PNT)

Pneumotachometer (Viasys Masterscope CT; Viasys Healthcare GmbH, Höchberg, Germany) is a device that measures airflow, by converting the airflow passing through its mouthpiece into a relative pressure-difference either side of a pressure transducer. A flow signal is produced, and a volume signal is also quantified by integrating the flow signal with respect to time. Viasys Masterscope was used, with a sampling rate of 100 Hz, flow range 0 to ±20 L/Sec, and flow accuracy of 2%. A 3-L syringe was used for the calibration prior to the arrival of every subject, ambient temperature, pressure and humidity were recorded.

8.7.2.2 Vicon Motion Capture System

The Vicon (Vicon Ltd, Oxford) system is a motion capturing system, which consists of multiple high-resolution cameras fixed at different locations around a capture volume. Each camera has a ring of light emitting diodes (LEDs) fitted around the lens. The LEDs project infrared light into the capturing volume, and the light reflected from retroreflective markers attached to a subject is detected by the lens to identify their exact locations.

The Vicon system is used clinically to examine human body-parts movement, by attaching a number of reflective markers on specific body parts, and tracking marker positions in real time. Positions of the markers in 3-dimensions are then used to quantify its: velocity, acceleration and jerk with high accuracy. Vicon is considered the gold standard in movement analysis.

The markers were placed on a specific (bony) visible locations Figure 8-8. The placement of the markers was based on the assumption that the bony parts of the shoulders (front and back) and the C7 do not move with the movement of TA wall during breathing. This assumption was

confirmed by quantifying distances variations between (front - back, left - right shoulder) markers, which have shown to be within one millimetre that was considered negligible (compared to TA wall movement during tidal breathing). Thus, we assumed the rigidity of upper-thorax, and we dealt with the segment of five markers as one unit.

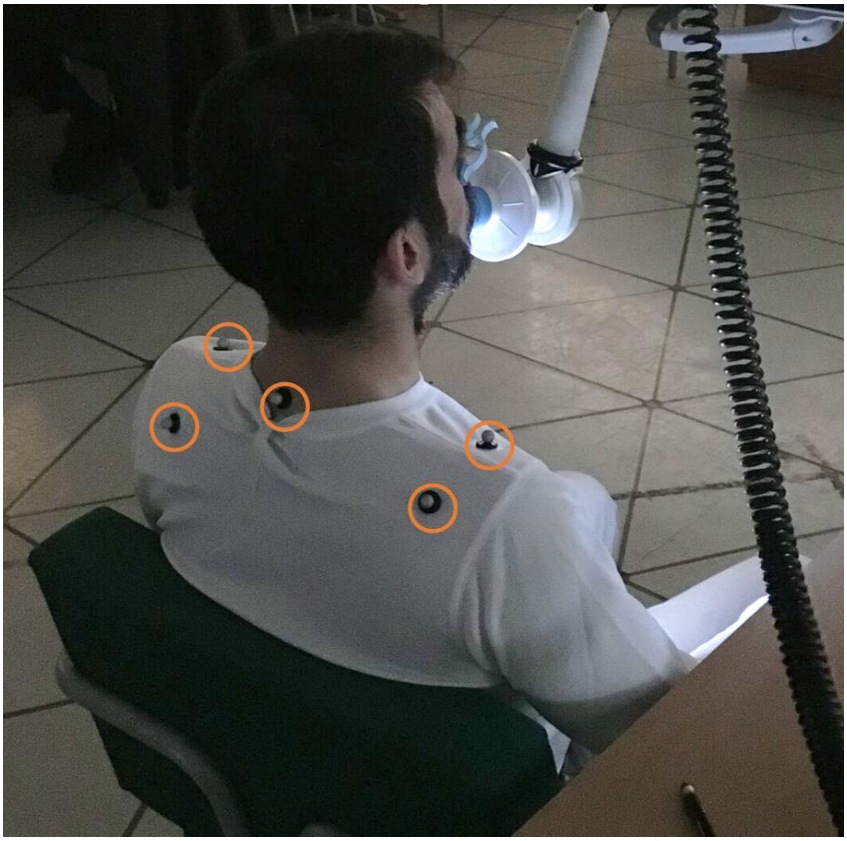

Figure 8-8. Markers placement on the subject's shoulder and C7

8.7.2.3 SLP (Thora-3Di™, PneumaCare, Ltd., Cambridgeshire, UK).

For each assessment, tidal breathing was recorded for five minutes using an SLP device.

8.7.3 Study divisions

This study was divided into three investigations, special conditions of each investigation will be discussed individually. However, certain conditions were shared by all three, which are:

Every subject was asked to put on a close-fitting white T-shirt, and to sit in a high-backed chair with arms as far back in the seat as possible. Five reflective markers were attached on top of the t-shirt at Front Right Shoulder (FRSH), Back Right Shoulder (BRSH), Front Left Shoulder (FLSH), Back Left Shoulder (BLSH) and C7. PNT was suspended from the ceiling, stabilised

and positioned at a height that allows the participant to place the mouthpiece in their mouths comfortably, gravity-eliminated position Figure 8-9. This method of positioning was done to avoid blocking the SLP grid. A nose-clip was used to block the subject's nose.

SLP machine was positioned one metre away from the subject, the height and angle of SLP head were adjusted such that the optical axis of the cameras were perpendicular to the subject's chest wall. The projected light was aligned to cover the Thoracoabdominal (TA) area of the subject, with the cross point of the projected light placed at the base of the xiphisternum. The area above a hypothetical horizontal line at xiphisternum level is identified as the thorax and below it as the abdomen.

As a part of normal operating conditions for SLP, room lights were switched off to allow a better grid visualisation by the SLP cameras. PNT and SLP recorded tidal breathing, and Vicon recorded upper-body movements all at the same time for five minutes.

Figure 8-9. Study setup. The subject is sitting as far back in a high-backed chair as possible with his arms on the chair arms. The PNT suspended from the ceiling to avoid blocking SLP-grid.

8.7.3.1 Sitting still and breathing

In this part of the study, participants were instructed to sit as still as possible and breathe naturally.

8.7.3.2 Breathing with Upper-body movements

In this part of the study; participants were asked to sit still and breathe and were instructed to move their upper-extremity forward-backwards once a minute at different speeds. The movements were introduced to mimic the real upper-extremity movements which might occur during an SLP recording.

8.7.3.3 Breathing with Coughing

Participants were asked to sit still and were instructed to cough once every one minute at different strengths and to try to keep the coughs as natural as possible. Coughs were introduced to mimic the real coughs which might occur during an SLP recording.

8.8 Study Aims

This study had three investigations; each has a specific purpose contributing toward the overall aim of the study, as follows:

The first trial aimed to identify the optimal recording time to obtain the least differences between SLP and PNT parameters. The agreement between the estimated parameters from both devices was then assessed.

The second trial aimed to assess the effect of upper-body movements on the agreement between the estimated parameters. Different approaches to remove upper-body movements from the SLP signal were investigated.

The third trial aimed to assess the effect of coughs on the estimated parameters. The effect of removing coughs on parameters estimation was assessed.

8.9 Software and Data Analysis

8.9.1 Pre-processing

PNT volume-derived signal was exported for each subject using Jscope software (Viasys Healthcare GmbH). Pneumaview-3D™ software (PneumaCare Ltd) was used to export TA wall displacement-signals.

Due to the difference of sampling frequencies between both devices (PNT: 100 Hz; SLP: 30 Hz), SLP signals were resampled to match the sampling rate of the PNT signals. This was done using a piecewise cubic Hermite interpolating polynomial. This interpolation was used previously by Motamedi-Fakhr et al., 2017, because it minimally affects the morphology of the signal (i.e. shape-preserving) (Kahaner et al., 1989). The algorithm explained in 4.3.3 was used for breaths.

Continuous wavelet transformation (cwt) was used to investigate frequency components of breathing, movements and coughs. Spectral subtraction and abnormalities-removal algorithms were applied in a trial to remove upper-body movements and coughs.

8.9.2 Calculation of Tidal Breathing Parameters

Inspiratory start times, expiratory start times, and expiratory end times were indicated. Each trough in the traces (PNT, and SLP) is considered as inspiratory start time (which in turn is considered the end time of the previous expiratory period), and each peak is considered as expiratory start time Figure 8-10. This method of identifying respiratory cycles is beneficial for calculating timing indices (Motamedi-Fakhr et al., 2017).

Following (Stocks, 1996) definitions, the parameters were calculated as follows:

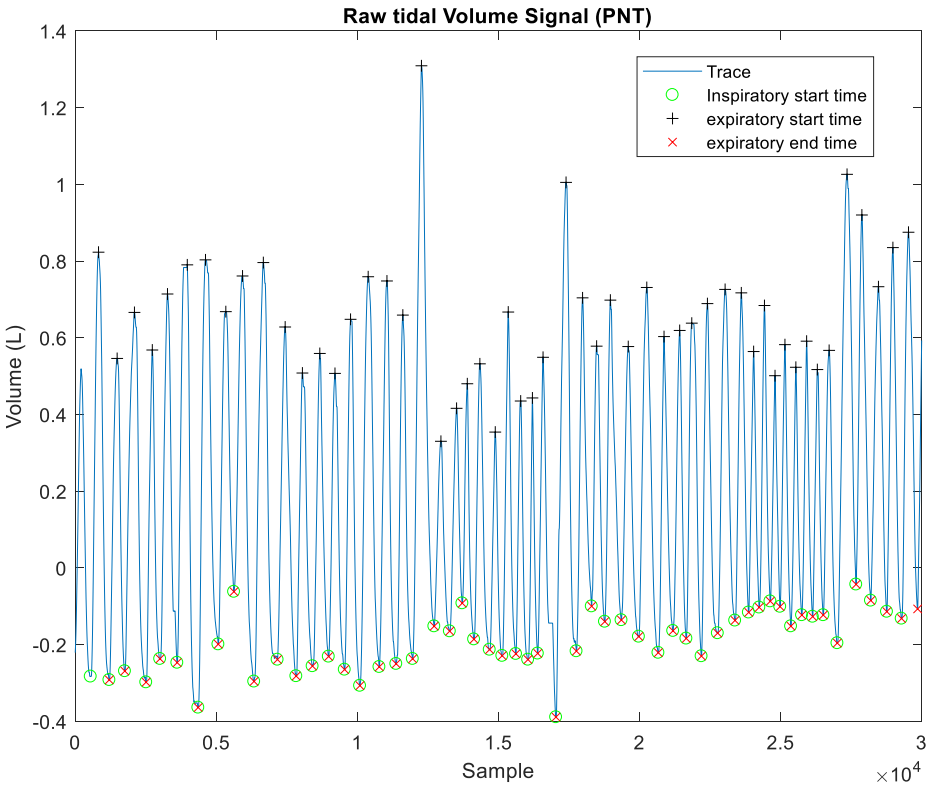

Figure 8-10. Tidal volume signal (PNT), with the peaks and troughs localized. Inspiratory, expiratory start times and expiratory end times identified.

tI = Expiratory start time – Inspiratory start time
tE = Expiratory End time – Expiratory start time
tTot = tI+ tE
RR = 60/tTot
IE50 = TIF50/TEF50

More details about the calculations of the parameters, is discussed in Chapter Four.

8.9.3 Statistical Analysis

8.9.3.1 Sitting still and breathing

Median of each tidal breathing parameter was calculated from both SLP and PNT signals using a total signal length of 10, 20, 30, 40 and 47 Breaths. Means of differences and Confidence intervals were quantified at each breath count, to find the period which offers the lowest mean difference and the narrowest CI range. The upper and lower confidence intervals were calculated as:

Mean of differences ± 1.96* (standard deviation / Sqrt (sample size) for each parameter.

For the chosen breath count, a Bland-Altman plot (Bland and Altman, 1986) was used to assess the agreement between tidal breathing parameters measured by SLP and PNT. Upper-limit of agreement (ULOA) and the Lower-limit of agreement (LLOA) are evaluated as mean of differences ±1.96(SD). Since PNT is considered as a gold standard for measuring those tidal breathing parameters, the x-axis in the Bland-Altman plot represented the PNT values. Bland-Altman plot contained 14 points for each parameter such that a point for each subject.

Percentage differences were also calculated for each parameter: $(X_{SLP}- X_{PNT})/X_{PNT}$, and X is any of the tidal breathing parameters.

8.9.3.2 Breathing with upper-body movements

Bland-Altman plots (Bland and Altman, 1986) were used to assess the agreement between the parameters after the introduction of upper-body movement (SLP_{Mov} and PNT_{Mov}). Changes in the estimated parameters in both devices were also quantified to assess the effect of upper-body movements on parameters estimation.

Mean of differences between SLP and PNT, ULOA and LLOA were used to assess spectral subtraction and abnormalities removal performances.

8.9.3.3 Breathing with Coughing

Differences in the parameters between SLP_{Still} and SLP_{Cough} were quantified, and then the parameters were quantified from SLP_{Cough} after coughs removal and compared with SLP_{Still}.

8.9.4 Results

14 subjects (7M:7F) were recruited, with an age range of 19-49 years; mean (SD) 29.9 (9.55) years.

Table 8-1. Participants demographics;
Data for each subject: age, height, weight and gender; F: female; M: male.

Subject number	Age (yrs.)	Height (cm)	weight (Kg)	Gender
Sub_01	36	164.5	67	M
Sub_02	28	176.5	77.5	M
Sub_03	49	168.5	85	M
Sub_04	26	178	82.8	M
Sub_05	31	164.5	62	F
Sub_06	47	178	92	M
Sub_07	19	179	89	M
Sub_08	20	172	64.2	F
Sub_09	33	169	62	F
Sub_10	36	162	68	M
Sub_11	26	165	71	F
Sub_12	26	170	57	F
Sub_13	20	168	66	F
Sub_14	21	162	74	F
Total (Mean:SD)	29.9 (9.55)	169.79 (6.05)	72.68 (10.98)	7M:7F

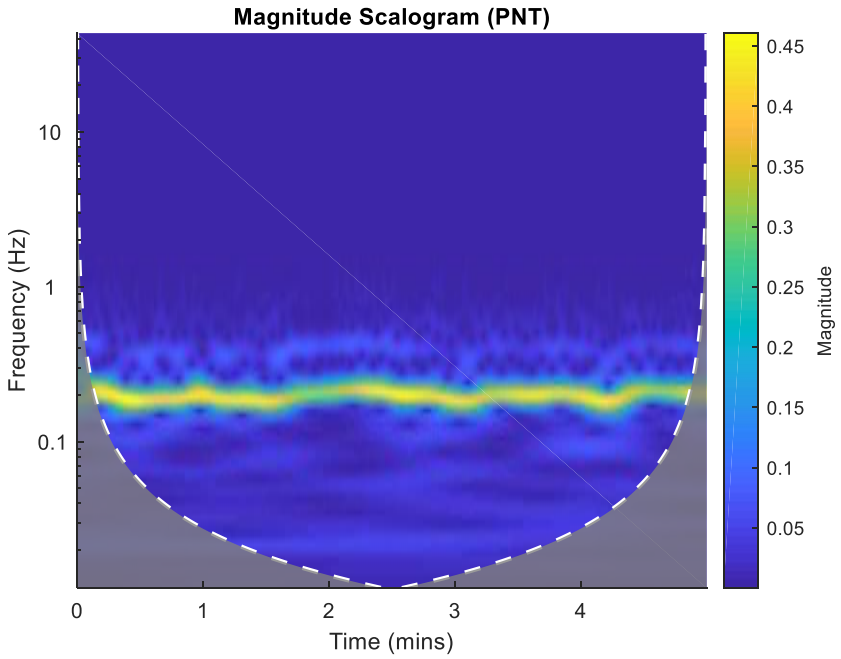

Figure 8-11. Continuous wavelet transformation of a PNT signal recorded from Subject_03 in Sitting still session.
The grey area marked with the dashed-line shows the area where edge effects become significant

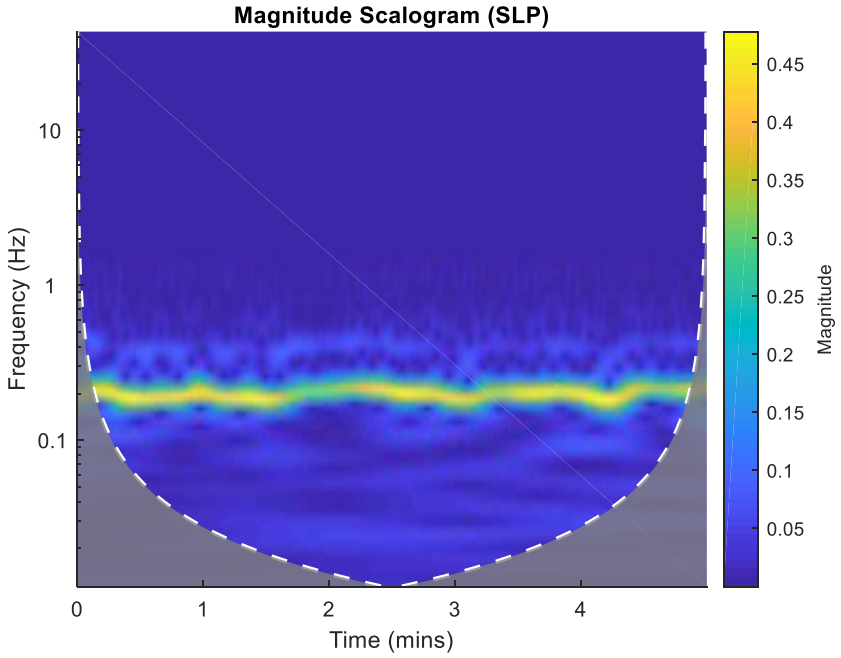

Figure 8-12. Continuous wavelet transformation of a SLP signal recorded simultaneously from Subject_03 in Sitting still session.

8.9.4.1 The agreement between SLP_{Still} and PNT_{Still}

Respiratory Rate (RR)

Respiratory rate median values range between 8.73 – 20.69 brpm. Figure 8-13 shows means of differences and CIs at different breath numbers. Means of differences ranged between 0.036 – 0.103 brpm with the smallest RR mean difference of 0.036 brpm obtained at 10 breaths period.

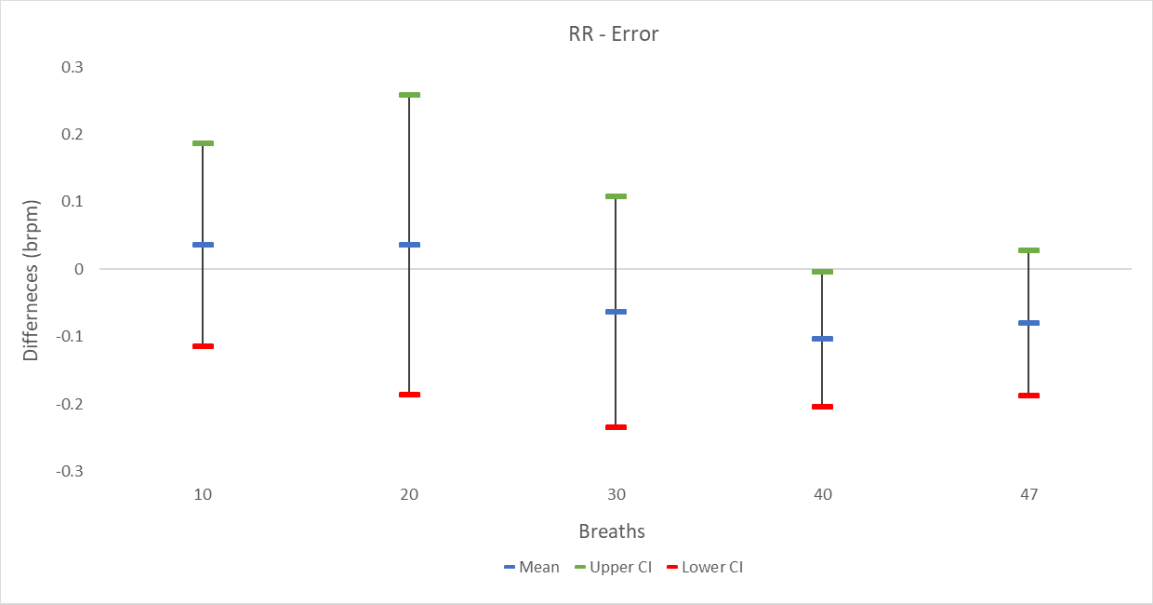

Figure 8-13. Mean differences between RR_{SLP} and RR_{PNT} and CIs at 10, 20, 30, 40 and 47 breaths.

Inspiratory Time (tI)

Inspiratory time (tI) median values range between 1.29 – 2.84 sec. Figure 8-14 shows mean differences and CIs at different breath numbers. Mean of differences ranged between 0.065 – 0.079 sec with the smallest tI mean difference of 0.065 sec obtained at 10 breaths period.

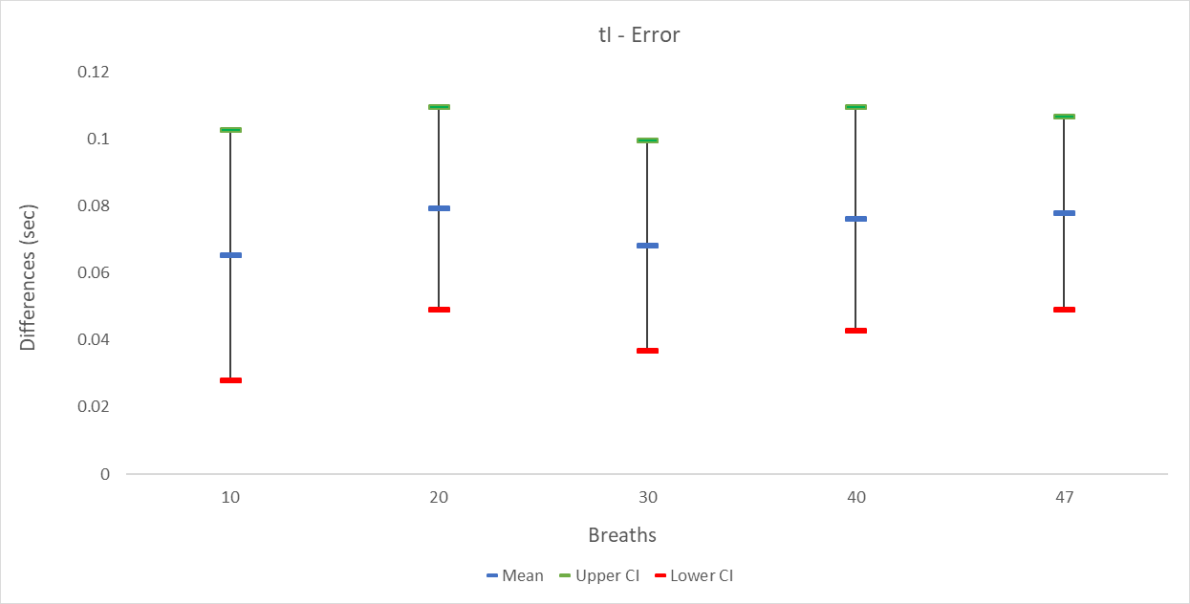

Figure 8-14. Mean differences between tI_{SLP} and tI_{PNT} and CIs at 10, 20, 30, 40 and 47 breaths.

Expiratory Time (tE)

Expiratory time (tE) median values range between 1.62 – 4.18 sec. Figure 8-15 shows mean differences and CIs at different breath numbers. Means of differences ranged between 0.036 – 0.064 sec with the smallest tE mean difference of 0.036 sec obtained at 20 breaths period.

Figure 8-15. Mean differences between tE_{SLP} and tE_{PNT} and CIs at 10, 20, 30, 40 and 47 breaths.

Total Breath Time (tTot)

Total Breath time (tTot) median values range between 2.9 – 6.87 sec. Figure 8-16 shows mean differences and CIs at different breath numbers. Means of differences ranged between 0.013 – 0.043 sec with the smallest tTot mean difference of 0.013 sec obtained at 20 breaths period.

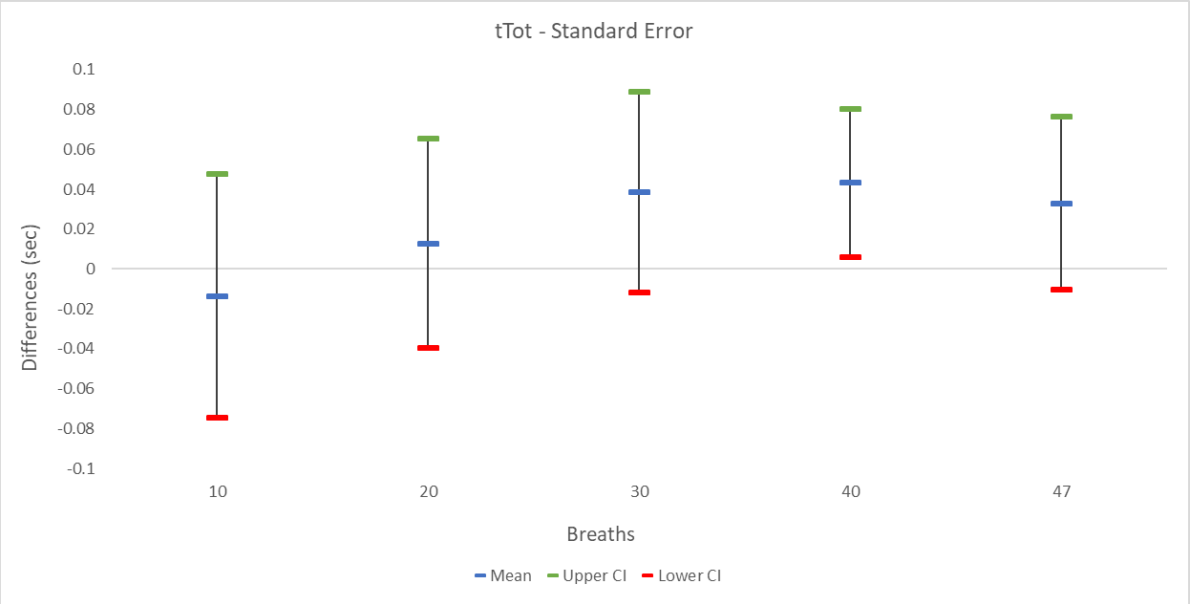

Figure 8-16. Mean differences between $tTot_{SLP}$ and $tTot_{PNT}$ and CIs at 10, 20, 30, 40 and 47breaths.

Inspiratory/Expiratory Time Ratio (tI/tE)

Inspiratory /expiratory time (tI/tE) median values range between 0.501 – 0.841. Figure 8-17 shows mean differences and CIs at different breath numbers. Mean of differences ranged between 0.041 – 0.045 with the smallest tI/tE mean difference of 0.041 obtained at 10 and 20 breaths period.

Figure 8-17. Mean differences between tI/tE_{SLP} and tI/tE_{PNT} and CIs at 10, 20, 30, 40 and 47 breaths.

Duty Cycle (tI/tTot)

Duty cycle (tI/tTot) median values range between 0.334 – 0.457. Figure 8-18 shows mean differences and CIs at different breath numbers. Mean of differences ranged between 0.015 – 0.016 with the smallest tI/tTot mean difference of 0.015 obtained at 10, 20 and 47 breaths period.

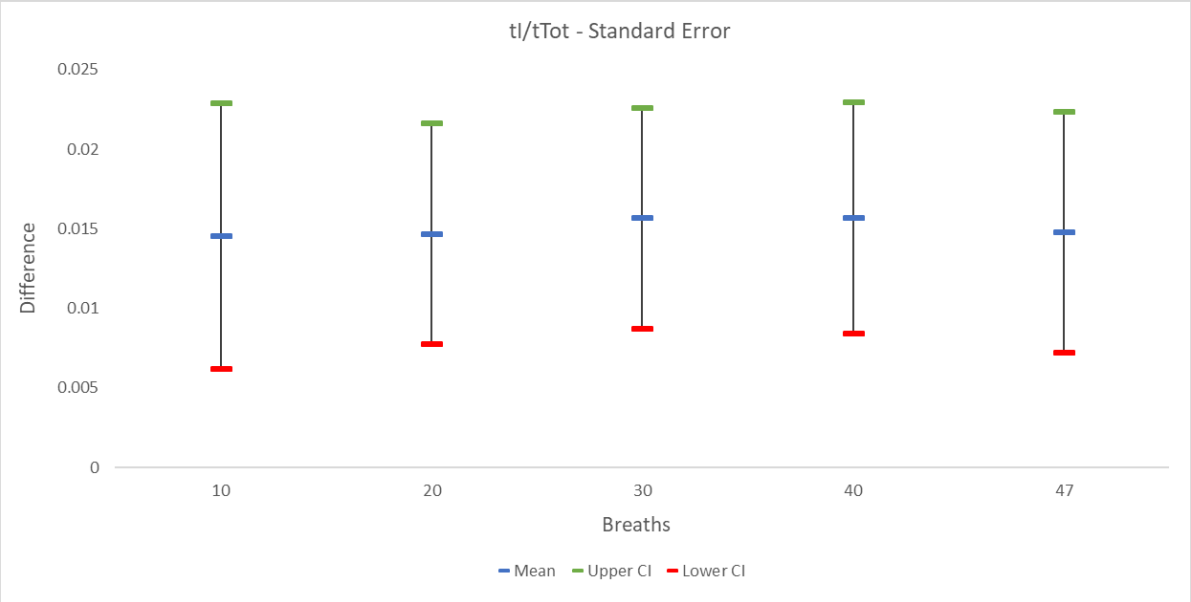

Figure 8-18. Mean differences between $tI/tTot_{SLP}$ and $tI/tTot_{PNT}$ and CIs at 10, 20, 30, 40 and 47 breaths

IE50

IE50 median values range between 0.791 – 1.754. Figure 8-19 shows mean differences and CIs at different breath numbers. Mean of differences ranged between 0.005 – 0.072 with the smallest IE50 mean difference of 0.005 obtained at 40 breaths period.

Table 8-2 presents the absolute and percentage differences and 95% LOAs at 40 breaths. The agreement between PNT and SLP is assessed using the LOAs and the mean of differences.

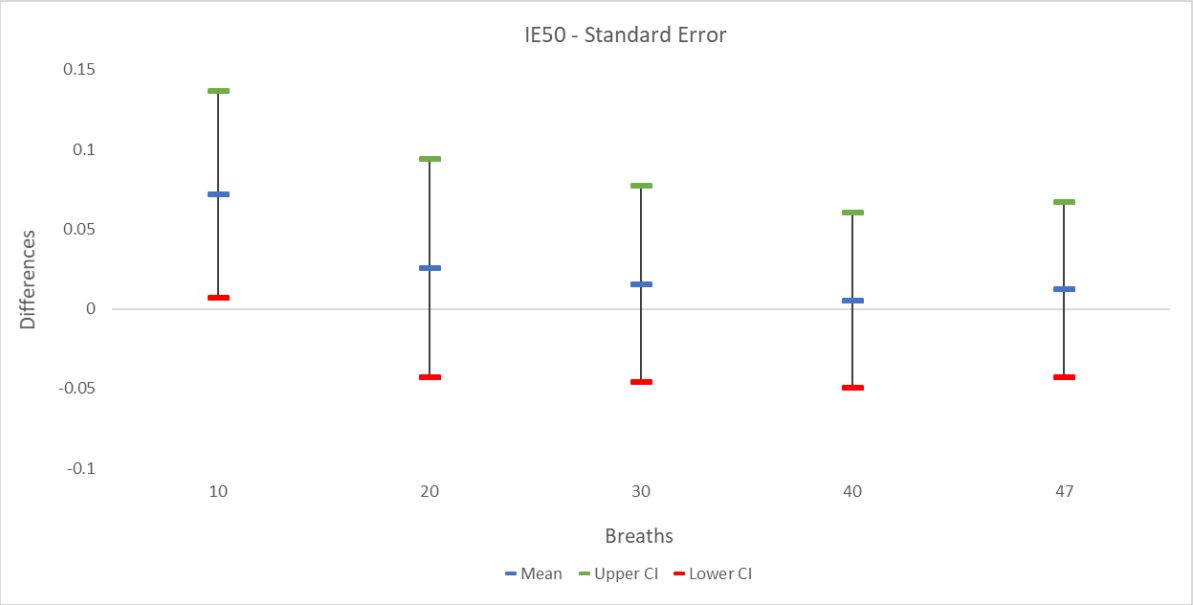

Figure 8-19 Mean differences between $IE50_{SLP}$ and $IE50_{PNT}$ and CIs at 10, 20, 30, 40 and 47 breaths.

Table 8-2 Absolute and Percentage differences between tidal breathing parameters measured simultaneously by SLP and PNT at 40 breaths.

Tidal breathing parameters	Absolute differences (over 40 breaths)	Percentage differences (over 40 breaths)
RR(brpm)	-0.10 [-0.48, 0.27]	-0.84 [-3.61, 1.94]
tI (sec)	0.08 [-0.05, 0.20]	4.93[-2.89, 11.67]
tE (sec)	-0.06 [-0.2, 0.07]	-2.57 [-7.43, 2.28]
tTot (sec)	0.04 [-0.1, 0.18]	0.86 [-1.99, 3.71]
tI/tE	0.04 [-0.03, 0.12]	6.91 [-4.91, 18.74]
tI/tTot	0.02 [-0.01, 0.04]	4.03 [-2.86, 10.91]
IE50	0.01 [-0.20, 0.21]	0.67 [-15.76, 17.09]

8.9.4.2 The effect of upper-body movements on derived tidal breathing parameters

SLP is a contactless measure of breathing signals, in which signals are acquired by measuring the movement of the TA wall during breathing. Upper-body movements could be captured during breathing measurements, which could deteriorate the quality of the signal (Motamedi-Fakhr, Wilson and Iles, 2017), and might provide the clinician with unrealistic breathing parameters. Figure 8-20 represents SLP, and PNT signals measured simultaneously, upper body-movements affect both signals, and it is clear that the SLP signal is more sensitive to this artefact. The agreement of the parameters between SLP and PNT was quantified at still and movement, then the differences in the parameters between movement and still were calculated for both devices Table 8-3.

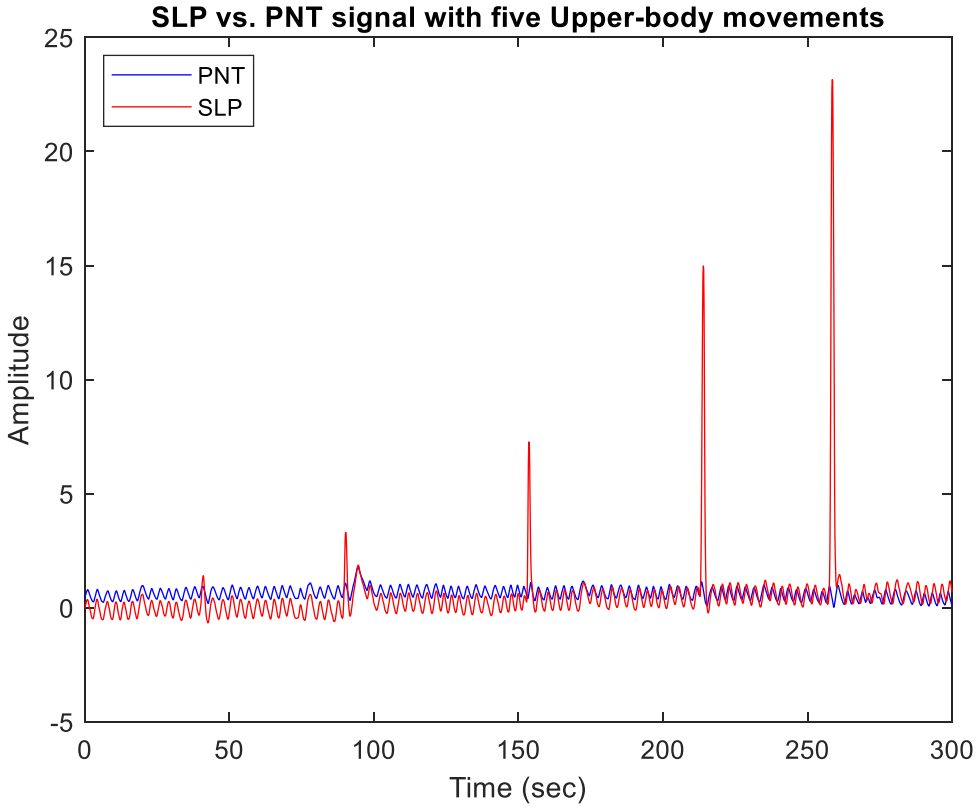

Figure 8-20. The effect of upper-body movement on SLP and PNT signals measured simultaneous. The effect of the movements on SLP is much bigger than on the PNT signal.

Continuous wavelet transformation was used to investigate frequency contents of the signals. Figure 8-21 and Figure 8-22 show the time-frequency plane of still SLP and PNT signals respectively, the bright colour extending at all times in both figures represent the frequency range of breathing 0.3 to 0.4 Hz.

Figure 8-23 shows the effects of upper-body movements on SLP frequency content, the five spikes that occupy the frequency range from 0.3 to 6 Hz represent upper-body movements' frequency content. Figure 8-24 shows that the effect of the movement on PNT frequency content was barely noticeable. Hence, there is an overlap in frequency-bands between the

signal of interest and the interference in the SLP signal. Figure 8-25 shows the wavelet transformation of a Vicon signal which represents frequency components of upper-body movement for that specific subject.

The continuous wavelet transform is an efficient technique for detecting transient components and sudden changes (Leonard et al., 2006). Therefore, it was used to identify and localise the intermittent components of upper-body movements.

Table 8-3. The agreement between PNT and SLP in both study conditions.
The first row represents the mean of differences and LOAs in still condition and the second in movement. LOA is measured as Mean (Diff) ± 1.96(SD).

Study Condition	The difference (SLP - PNT)	Tidal Breathing Parameters						
		RR (brpm)	tE (sec)	tI (sec)	tTot (sec)	tI/tE	tI/tTot	IE50
Still	Mean	-0.05	-0.01	0.02	0.03	0.03	0.01	0.07
	LOAs	[-0.69, 0.60]	[-0.22, 0.19]	[-0.14, 0.19]	[-0.17, 0.22]	[-0.06, 0.13]	[-0.02, 0.04]	[-0.22, 0.36]
Movement	Mean	0.27	-0.05	-0.01	-0.08	0.00	0.00	0.03
	LOAs	[-0.64, 1.17]	[-0.23, 0.13]	[-0.14, 0.12]	[-0.33, 0.17]	[-0.11, 0.11]	[-0.03, 0.03]	[-0.28, 0.34]

Table 8-4. Changes in the estimated parameters between both study conditions observed from both machines.
The first row represents the mean of differences and LOAs in SLP, and the second in PNT. LOA is measured as Mean (Diff) ± 1.96(SD).

Machine type	Difference (Mov – Still)	Tidal Breathing Parameters						
		RR (brpm)	tE (sec)	tI (sec)	tTot (sec)	tI/tE	tI/tTot	IE50
SLP	Mean	1.98	-0.38	-0.18	-0.59	0.03	0.01	-0.08
	LOAs	[-3.88, 7.84]	[-1.54, 0.78]	[-1.00, 0.64]	[-2.42, 1.24]	[-0.10, 0.15]	[-0.03, 0.05]	[-0.59, 0.43]
PNT	Mean	1.67	-0.34	-0.15	-0.48	0.05	0.02	-0.04
	LOAs	[-4.35, 7.69]	[-1.49, 0.81]	[-1.01, 0.72]	[-2.37, 1.41]	[-0.13, 0.23]	[-0.04, 0.07]	[-0.63, 0.55]

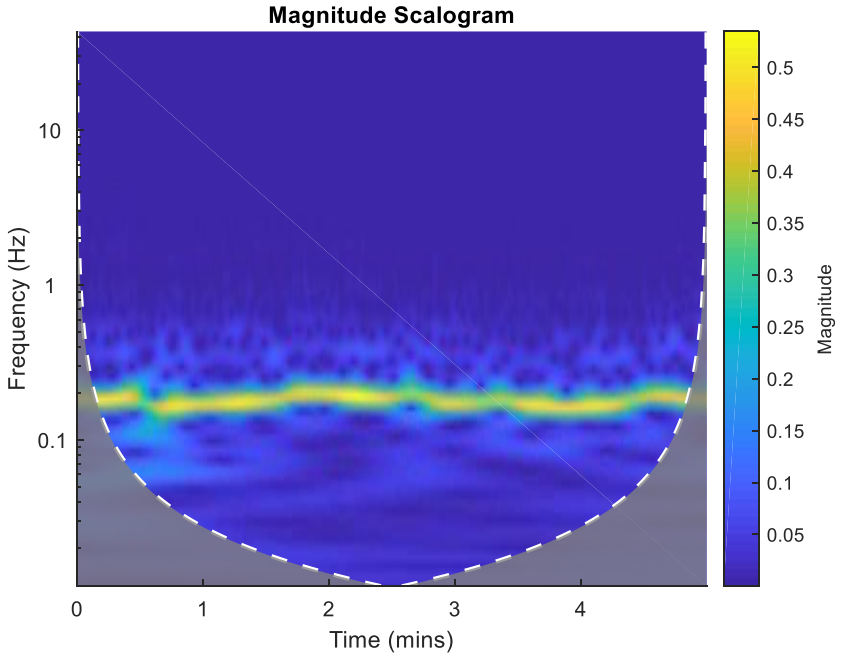

Figure 8-21. Continuous wavelet representation of a still SLP signal for Sub_01.

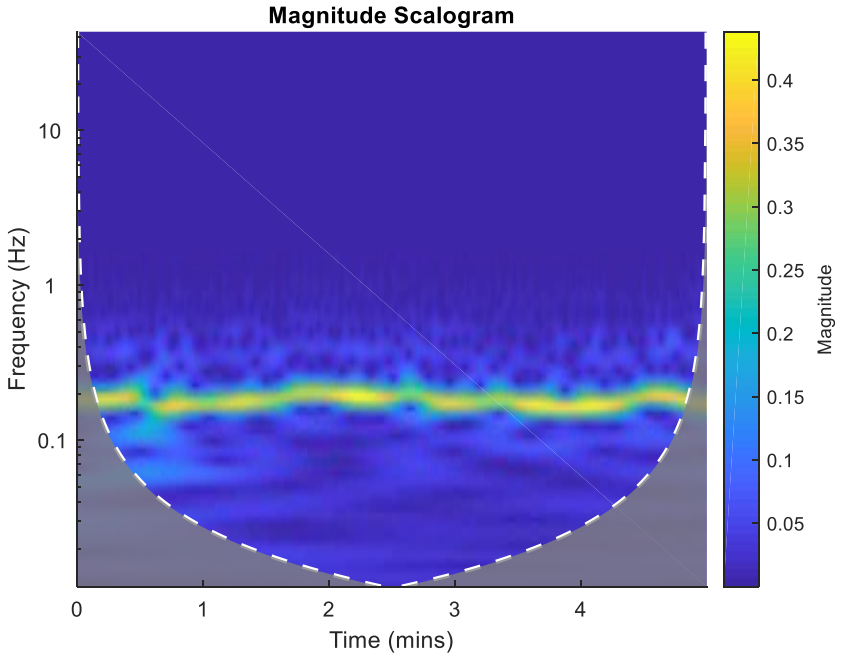

Figure 8-22. Continuous wavelet representation of a still PNT signal for Sub_01

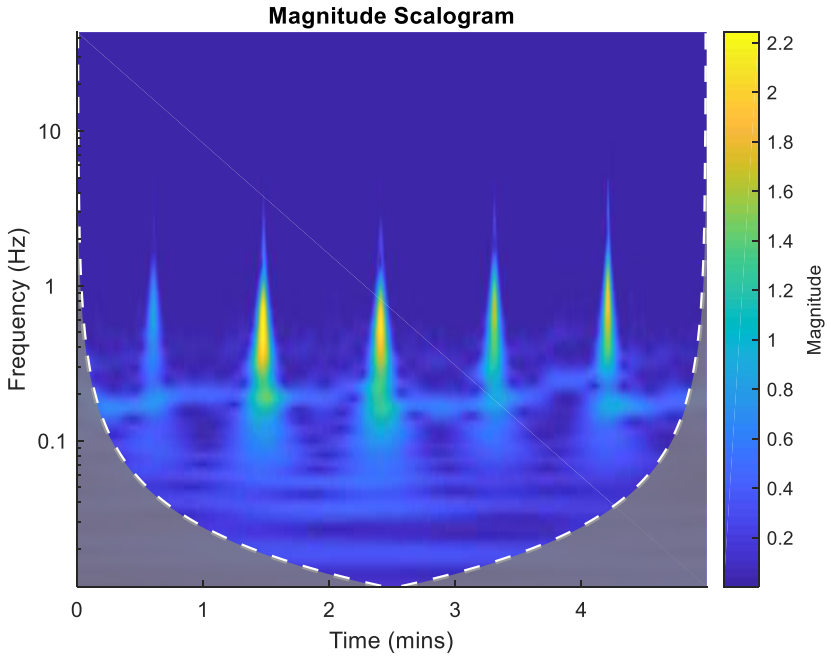

Figure 8-23. Continuous wavelet representation of SLP-signal with five upper-body movements for Sub_01.

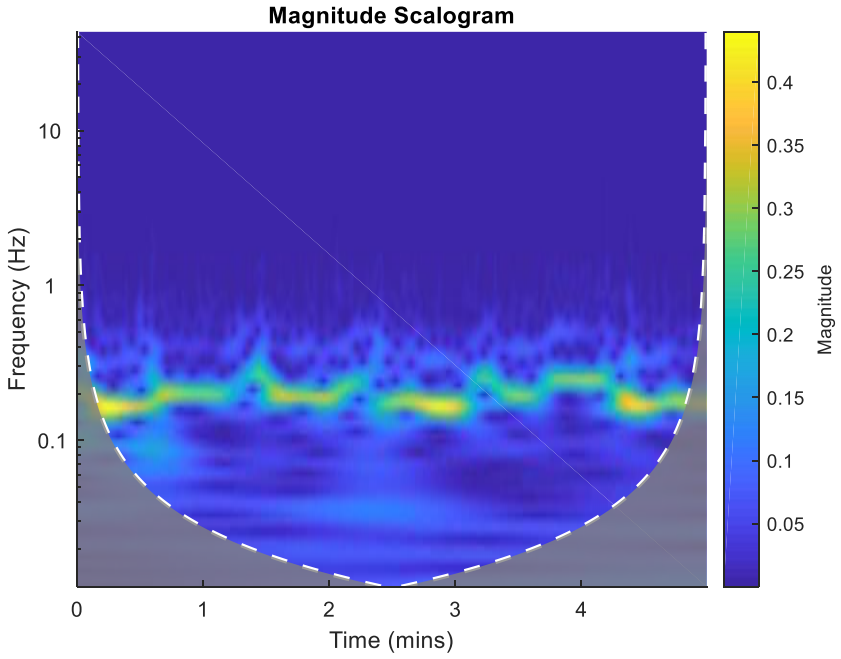

Figure 8-24. Continuous wavelet representation of a PNT-signal with five upper-body movements for Sub_01.

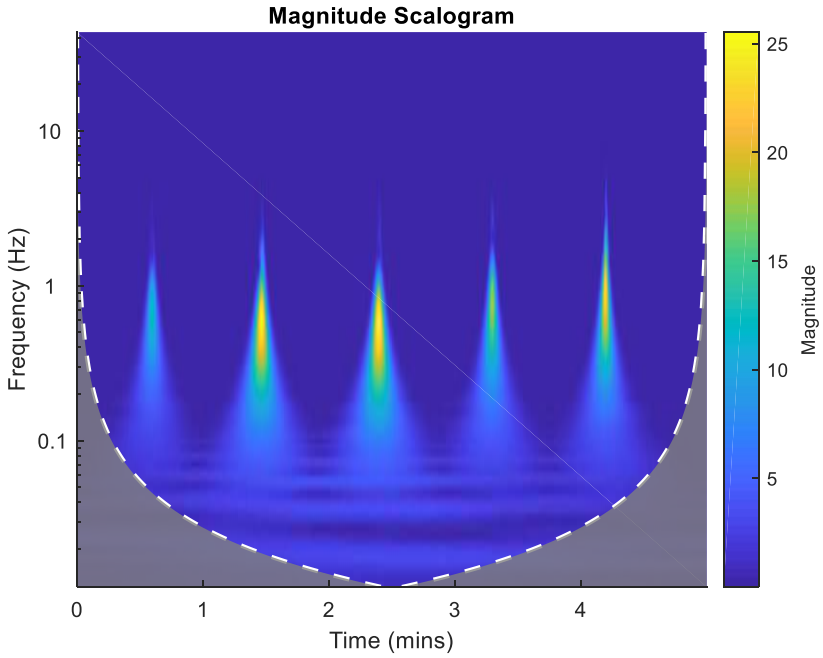

Figure 8-25. Continuous wavelet representation of the Vicon signal with the five body movements sub_01

Spectral subtraction was employed in an attempt to remove upper-body movements from SLP signals, by subtracting the frequency contents of upper -body movements (Vicon), from the frequency content of SLP for each subject. Figure 8-26 shows the result of applying spectral subtraction on an SLP signal (blue), using the reference noise recorded by Vicon (green). The red trace shows the filtered signal; movement peaks were significantly suppressed using this approach with a minimal effect on the breathing parts of the signal. However, the reduced peaks did not reach a normal-breathing level, and some of them created a high-frequency oscillation in the place of the movement.

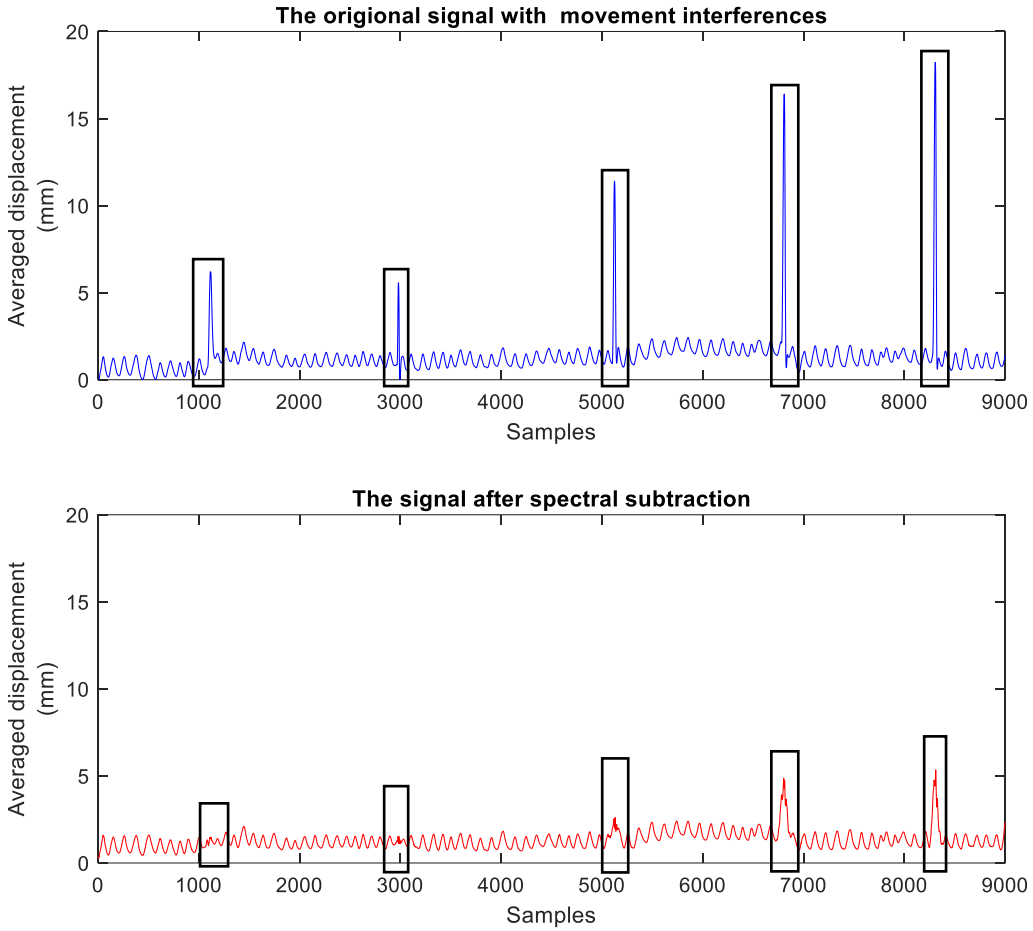

Figure 8-26. Spectral subtraction outcome for Sub_06.
Top, blue is the SLP signal with upper-body movements interferences; red is the signal post-spectral subtraction. Upper-body movements are highlighted in a black box.

The performance of spectral subtraction filtering approach was assessed using the agreement between tidal breathing parameters measured by SLP (Pre and Post-filtering) and PNT_{Mov}.

Abnormalities removal algorithm was applied to remove upper-body movements and any other abnormal breath cycles as explained earlier on page 97. The algorithm successfully identified all upper-body movements as they have higher amplitudes than breathing peaks.

Table 8-6 shows the agreement between tidal breathing parameters measured by SLP and PNT at still, movement, post spectral subtraction and post movement removal.

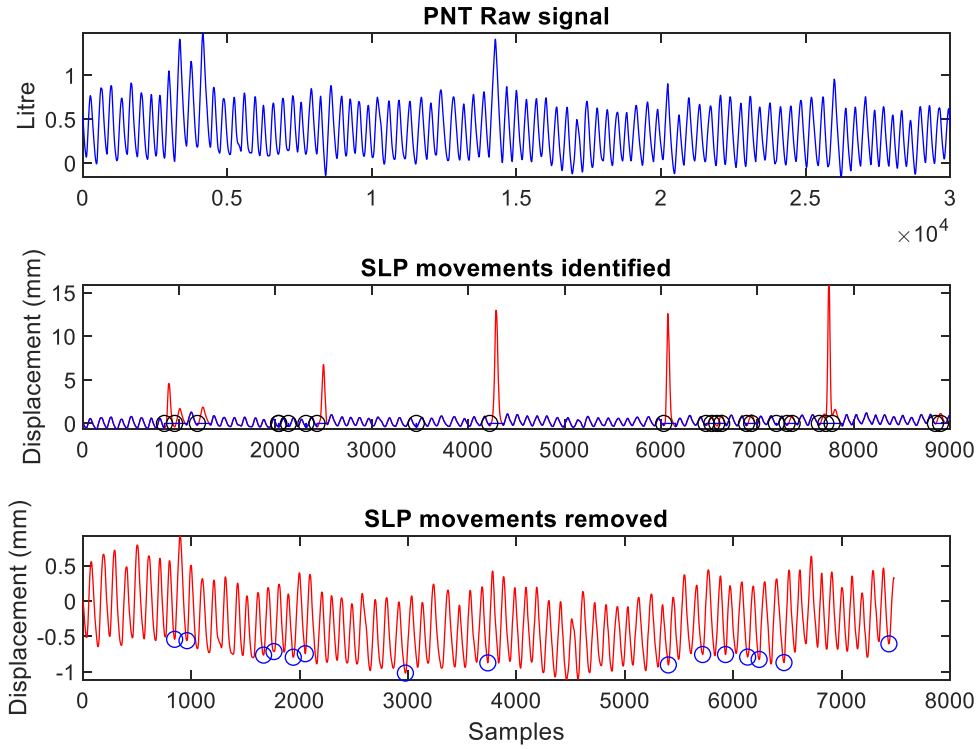

Figure 8-27. Upper-body movements identification and removal from SLP signal (Sub_10) using abnormalities removal algorithm.
On top a raw PNT signal which shows the minimal effect of upper-body movements on the gold standard; in the middle, an SLP signal with movement-peaks identified and set to zero, and on the bottom, the identified peaks are removed, and the trace is attached at the cutting locations.

Table 8-5. The sensitivity and specificity of the abnormalities-removal algorithm in detecting upper-body movements for subjects Sub_01-14.

Subject Number		
	Sensitivity (%)	Specificity (%)
Sub_01	100	92
Sub_02	100	97
Sub_03	100	95
Sub_04	100	89
Sub_05	100	99
Sub_06	100	85
Sub_07	100	95
Sub_08	100	91
Sub_09	100	96
Sub_10	100	87
Sub_11	100	97
Sub_12	100	100
Sub_13	100	88
Sub_14	100	100
Average	**100**	**94**

Table 8-6. The agreement between tidal breathing parameters measured by PNT and SLP at still, movement, post spectral subtraction and post movement removal.
Values are mean [LOA].

Tidal Breathing Parameters	Absolute Differences between tidal breathing parameters measured by PNT and SLP at Still, movement ,post spectral subtraction and post abnormalities removal algorithm			
	Still	**Movement**	**Post spectral sub**	**Post mov removal**
RR (brpm)	-0.05 [-0.69, 0.60]	0.27 [-0.64, 1.17]	0.92 [-1.03, 2.86]	-0.02 [-0.49, 0.46]
tE (sec)	-0.01 [-0.22, 0.19]	-0.05 [-0.23, 0.13]	-0.22 [-0.73, 0.30]	-0.01 [-0.15, 0.13]
tI (sec)	0.02 [-0.14, 0.19]	-0.01 [-0.14, 0.12]	-0.06 [-0.27, 0.16]	0.01 [-0.10, 0.11]
tTot (sec)	0.03 [-0.17, 0.22]	-0.08 [-0.33, 0.17]	-0.26 [-0.93, 0.40]	-0.01 [-0.13, 0.12]
tI/tE	0.03 [-0.06, 0.13]	0.00 [-0.11, 0.11]	0.02 [-0.12, 0.17]	-0.01 [-0.10, 0.08]
tI/tTot	0.01 [-0.02, 0.04]	0.00 [-0.03, 0.03]	0.01 [-0.04, 0.05]	0.00 [-0.03, 0.03]
IE50	0.07 [-0.22, 0.36]	0.03 [-0.28, 0.34]	-0.03 [-0.37, 0.31]	0.06 [-0.22, 0.33]

8.9.4.3 The Effect of coughing on SLP-derived tidal breathing parameters

Figure 8-28 represents raw PNT and SLP signals measured simultaneously, the effect of the five-coughs on both traces is comparable. Differences between tidal breathing parameters estimated from SLP_{Still} and SLP_{Cough} were quantified in Table 8-8.

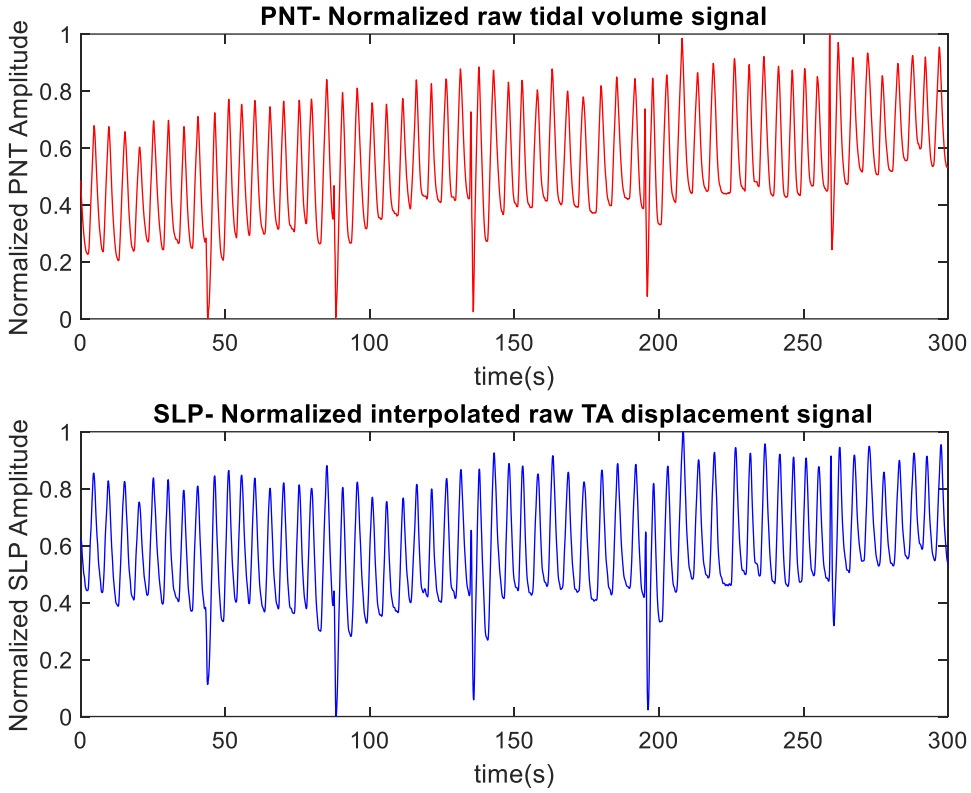

Figure 8-28. A comparison between PNT and SLP signals for one subject, both traces were normalized to facilitate visual comparison.

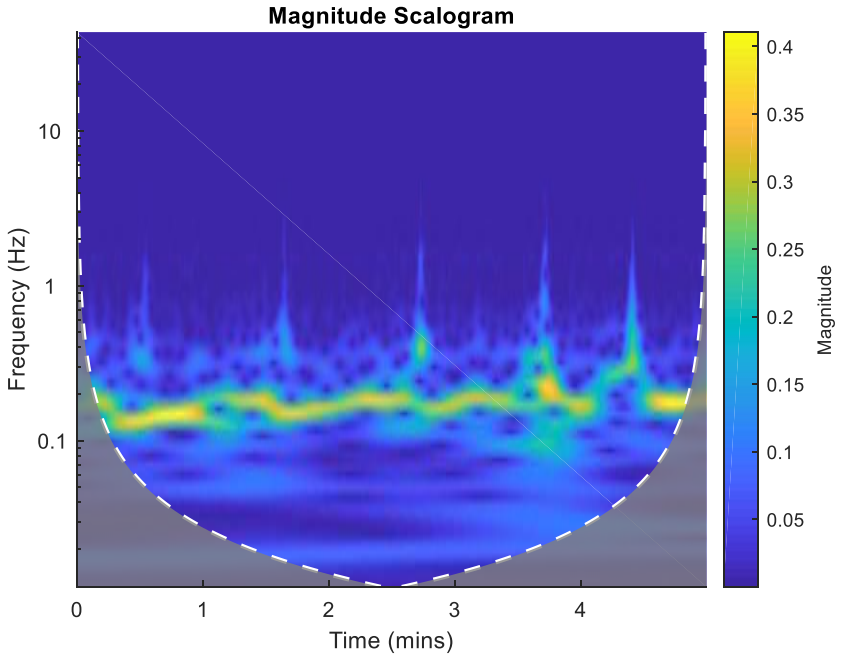

Figure 8-29. Continuous wavelet representation of SLP signal with five coughs from Sub_01.

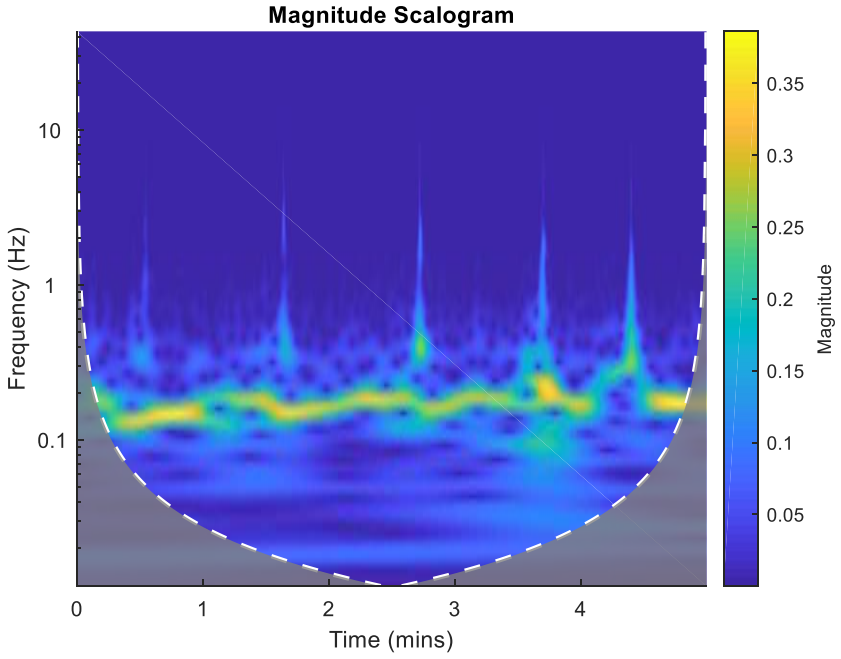

Figure 8-30. Continuous wavelet representation of a PNT signal with five coughs from Sub_01.

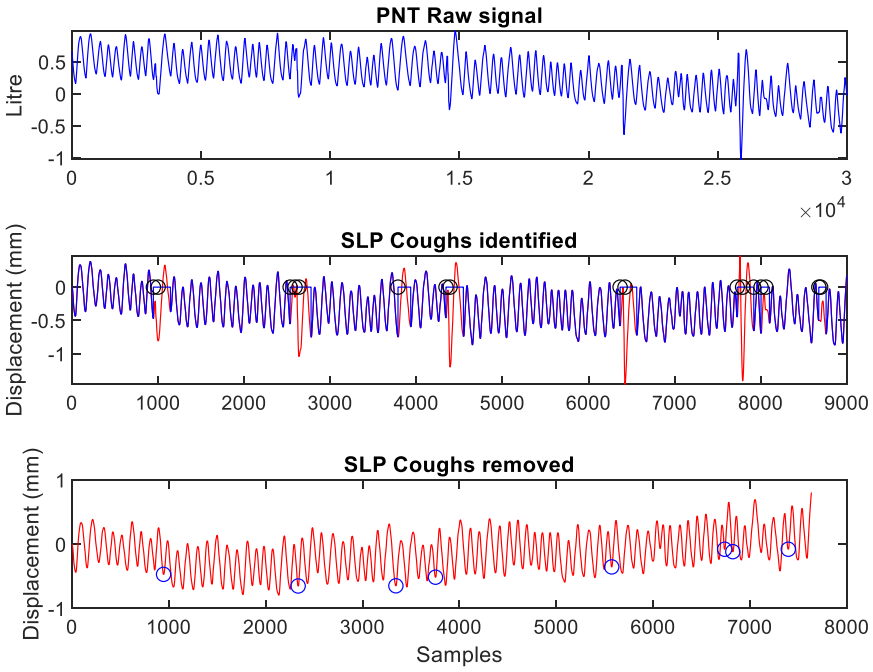

Figure 8-31. Coughs identification and removal from SLP signal using abnormalities-removal algorithm. On top a raw PNT signal which show the effect of coughs on the gold standard; in the middle SLP signal with the coughs identified; and on the bottom the identified peaks are removed, and the trace is attached at the cutting locations (identified by blue circles).

Table 8-7. The sensitivity of abnormalities-removal algorithm in detecting coughs.

Subject Number	Sensitivity (%)	Specificity (%)
Sub_01	100	98
Sub_02	100	89
Sub_03	100	94
Sub_04	100	96
Sub_05	100	96
Sub_06	100	77
Sub_07	100	90
Sub_08	100	96
Sub_09	100	96
Sub_10	80	91
Sub_12	80	100
Sub_13	80	95
Sub_14	100	100
Average	**95**	**94**

Table 8-8. Differences in tidal breathing parameters measured by SLP_{Still} and SLP_{Cough}.

Tidal Breathing Parameter	Still		Coughing		Differences	
	Mean	SD	Mean	SD	Mean	SD
RR (brpm)	13.86	2.79	14.83	2.40	0.97	-0.39
tE (sec)	2.59	0.59	2.36	0.46	-0.23	-0.13
tI (sec)	1.88	0.32	1.75	0.29	-0.13	-0.03
tTot (sec)	4.49	0.87	4.15	0.71	-0.34	-0.16
tI/tE	0.75	0.07	0.77	0.09	0.02	0.02
tI/tTot	0.43	0.02	0.43	0.03	0.00	0.01
IE50	1.51	0.26	1.55	0.35	0.04	0.09

Table 8-9. Differences in tidal breathing parameters measured by SLP_{Still} and SLP_{Cough} post the removal of coughs using the abnormalities-removal algorithm.

Tidal Breathing Parameter	Still		Post-Cough removal		Differences	
	Mean	SD	Mean	SD	Mean	SD
RR (brpm)	13.86	2.79	14.77	2.44	0.91	-0.35
tE (sec)	2.59	0.59	2.39	0.48	-0.2	-0.11
tI (sec)	1.88	0.32	1.77	0.30	-0.11	-0.02
tTot (sec)	4.49	0.87	4.18	0.74	-0.31	-0.13
tI/tE	0.75	0.07	0.77	0.09	0.02	0.02
tI/tTot	0.43	0.02	0.43	0.03	0.00	0.01
IE50	1.51	0.26	1.55	0.37	0.04	0.11

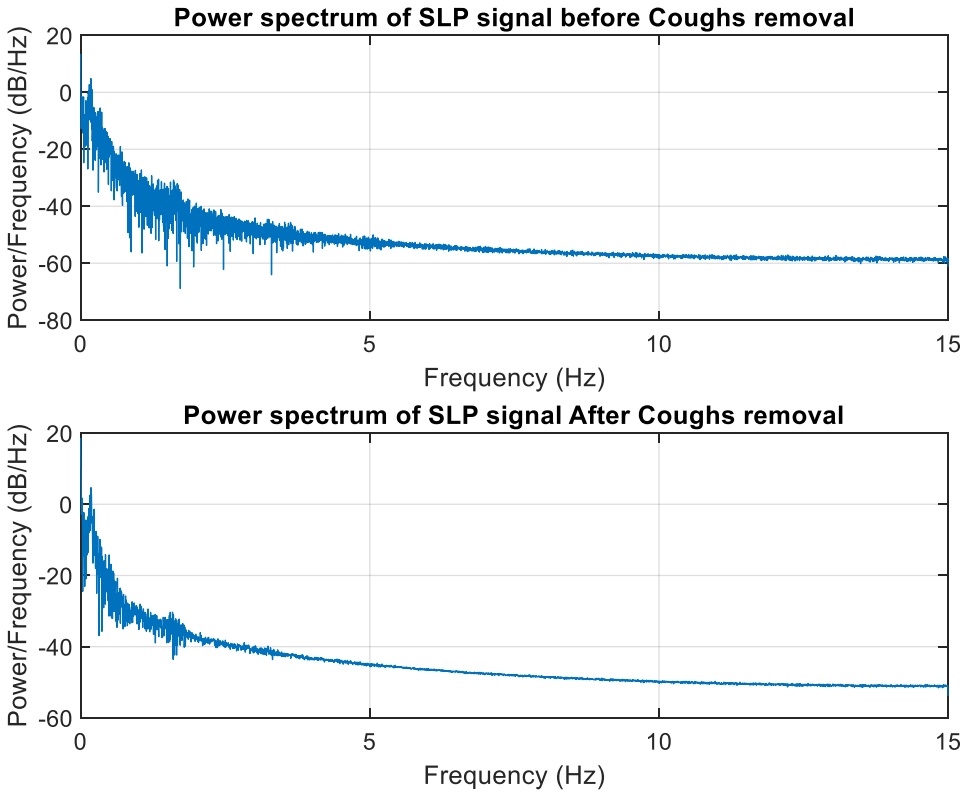

Figure 8-32. Power spectrums of an SLP signal before and after coughs removal. A part of the power of high frequencies is removed after removing the coughs.

8.10 Discussion

8.10.1 Sitting Still and Breathing

Measuring respiratory functions (i.e. flow and volume) can be performed by many techniques; however, Pneumotachograph is considered the gold standard via widespread use, among researchers and clinicians (Stick, 1996). SLP measures the displacement of the TA wall, which is a different approach for measuring tidal breathing parameters. Therefore, differences between PNT and SLP are expected (Motamedi-Fakhr et al., 2017). In this study, we have assessed the agreement between tidal breathing parameters measured simultaneously by PNT and SLP.

In the first part of this study, errors of measurement were quantified at 10, 20, 30, 40 and 47 breaths count. All subjects breathed a minimum of 47 breaths. Hence, it was the maximum value that could be chosen while not excluding any subjects. Errors were defined as the absolute means of differences between parameters from PNT and SLP and were quantified for each parameter. The optimal recording period for each parameter was then defined as the breath count associated with the minimum absolute difference between both devices. For each participant, the median value for each parameter over 10, 20, 30, 40, 47 breaths was calculated to quantify its magnitude.

Figure 8-13, Figure 8-14, Figure 8-17 and Figure 8-18 illustrate that the 10-breath period was sufficient to obtain the least error between PNT and SLP for: RR (CI ranging: 0.036 - 0.103 brpm), tI (ranging: 0.065 - 0.079 sec), tI/tE (ranging: 0.041 - 0.045) and tI/tTot (ranging: 0.015 - 0.016) respectively.

However, Figure 8-15 and Figure 8-16 show that more breaths (20-breath period) were required to get the least errors for both: tE (CI range: 0.036 - 0.064 sec) and tTot (CI range: 0.013 - 0.043 sec) respectively. Finally, Figure 8-19 shows that even more breaths (40-breath period) were needed to obtain the minimum error for IE50 (ranging: 0.005 – 0.072).

From that we can conclude that in order to obtain the least error for all the tidal breathing parameters investigated, the 40-breath period should be recorded. The Absolute and percentage differences between tidal breathing parameters measured by PNT and SLP were then quantified at 40-breaths (which correspond on average to one minute for infants, and two minutes for children).

According to (Smith and Mackay, 2011) and (Parker et al., 2016), differences in RR within two brpm are considered clinically insignificant. For this study we considered this threshold to report similarity or agreement between RR_{SLP} and RR_{PNT}. Table 8-2 shows the absolute and percentage differences between PNT and SLP in measuring RR at 40-breath period. Absolute difference and LOAs -0.10 [-0.48, 0.27], were within the clinically acceptable limit. Based on this, we concluded that RR_{SLP} and RR_{PNT} are in agreement, which is in line with the results shown in a previous study by (Motamedi-Fakhr et al., 2017).

There are no recognised clinically acceptable limits for some parameters such as tTot (Motamedi-Fakhr et al., 2017), but knowing the mathematical relation between RR and tTot and their corresponding LOAs we could infer some information.

LOAs of the absolute difference in quantifying tTot ranged between (-0.1 to 0.18 sec), and by knowing that we have previously concluded that RR_{SLP} and RR_{PNT} are in agreement at the 40-breath period. Therefore, we could anticipate that $tTot_{SLP}$ and $tTot_{PNT}$ also agree over that range. From a more precise view, low-pass filtering with 0.5 Hz cut-off is frequently used to smooth respiratory traces (Chervin, Malhotra and Burns, 2008; Walter and Vaughn, 2013), this kind of filtering can move the inspiratory and expiratory markers by up to 0.5 sec, which could indicate that such a difference is considered clinically insignificant. This might support our finding since LOAs range (-0.1 to 0.18) fall within this clinically acceptable limit. Similarly, the LOAs for tI and tE can be considered in the agreement between SLP and PNT as they all fall within that range of ±0.5 sec.

LOAs of the absolute difference in calculating tI/tE were within ±0.12 and up to 18.74% percentage difference. In the agreement study conducted by (Motamedi-Fakhr et al., 2017) over 45-sec recording, a disagreement in quantifying tI/tE over 20% was considered significant. However, the agreement was assumed to be an application dependent. Both LOAs in this study were within the reported limit. From another view, mechanical ventilation studies usually require choosing inspiration to expiration (I:E) ratios, in order to enhance patient's ventilation. tI/tE is obtained by taking the ratio between two integers; such as 1:2 or 1:4 which are commonly used settings in these studies. Hence it is unlikely that an error of 0.12 in quantifying tI/tE is clinically significant. Therefore, we have concluded that tI/tE_{SLP} and tI/tE_{PNT} are in agreement.

Differences in quantifying Duty cycle (tI/tTot) have shown a narrower LOAs range than in tI/tE -0.01 and 0.04 in terms of absolute difference, which is not known if it is clinically significant. In a previous study to validate RIP against PNT in sleeping infants, it was stated that LOAs of the difference in quantifying tI/tTot ranged between -0.016 and 0.064 (Stick et al., 1992). The LOA for our comparison was a little narrower with the mean difference close to zero, suggesting a higher agreement.

IE50 showed a relatively higher disagreement compared to the timing indices, this could be reasoned to the fact that IE50 describes the shape of the flow-volume loop from PNT signal, and the TA displacement - TA displacement rate loop from SLP signal. In (Motamedi-Fakhr *et al.*, 2017) validation study absolute and percentage mean differences over a 45-sec scan were 0.05 and 4.85 respectively, in their study they have anticipated that an improvement in the agreement could be obtained by increasing the capturing period. In this study, 40-breath period was analysed, and the mean and percentage differences in quantifying IE50 were: 0.01 and 0.67 respectively, which confirms their assumption. In their study, A 95% LOA ranging from -0.15 to 0.25 was considered relatively narrow, which was not highly affected by a longer capturing period in this study -0.2 to 0.21.

In the first part of the study, measurement errors were quantified at different breath counts 10, 20, 30, 40 and 47. 40-breath period was selected as an optimal recording period as it has provided the smallest absolute error between parameters measured by PNT and SLP. In the second part of this section, the agreement between tidal breathing parameters measured by both devices was assessed at 40-breath period using the mean of differences and 95% LOA. From the previous discussion and by adopting the same assumptions by (Motamedi-Fakhr et al., 2017), that percentage difference of 10% or less is considered clinically insignificant; we might conclude that: RR, tI, tE, tTot and tI/tTot were in agreement between SLP and PNT. tI/tE and IE50 differed by more than 10% between both devices, but the differences were lower than what have been reported by (Motamedi-Fakhr et al., 2017), this confirms their assumption; that an improvement in the agreement might be achieved by a longer capturing period.

LOAs using mean and SD could also not be representative of the true ones since most of the distributions of differences were not normally distributed. LOA ranges determined in this way are likely to be higher and should not show a false disagreement (Bland and Altman, 1999).

8.10.2 The Effect of Upper-Body Movements on the Derived Tidal Breathing Parameters

In the previous part of the study, we have examined the agreements between tidal breathing parameters quantified from SLP_{Still} and PNT_{Still} in simultaneous measurements. We have shown that including 40 breaths in the analysis offered the best agreement between the parameters if all the parameters including IE50 are considered. A much shorter recording period is required if IE50 is not to be included. The main challenge when scanning young children is their excessive movement; this movement might affect some tidal breathing parameters according to Motamedi-Fakhr, Wilson and Iles, (2017). In children, respiratory signal is one of the most difficult to establish due to movement artefacts (Almazaydeh et al., 2013), therefore understanding the effect of upper-body movement on tidal breathing parameters is crucial.

Children may be uncooperative, easily distracted and in motion. Moreover, children are less tolerant to monitoring machines. Assessing signals in such cases can be quite challenging, and the readings obtained can be misleading (Leonard et al., 2006). Incorrect readings could be dangerous in that patients could be given the wrong medications or medical procedures. Therefore, in this part of the study, we have examined the effect of upper-body movements on tidal breathing parameters, by introducing five upper body-movements during five minutes of SLP-recording. The effect of five pre-defined, artificial upper-body movements on both SLP and PNT signals was assessed by measuring the agreements between tidal breathing parameters measured by SLP and PNT in still and movement and by quantifying changes in parameters from each device between still and movement.

From Table 8-3, the agreement between PNT and SLP was affected slightly by the introduction of five-upper body movements. Means of differences and ranges of LOAs have shown an increase for both RR and tTot, an increase in the mean difference for tE and the range of LOAs for IE50 were observed. Smaller changes in the agreement were detected in tI, tI/tE and tI/tTot.

However, the changes in the agreements for all the estimated parameters remained within the clinically acceptable limits explained in the previous section.

Table 8-4 represents the changes in the parameters observed from both devices after the introduction of upper-body movements. The results show that the changes were comparable between PNT and SLP. Means of difference and LOAs ranges indicate that SLP was more influenced than PNT by this kind of artefact, which can be confirmed by purely viewing both traces on Figure 8-20. The observed increase in RR in both devices could be attributed to an increase in subjects' breathing rate as a reason of movement, and not only to the effect of movements on the estimated parameters.

For each participant, the median value for each parameter over the 5-min assessment was calculated to quantify its magnitude. The number of breaths included in the calculation varied between participants and ranged between 53 and 93 breaths. SLP-derived parameters were more likely to be influenced by upper-body movements than PNT.

Median was used to calculate parameters' magnitudes as it is a robust measure against outliers. However, the agreement between PNT and SLP derived parameters was slightly affected. This could be attributed to the artificial and exaggerated nature of the introduced movements (subjects were instructed to perform them), with higher peak-to-peak amplitudes than breathing peak-to-peak amplitudes.

Median is the value which separates the data into two halves after ranking them from lower to higher values. Hence, it is a robust measure to outliers, which could explain the small reduction in the agreement between SLP and PNT derived parameters. The agreement might be affected further if a higher number of upper-body movements is introduced to the SLP signal, as they will introduce more extreme points in each parameter's series and might have a larger effect on parameters' magnitudes.

From the previous discussion, five upper body-movements could be considered as outliers relative to the total number of breaths analysed. Moreover, these artefacts are not likely to significantly affect parameters estimation, because of the way those parameters were calculated.

SLP and PNT signals with movement artefact were further investigated using the continuous wavelet transformation (CWT), in order to identify the added frequency components on both signals. CWT was used because of its ability to reveal the time-frequency information of the signal. Figure 8-21and Figure 8-22 show the time-frequency domain of a still SLP and PNT recordings respectively, frequencies at 0.2-0.3 Hz exist at all times which are the dominant frequencies of breathing. Figure 8-23 and Figure 8-24 respectively, show the added frequencies on SLP and PNT signals due to five-upper body movements. Movement-effect could be seen clearly on the time-frequency representation of the SLP signal but not on the PNT signal, the added frequencies on the SLP extended from 0.2 to 6 Hz at the times when body-movements

occurred. Figure 8-25 shows the wavelet transformation of the reference noise (body-rocking) recorded simultaneously using Vicon, which was used to confirm that the identified added frequencies in Figure 8-23 are due to body-movements.

It was not possible to completely separate movement signal from the breathing signal using various techniques such as band-pass filtering or wavelet filtering, due to the overlap in the frequency contents of breathing and body movements at the times of movement. Applying any of those filtering approaches to remove body-movement have affected breathing parts. Therefore, spectral subtraction method was employed in a trial to use Vicon reference-noise signal in the filtering process.

Spectral subtraction successfully suppressed big parts of upper-body movements while minimally affected breathing signal. Movement peaks were reduced differently using this approach, few of them were reduced to breathing-peaks level Figure 8-26. Table 8-6 shows the increase in parameters' mean differences and LOAs ranges between SLP and PNT as a result of applying spectral subtraction. This could be attributed to the creation of new peaks (high-frequency ripples) in the place of movement peaks, which might have introduced more abnormal values. Hence, affected SLP parameters estimation and the agreement as a result. Furthermore, the reference noise signal might have contained some breathing components Figure 8-25 which could have further affected the outcomes of this filtering approach.

Table 8-6 shows the results obtained by applying the abnormalities-removal algorithm, means of differences and LOAs show an improvement in the agreement for most of the parameters. This statistical approach has shown superior performance over Spectral subtraction to recover the agreement between SLP and PNT. Rejecting peaks with abnormal amplitudes or timing was more effective and has slightly improved the robustness of parameters calculation. Furthermore, the Abnormalities-removal algorithm could identify and remove movements with high sensitivity without requiring a reference noise signal (which is not usually available in clinical settings).

As a summary, the introduced movements could be completely removed from the analysis using a statistical approach by applying the abnormalities-removal algorithm. This approach simply excludes any peak with an abnormal rising or falling amplitude (high or low) relative to the median rising or falling amplitudes of the entire trace, or an abnormal rising or falling duration (long or short) relative to the median rising or falling durations of the entire trace.

Five artificial upper-body movements were introduced to the signal and did not significantly affect the agreement between the parameters measured by SLP and PNT. Even though, this approach has successfully restored this slight effect of body movements on the agreement and thus improved the robustness of parameters calculation.

Movement removal algorithm was highly successful in identifying and removing peaks corresponding to upper-body movements. If a movement has an amplitude that falls within the amplitude range of breathing, the algorithm will use the duration (speed) of that peak to identify

it and vice versa. The sensitivity and specificity of the algorithm were 100% and 94% respectively; this shows that some real breaths that might be longer/shorter (or larger/ smaller) were excluded. The effect of removing abnormal real breaths is expected to be minimal since those values will be considered as outliers and removing them will have a small effect on the parameters. Hence, removing a real breath will be better than not removing a movement. In this study, movements were artificial, and of high amplitudes, the algorithm needs to be further assessed with more natural and complicated upper-body movements.

8.10.3 The Effect of Coughing on SLP-Derived Parameters

In the previous part of the study, we have shown that upper-body movements do not significantly affect SLP-estimated parameters. Furthermore, removing the peaks corresponding to the movements is advantageous in restoring the agreement between parameters measured simultaneously by SLP and PNT. One of the other challenges when scanning children with breathing disorders is coughing; therefore, understanding the effect of coughing on the estimated parameters is crucial.

In this part of the study, we have asked the participants to perform five coughs and to try keeping them as natural as possible, at a rate of one cough per minute. Figure 8-28 shows that the effect of the five coughs on both PNT and SLP signals is comparable. Thus, there was no point in assessing the agreement between tidal breathing parameters measured by both devices in this case.

SLP and PNT signals with coughs were further investigated using the continuous wavelet transformation (cwt), in order to identify the added frequency components on both signals. Added frequencies on both signals spread from 0.3 to 6 Hz, with the highest powers at the frequencies below 1 Hz Figure 8-29 and Figure 8-30. It was not possible to completely separate coughs from breathing signal using various filtering techniques such as band-pass filtering or wavelet filtering, due to the overlap in the frequency contents of breathing and coughing.

SLP-estimated parameters were compared between both sessions: still and with coughing, to quantify the effect of coughs on the parameters. Table 8-8 shows the differences between the means of the parameters at still and cough. Small differences were observed in almost all the parameters except tI/tTot which stayed the same. This could be attributed to the robustness of the algorithm used to calculate the parameters against outliers, as it uses the median value to quantify parameters' magnitudes.

Coughs should be considered as rejected breaths as they do not represent a normal tidal breathing cycle. Coughs have few features that distinguish them from tidal breathing; firstly, a high amplitude and secondly a shorter duration, both of those features could be identified using the abnormalities-removal algorithm. Figure 8-31 presents the identification and removal of coughs from one SLP signal; it shows the ability of the algorithm to detect the five coughs and remove them from the trace.

Table 8-7 shows the high sensitivity and specificity of the algorithm in detecting coughs 95% and 94% respectively. This confirms that most of the coughs were detected and removed. Few real breaths were removed because of their abnormal amplitude or duration, which is not expected to highly affect parameters estimation (as they were considered as outliers).

Table 8-9 represents the differences between the means of the parameters at still and coughs post coughs removal. There were clear drops in the differences in RR, tE, tI and tTot (mean and SD). Differences in tI/tE, tI/tTot and IE50 stayed the same.

Power spectrum in Figure 8-32 shows the removal of a part of the power of higher frequencies after removing the five coughs from an SLP signal.

As a summary; differences in tidal breathing parameters were observed between SLP_{Still} and SLP_{Cough}. Those differences could be caused by the introduction of the coughs or the normal difference (variability) between the two sessions. The application of abnormalities-removal algorithm has identified and removed most of the coughs and resulted in a drop in the differences for most of the parameters. A difference in RR, for example, stayed 0.91 brpm, which may indicate that this difference could have been caused by an increase in the breathing rate of the subjects as a result of coughing.

9 General Discussion

This thesis was informed by four main studies, all of which evaluated the reliability of SLP for measuring tidal breathing parameters. The purpose of this chapter is, therefore, to consolidate the results and discussions from individual chapters, relating to the aforementioned studies, into a summative conclusion and final discussion.

An accurate assessment of lung function is crucial for effective management of respiratory conditions (Beydon *et al.*, 2007; Wijngaart, Roukema and Merkus, 2015). Spirometry, conventionally used for the assessment of lung function, typically requires the patient to have a level of compliance and understanding when undertaking the assessment. Hence, it is often not appropriate for young children (Wijngaart, Roukema and Merkus, 2015). Alternative approaches include the use of PNT or RIP for the measurement of tidal breathing patterns. Their clinical usefulness for application in children is however limited, due to the testing equipment used, e.g. use of a mouthpiece in PNT can cause changes to breathing patterns, and slippage of the band can result in erroneous readings in RIP (Weissman *et al.*, 1984; Stick *et al.*, 1992; Caretti *et al.*, 1994; Laveneziana *et al.*, 2015a). SLP was therefore identified as a possible modality for overcoming these limitations, as it is a light-based, non-contact technique which allows a detailed assessment of tidal breathing patterns over successive breaths. SLP can be performed in either seated or supine positions and requires minimal subject cooperation. This is arguably a more suitable method for young children and infants. However, before SLP can be implemented clinically, it is important to ensure that the measures taken accurately reflect the patient's true lung function, as these measures may be used to diagnose respiratory conditions, monitor disease progression and responses to pharmacological interventions.

Therefore, the primary step in determining the reliability of SLP required an evaluation of SLP for lung function monitoring in a paediatric population. The first study therefore, investigated the use of SLP in assessing tidal breathing in school-age children (7-16 years). In order to identify if SLP could detect differences in lung function between normative and pathological populations, children with asthma were compared with healthy children in this study. Additionally, the effect of bronchodilator administration on both spirometry and SLP-estimated parameters in the asthmatic group were investigated. Our results showed that SLP could differentiate between school-age children with and without asthma and may detect responses to bronchodilation. The most informative parameter was $IE50_{SLP}$ ($IE50_{SLP}$, quantified as $TIF50_{SLP}/TEF50_{SLP}$), which was significantly higher in children with stable asthma compared to healthy controls of a similar age. As previously discussed, in asthma, the airways are narrowed due to the inflammation in the airway walls and constriction of smooth muscles surrounding them. This narrowing in the diameter becomes clear when exhalation occurs as exhalation causes further narrowing in these obstructed airways. Hence, a reduction in $TEF50_{SLP}$ was observed, which leads to an increased IE50 value in the asthmatic group.

This result is in line with the findings observed by (Papiris *et al.*, 2002; Tauber *et al.*, 2003). A high success rate for the procedure was shown in this age group, and hence, it was concluded

that SLP could be successfully utilised in school-age children (aged 7-16 years) and that it is sensitive enough to detect airways obstruction in the asthmatic group. All the above points suggest several relative clinical applicability advantages for SLP. Using SLP comes with several conveniences over spirometry. First, SLP is a non-invasive technique, and its minimal subjects' cooperation requirements make it more convenient for young children. In addition, the contactless nature of its procedure reduces the risk of cross-infection. Finally, the simplicity of the procedure and minimal training requirements, compared to spirometry, gives a superior clinical preference. In short, using spirometry accurately would require several factors to be considered: intensive training for the clinician, cooperation from the participant and in-session coaching and instructing to ensure that the child is cooperating correctly. All these features might give precedence to using SLP as a quick monitoring tool to assess lung functions of children in none-specialised health services, such as schools and GP practices.

Following this study, it was identified that further research was required before recommending the use of SLP in younger children, with or without respiratory pathology. Therefore, another study on children (2-12 years) recovering from acute asthma/wheeze was carried out. It was demonstrated that SLP could be performed successfully in children as young as two years of age. Many SLP parameters have differentiated between acute asthmatics and their healthy counterparts, specifically, $IE50_{SLP}$ and chest versus abdominal asynchrony TAA_{SLP}. The increased $IE50_{SLP}$ value in the acute asthma group is in line with the observations seen in older children with airways obstruction. However, $IE50_{SLP}$ stayed higher than normal after bronchodilation administration, which suggests no response to treatment, even though children were in the recovery phase of their disease. This contradicted the findings in the first study related to stable asthma, where $IE50_{SLP}$ dropped significantly after bronchodilation administration. TAA_{SLP} was also higher in children with acute asthma, which was expected because of the increased work of breathing they experience, resulting in a loss of thoracoabdominal synchrony (Lødrup, 2000; Giordano *et al.*, 2012). The within-subject variability in TAA was higher in children with acute asthma suggesting a compensatory mechanism in which spatial variability is introduced into the system when temporal variability is reduced. Within-subject variability of asynchrony was not observed in the first study, which might be attributed to the reduced chest wall compliance in older children, and hence, less tendency for regional variation. One parameter $vTPTEF/tE_{SLP}$ of the SLP was able to detect a response to bronchodilator administration in this study. SLP has shown a unique value in the preschool age group, where traditional airflow obstruction assessments are challenging. This may be useful for providing an accurate asthma diagnosis within this age group. Although the success rate of spirometry in preschool children was reported differently between studies (Aurora *et al.*, 2004), in a feasibility study by Kampschmidt *et al.* (2016), success rates of 45%, 65% and 87% for three, four and five years old, respectively was reported. The preliminary results reported in this study and the associated high success rate of 87% (93.7% for 6-12 years and 83.9% for 2-5 years), may support further investigations to assess the age-effect on breathing patterns. These points might suggest the use of SLP in obtaining objective clinical measures of lung function, specifically in pre-school children. This is because in this population obtaining accurate lung function measurements is challenging using conventional techniques.

Moreover, SLP can be used clinically to assess the natural recovery of asthma or the effect of different interventions. Further study on the technique and the data analysis methods is required before introducing SLP into routine clinical practice.

After showing the high success rate in children with airways obstruction above two years of age, the next study was carried out to check the feasibility of SLP in infants recovering from acute viral bronchiolitis (0-1 year). SLP-estimated tidal breathing parameters in the AVB group were compared with those in healthy infants. Differences in the parameters between admission and discharge in the AVB group were also investigated. In this study, even though a high success rate of the procedure was shown, excessive movement of infants did not allow a full five-minute scan to be obtained. However, this study showed that three SLP parameters, specifically, $IE50_{SLP}$, $vIE50_{SLP}$ and TAA_{SLP} were able to differentiate between healthy infants and those with AVB. $IE50_{SLP}$ was significantly lower in the AVB group, which contradicts our findings from the previous two studies on older children with asthma, where $IE50_{SLP}$ was significantly higher compared to healthy children. TAA_{SLP} was significantly higher in the AVB group compared to the healthy group, which is in line with what is reported in study two, that a loss of thoraco-abdominal synchrony is caused by the increased work of breathing resulted from airway obstruction.

The reduced value of $vIE50_{SLP}$ on admission and its increase on discharge toward the value seen in the healthy group was expected. This is in line with the previously reported results stating that an increased load on the respiratory system caused by the obstruction make it more rigid, hence reduces its within-subject variability. As a result of the natural recovery of the condition, the load on the respiratory system decreases and this, in turn, will reduce its rigidity leading to an increase in within-subject variability.

SLP has been proposed as a method for overcoming limitations associated with other methods used to obtain breathing measures. However, it is apparent that an optimal recording condition for SLP requires the child to remain still throughout, as upper-body movements would interfere with the signal. Five minutes of still recording (requested by the manufacturer) is a long period which is sometimes challenging to obtain in children. Therefore, the optimal recording time to obtain the minimum differences between SLP and PNT parameters was investigated. A total of 40 breaths, two minutes for a child and one minute for an infant, was found to be sufficient for meeting this condition. The agreement between parameters, measured by both devices at that duration, was found to fall within the clinically acceptable limits and the agreements were consistent with the finding observed by Motamedi-Fakhr *et al.* (2017).

In the previous studies, other sources of interference stemming from coughing and upper-body movement especially in the younger age group were observed during data acquisition. The effect of these movement artefact sources on SLP-estimated tidal breathing parameters had not been previously studied. Hence, the next study was carried out in order to quantify and evaluate the effect of these artefact sources on SLP measures. In the final study, upper-body movements

and coughs were introduced to the SLP signals in two separate lab settings, to investigate their effect on SLP and PNT simultaneous recordings.

The five-artificial upper-body movements, introduced to SLP recording, minimally affected the agreement between PNT and SLP. In addition, any changes in the parameters from both devices were comparable. These results have shown the stability of the algorithm, as it uses the robust median to calculate the parameter from successive breaths. The added movements would have introduced outliers to each parameter sequence but would have only minimally affected the parameter estimation. The study has also shown the overlap in frequency contents between upper-body movements and breathing, which made it challenging to separate movement signal from breathing using ordinary filtering techniques. A statistical approach for removing upper-body movements from the trace was used and demonstrated superior performance in improving the agreement between SLP and PNT over the spectral subtraction method. Spectral subtraction algorithm requires recording of the interference using an external system (Vicon) as a reference signal, which is not usually available in clinical settings.

For artefact stemming from coughs, these episodes were considered as rejected breaths because they did not represent tidal breathing cycles. Furthermore, they showed an overlap in frequency content with the breathing signal. The application of a statistical approach successfully identified and removed coughs, reducing the differences between SLP_{Still} and SLP_{Cough} for most of the studied parameters.

9.1 Limitations

The studies carried out in this research shows the possible advantages of using SLP to display the difference in respiratory disease compared to normal control data as well as showing changes as recovery from illness happen. However, the clinical usefulness of this method remains to be proven. If SLP succeeded in offering additional clinically meaningful information to help to improve our diagnosis and management, its adaptation in a clinical setting would be justified.

In preschool children, although SLP was successful in obtaining objective measurements of lung function, their link to certain pathological or physiological changes need to be further investigated. It is worth mentioning that, even though SLP has shown differences between health and disease in this group, it was not backed up by a gold standard method, spirometry, which is not used clinically in this age group at present.

It is also important to point out that the effects of upper-body movements and coughs were investigated. However, these were from healthy adults and were artificial. This might not represent the natural coughs and body movements encountered in diseased children in the actual clinical setting. Further study to assess the effectiveness of abnormality-removal algorithm on detecting and removing these artefacts in this age group is therefore needed.

10 Conclusion and Future Work

My research focused on finding a suitable technique to assess lung function, as there is a need for accurate assessment that is convenient for the patient and suitable for younger ages. The difficulties in lung function assessment in children are well established and have been described in this thesis.

Tidal breathing was considered as an alternative approach to forced manoeuvres for measuring breathing, but the clinical non-practicality of the measuring devices used for this purpose have limited its use. SLP is a novel technique to measure tidal breathing which would arguably solve the shortcoming of the previous techniques and provide a new approach for assessing lung function in children.

The main findings of this thesis are that SLP can be considered a reliable measure for assessing lung function in children aged 0 to 17 years, with each of the three studies showing development in the assessment in terms of the ages of the children. The target was to allow a non-invasive method for children as young as few weeks old, ensuring that data collected is accurate and provide data for children that have been presented with normal lung function as well as those with affected lung function, specifically stable asthma, acute asthma/wheeze and acute viral bronchiolitis.

The first study showed that $IE50_{SLP}$ was able to detect airways obstruction and identify responses to bronchodilator in children with stable asthma (6-17 years). In this study, I determined the reality of SLP in quantifying lung functions; the children were tested with both spirometry and SLP to establish a comparison between the techniques, with spirometry being a suitable technique to show lung obstruction and the effect of the treatment used. SLP was used here to check the feasibility of SLP in those children and to check if the parameters are sensitive enough to classify between asthmatics and healthy patients.

The second study showed that $IE50_{SLP}$ and asynchrony parameters, along with the within-subject variability of multiple parameters differentiated between children with acute asthma (2-12 years) and their healthy counterparts and had detected recovery. In this study, SLP has shown usefulness in preschool children where assessment of airflow obstruction is challenging.

The third study showed again that $IE50_{SLP}$ and TAA_{SLP}, along with the within-subject variability of multiple parameters could be used to differentiate between infants with AVB and healthy infants; $vIE50_{SLP}$ may also be used to detect recovery. This study is a feasibility study that shows that even younger children can be scanned using SLP. The main progression within each of these tests is the age groups of the patients, with the first a larger older range of 7-16 years old, the second a more focused age group of 2-12 years old and the third most specific for those under 2 years of age.

These preliminary results look promising and support further study and refinement of the technique and data analysis methods with an aim toward introducing it to routine clinical

practice. Further study to evaluate the effects of age on breathing patterns is also required; SLP may represent a method for assessing lung function in patient populations in whom traditional techniques such as spirometry cannot be conveniently used.

A more detailed investigation of thoracoabdominal asynchrony (TAA) parameter could be useful, by quantifying the inspiratory and expiratory TAA separately. This separation can provide a detailed information about the phase when asynchrony between thoracic and abdomen become apparent, which might help clinicians in supporting their diagnosis based on the physiological basis of each condition.

In addition, a larger study would help in determining the diagnostic ability of SLP in children with asthma. More investigations are also required on infants with AVB, as the findings in this cohort contradicted our hypothesis about obstruction. Furthermore, different respiratory and neuromascular conditions in younger population could be investigated using SLP, which might help clinicians in monitoring and managing theese condition.

SLP could be a promising technique in conditions that involve chest wall deformities particularly in children, and to monitor the changes in breathing after a surgical intervention, more researches in this area are recommended.

In Adults, SLP might be a promising technique in elderly and severely ill patients (such as patients in the ICU) as a quick scanning tool to assess their lung functions when their cooperation cannot be achieved.

Whilst the sources of artefact were identified, these could be overcome by implementing a statistical approach to remove them from the analysis rather than trying to filter them out of SLP signal, as those artefacts overlap in frequency with breathing. Further investigation on the abnormalities-removal algorithm is required to assess its robustness in detecting more complex upper-body movements (child's movement in real clinical setting). Furthermore, SLP data could have been filtered using different approaches if the displacement of every single square of the projected light was provided. Upper-body movements could be then identified by looking at the movement of the squares in each corner of the grid and compare their movements with respect to each other. This could help in identifying different nature of movements and can possibly be used in adaptively removing this movement from the raw data.

Researches on the potential use of SLP in continuous monitoring could be conducted especially with young infants with sleeping apnoea, who will be lying in a supine position, and SLP might help in further understanding the changes in their breathing patterns at different sleeping stages. The feasibility of SLP in those infant need to be investigated, accounting for the possibility that infants might frequently change their sleeping position.

In summary, SLP may offer a new approach to assess lung function in children, especially pre-school children, where conventional techniques such as spirometry are not usually obtainable. Due to its ease of use and limited requirement of training, such technique can be used in health

centres, within schools or other institutions to bring about a quick assessment of lung function of the patient. The study shows that SLP can be used for children, and not only in adults, it is sensitive to obstruction and matches data used in spirometry for older children.

11 References:

Adams, J. A. *et al.* (1993) 'Measurement of breath amplitudes: comparison of three noninvasive respiratory monitors to integrated pneumotachograph', *Pediatric pulmonology*. Wiley Online Library, 16(4), pp. 254–258.

Allen, J. L. *et al.* (1990) 'Thoracoabdominal asynchrony in Infants with', *Am Rev Respir Dis*. Am Thoracic Soc, 141, pp. 337–342.

Almazaydeh, L. *et al.* (2013) 'Apnea detection based on respiratory signal classification', *Procedia Computer Science*. Elsevier Masson SAS, 21, pp. 310–316. doi: 10.1016/j.procs.2013.09.041.

Anatomy-medicine (2018) *Respiratory System*. Available at: https://anatomy-medicine.com/respiratory-system/22-respiratory-system.html (Accessed: 12 January 2017).

Angus, G. E. and Thurlbeck, W. M. (1972) 'Number of alveoli in the human lung.', *Journal of applied physiology*. Am Physiological Soc, 32(4), pp. 483–485.

Asthma UK (2018) *Asthma facts and statistics*. Available at: //www.asthma.org.uk/about/media/facts-and-statistics/.

Aurora, P. *et al.* (2004) 'Quality control for spirometry in preschool children with and without lung disease', *American journal of respiratory and critical care medicine*. American Thoracic Society, 169(10), pp. 1152–1159.

Baker, R. R. *et al.* (2000) 'Poor perception of airway obstruction in children with asthma', *Journal of asthma*. Taylor & Francis, 37(7), pp. 613–624.

Banovcin, P., Seidenberg, J. and der Hardt, H. (1995) 'Assessment of tidal breathing patterns for monitoring of bronchial obstruction in infants', *Pediatric research*. Nature Publishing Group, 38(2), p. 218.

Banovcin, P., Seidenberg, J. and Von Der Hardt, H. (1995) 'Assessment of tidal breathing patterns for monitoring of bronchial obstruction in infants', *Pediatric Research*, 38(2), pp. 218–220. doi: 10.1203/00006450-199508000-00014.

Bateman, E. D. *et al.* (2008) 'Global strategy for asthma management and prevention: GINA executive summary', *European Respiratory Journal*. Eur Respiratory Soc, 31(1), pp. 143–178.

Bates, J. H. *et al.* (2000) 'Tidal breath analysis for infant pulmonary function testing. ERS/ATS task force on standards for infant respiratory function testing. European respiratory society/American thoracic society', *European Respiratory Journal*. Eur Respiratory Soc, 16(6), pp. 1180–1192.

Beachey, W. (2018) *Respiratory care anatomy and physiology: foundations for clinical practice*. Elsevier Health Sciences.

Beydon, N. *et al.* (2007) 'An official American Thoracic Society/European Respiratory Society statement: pulmonary function testing in preschool children', *American journal of respiratory*

and critical care medicine. Am Thoracic Soc, 175(12), pp. 1304–1345.

Björgvinsson, T. and Kerr, P. (1995) 'Use of a common language effect size statistic.', *The American journal of psychiatry*. American Psychiatric Assn.

Black, J. *et al.* (2004) 'Assessment of Airway Function in Young Children with Asthma: Comparison of Spirometry, Interrupter Technique, and Tidal Flow by Inductance Plethsmography', *Pediatric pulmonology*. Wiley Online Library, 37(6), pp. 548–553.

Bland, J. M. and Altman, D. G. (1986) 'Statistical Methods for Assessing Agreement Between Two Methods of Clinical Measurement', *Lancet*, 327, pp. 307–310. doi: 10.1016/S0140-6736(86)90837-8.

Bland, J. M. and Altman, D. G. (1999) 'Measuring agreement in method comparison studies', *Statistical Methods in Medical Research*, 8(2), pp. 135–160. doi: 10.1191/096228099673819272.

Blanken, M. O. *et al.* (2013) 'Respiratory syncytial virus and recurrent wheeze in healthy preterm infants', *New England Journal of Medicine*. Mass Medical Soc, 368(19), pp. 1791–1799.

Blinowska, K. J. and Zygierewicz, J. (2012) *Practical Biomedical Signal Analysis Using MATLAB*, *Eshwar Books*. doi: 10.1201/b11148.

Boer, W. H. De *et al.* (2010) 'SLP: A Zero-Contact Non-Invasive Method for Pulmonary Function Testing', *Procedings of the British Machine Vision Conference 2010*, p. 85.1-85.12. doi: 10.5244/C.24.85.

Boll, S. (1979) 'Suppression of acoustic noise in speech using spectral subtraction', *IEEE Transactions on acoustics, speech, and signal processing*. IEEE, 27(2), pp. 113–120.

Brack, T., Jubran, A. and Tobin, M. J. (2002) 'Dyspnea and decreased variability of breathing in patients with restrictive lung disease', *American journal of respiratory and critical care medicine*. Am Thoracic Soc, 165(9), pp. 1260–1264.

Brand, P. L. P. *et al.* (2008) 'Definition, assessment and treatment of wheezing disorders in preschool children: an evidence-based approach', *European Respiratory Journal*. Eur Respiratory Soc, 32(4), pp. 1096–1110.

Brouillette, R. T. *et al.* (1987) 'Comparison of respiratory inductive plethysmography and thoracic impedance for apnea monitoring', *The Journal of pediatrics*. Elsevier, 111(3), pp. 377–383.

Brusasco, V., Crapo, R. and Viegi, G. (2005) 'Coming together: the ATS/ERS consensus on clinical pulmonary function testing'. Eur Respiratory Soc.

Bryan, A. C. and Wohl, M. E. B. (2011) 'Respiratory mechanics in children', *Comprehensive Physiology*. Wiley Online Library.

BTS (2006) 'The Burden of Lung Disease 2nd ed.', *The British Thoracic Society*, pp. 1–47.

Burgel, P. R. *et al.* (2009) 'Update on the roles of distal airways in asthma', *European Respiratory Review*. Eur Respiratory Soc, 18(112), pp. 80–95.

Burrus, C. S., Gopinath, R. a and Guo, H. (1998) *Introduction to Wavelets and Wavelet Transforms: A Primer*, *Recherche*. Available at: http://www.amazon.com/Introduction-Wavelets-Wavelet-Transforms-Primer/dp/0134896009.

Bush, A. and Davies, J. (2005) 'Early detection of lung disease in preschool children with cystic fibrosis', *Current opinion in pulmonary medicine*. LWW, 11(6), pp. 534–538.

Bush, A., Grigg, J. and Saglani, S. (2014) 'Managing wheeze in preschool children', *BMJ (Online)*, 348(February), pp. 1–7. doi: 10.1136/bmj.g15.

Bush, A. and Thomson, A. H. (2007) 'Acute bronchiolitis', *Bmj*, 335(7628), pp. 1037–1041. doi: 10.1136/bmj.39374.600081.AD.

Caretti, D. M. *et al.* (1994) 'Reliability of respiratory inductive plethysmography for measuring tidal volume during exercise', *American Industrial Hygiene Association Journal*. Taylor & Francis, 55(10), pp. 918–923.

Carlsen, K. C. L. *et al.* (1995) 'Eosinophil cationic protein and tidal flow volume loops in children 0-2 years of age', *European Respiratory Journal*. Eur Respiratory Soc, 8(7), pp. 1148–1154.

Castro-Rodriguez, J. A., Rodriguez-Martinez, C. E. and Custovic, A. (2012) 'Infantile and preschool asthma', *Paediatric asthma. Eur Respir Monogr*. Copyright ERS, 56, pp. 10–21.

Challis, R. E. and Kitney, R. I. (1982) 'The Design of Digital Filters for Biomedical Signal Processing Part 1 : Basic Concepts', *Journal of Biomedical Engineering*, 4, pp. 267–278.

Chervin, R. D., Malhotra, R. K. and Burns, J. W. (2008) 'Respiratory cycle-related EEG changes during sleep reflect esophageal pressures.', *Sleep*, 31, pp. 1713–1720.

Chu, W. C. W. *et al.* (2006) 'Dynamic magnetic resonance imaging in assessing lung volumes, chest wall, and diaphragm motions in adolescent idiopathic scoliosis versus normal controls', *Spine*. LWW, 31(19), pp. 2243–2249.

Clinicalgate (2015) *Pulmonary Function Testing Equipment*. Available at: https://clinicalgate.com/pulmonary-function-testing-equipment/ (Accessed: 22 March 2018).

Cooper, P. J. *et al.* (1990) 'Variability of pulmonary function tests in cystic fibrosis', *Pediatric pulmonology*. Wiley Online Library, 8(1), pp. 16–22.

Cotes, J. E., Chinn, D. J. and Miller, M. R. (2009) *Lung function: physiology, measurement and application in medicine*. John Wiley & Sons.

Crenesse, D. *et al.* (2001) 'Spirometry in children aged 3 to 5 years: reliability of forced expiratory maneuvers', *Pediatric pulmonology*. Wiley Online Library, 32(1), pp. 56–61.

Davenport, P. W. and Kifle, Y. (2001) 'Inspiratory resistive load detection in children with life-threatening asthma', *Pediatric pulmonology*. Wiley Online Library, 32(1), pp. 44–48.

Davies, J. C. and Alton, E. W. F. W. (2009) ‘Monitoring respiratory disease severity in cystic fibrosis’, *Respiratory care*. Respiratory Care, 54(5), pp. 606–617.

Davis, C. *et al.* (1999) ‘A new sensor for monitoring chest wall motion during high-frequency oscillatory ventilation’, *Medical engineering & physics*. Elsevier, 21(9), pp. 619–623.

Davis, G. M. (2002) *Noise reduction in speech applications*. CRC Press.

Decramer, M. (1997) ‘Hyperinflation and respiratory muscle interaction’, *European Respiratory Journal*, 10(4), pp. 934–941. doi: 10.1183/09031936.97.10040934.

Dehkordi, P. *et al.* (2014) ‘Assessment of respiratory flow and efforts using upper-body acceleration’, *Medical & biological engineering & computing*. Springer, 52(8), pp. 653–661.

Delgutte (2007) ‘INTRODUCTION TO BIOMEDICAL SIGNAL AND IMAGE c Bertrand Delgutte 1999 Signals convey information Stages in biomedical signal processing’, *Image Processing*, pp. 1–2.

Dellaca, R. L. *et al.* (2010) ‘Measurement of total and compartmental lung volume changes in newborns by optoelectronic plethysmography’, *Pediatric research*. Nature Publishing Group, 67(1), p. 11.

Deshpande, S. A. and Northern, V. (2003) ‘The clinical and health economic burden of respiratory syncytial virus disease among children under 2 years of age in a defined geographical area’, *Archives of disease in childhood*. BMJ Publishing Group Ltd, 88(12), pp. 1065–1069.

Devlieger, H. *et al.* (1991) ‘The diaphragm of the newborn infant: anatomical and ultrasonographic studies.’, *Journal of developmental physiology*, 16(6), pp. 321–329.

Douglas, G. *et al.* (2008) ‘British guideline on the management of asthma: a national clinical guideline’, *Thorax*. BMJ Group, 63(Suppl. 4), pp. iv1--iv121.

Drakatos, P. *et al.* (2016) ‘The utility of respiratory inductance plethysmography in REM sleep scoring during multiple sleep latency testing’, *Respiratory physiology & neurobiology*. Elsevier, 230, pp. 1–4.

Elshafie, G. *et al.* (2016) ‘Measuring changes in chest wall motion after lung resection using structured light plethysmography: A feasibility study’, *Interactive Cardiovascular and Thoracic Surgery*, 23(4), pp. 544–547. doi: 10.1093/icvts/ivw185.

van der Ent, C. K. *et al.* (1996) ‘Tidal breathing analysis as a measure of airway obstruction in children three years of age and older.’, *American Journal of Respiratory and Critical Care Medicine*, 153(4), pp. 1253–1258. doi: 10.1164/ajrccm.153.4.8616550.

Faugeras, O. *et al.* (1993) *Real time correlation-based stereo: algorithm, implementations and applications*.

Faugeras, O. (1993) *Three-Dimensional computer vision (artificial intelligence)*. The MIT Press Cambridge. doi: 9780262061582.

Ferrigno, G. *et al.* (1994) 'Three-dimensional optical analysis of chest wall motion', *Journal of Applied Physiology*. Am Physiological Soc, 77(3), pp. 1224–1231.

Flume, P. A. *et al.* (2007) 'Cystic Fibrosis Foundation, Pulmonary Therapies Committee. Cystic fibrosis pulmonary guidelines: chronic medications for maintenance of lung health', *Am J Respir Crit Care Med*, 176(10), pp. 957–969.

Frey, U. and Merkus, P. (2010) *Paediatric Lung Function: European Respiratory Monograph*. European Respiratory Society.

Gajdos, V. *et al.* (2010) 'Effectiveness of chest physiotherapy in infants hospitalized with acute bronchiolitis: A multicenter, randomized, controlled trial', *PLoS Medicine*, 7(9). doi: 10.1371/journal.pmed.1000345.

Gaultier, C. (1995) 'Respiratory muscle function in infants', *European Respiratory Journal*, 8(1), pp. 150–153. doi: 10.1183/09031936.95.08010150.

Gaultier, C. and Gallego, J. (2005) 'Development of respiratory control: evolving concepts and perspectives', *Respiratory physiology & neurobiology*. Elsevier, 149(1–3), pp. 3–15.

Ghezzi, M. *et al.* (2017) 'Structured Light Plethysmography (SLP): Management and follow up of a paediatric patient with pneumonia', *Respiratory Medicine Case Reports*. Elsevier Ltd. doi: 10.1016/j.rmcr.2017.06.004.

Gilbert *et al.* (1972) 'Changes in tidal volume, frequency, and ventilation induced by their measurement.', *Journal of Applied Physiology*, 33(2), pp. 252–254.

Giordano, K. *et al.* (2012) 'Pulmonary function tests in emergency department pediatric patients with acute wheezing/asthma exacerbation', *Pulmonary medicine*. Hindawi, 2012.

Glass, R. B. J. *et al.* (2002) 'Pediatric ribs: a spectrum of abnormalities', *Radiographics*. Radiological Society of North America, 22(1), pp. 87–104.

Glezen, W. P. *et al.* (1986) 'Risk of primary infection and reinfection with respiratory syncytial virus', *American journal of diseases of children*. American Medical Association, 140(6), pp. 543–546.

Goldman, M. D., Smith, H. J. and Ulmer, W. T. (2005) 'Whole-body plethysmography', *European Respiratory Monograph*. European Respiratory Society, 31, p. 15.

Green, C. A. *et al.* (2016) 'Admission to hospital for bronchiolitis in England: Trends over five decades, geographical variation and association with perinatal characteristics and subsequent asthma', *Archives of Disease in Childhood*, 101(2), pp. 140–146. doi: 10.1136/archdischild-2015-308723.

Greenough, A. (2003) 'Transient tachypnea of the newborn (TTN)', *Neonatal Respiratory Disorders. London, England: Arnold Publishers*, pp. 272–277.

Greenough, A. (2009) 'Role of ventilation in RSV disease: CPAP, ventilation, HFO, ECMO', *Paediatric respiratory reviews*. Elsevier, 10, pp. 26–28.

Grol, M. H. *et al.* (1999) 'Risk factors for growth and decline of lung function in asthmatic individuals up to age 42 years: a 30-year follow-up study', *American journal of respiratory and critical care medicine*. Am Thoracic Soc, 160(6), pp. 1830–1837.

Haddad, G. G., Abman, S. H. and Chernick, V. (2002) *Chernick-Mellins basic mechanisms of pediatric respiratory disease*. London: BC Decker Inc.

Hall, C. B. *et al.* (2009) 'The burden of respiratory syncytial virus infection in young children', *New England Journal of Medicine*. Mass Medical Soc, 360(6), pp. 588–598.

Hamid, Q., Shannon, J. and Martin, J. (2005) *Physiologic basis of respiratory disease*. London: BC Decker Inc.

Hargrove, J., Zemper, E. D. and Jannausch, M. L. (2009) 'Respiratory measurement utilizing a novel laser displacement technique: normal tidal breathing', *Biomedical instrumentation & technology*, 43(4), pp. 327–331.

Heldt, G. P. (1988) 'Simultaneous quantification of chest wall distortion by multiple methods in preterm infants', *Am Rev Respir Dis*, 138(1), pp. 20–25.

Herrmann, K. A. *et al.* (2006) 'Cine MRI of the thorax in patients with pectus excavatum; CINE-MRT des Thorax bei Patienten mit Pectus excavatum'.

Hershenson, M. B. *et al.* (1990) 'Changes in the Contribution of the Rib Cage to Tidal Breathing during Infancy1-3', *Am Rev Respir Dis*. Am Thoracic Soc, 141, pp. 922–925.

Hmeidi *et al.* (2017) 'Tidal breathing parameters measured using structured light plethysmography in healthy children and those with asthma before and after bronchodilator', 5, pp. 1–12. doi: 10.14814/phy2.13168.

Hmeidi, H. *et al.* (2015) 'Non-invasive, non-contact measurement of tidal breathing parameters in children aged 3-17 years using structured light plethysmography (SLP)'. European Respiratory Journal, 46(59), p. 3643.

Hmeidi, H. *et al.* (2016) 'Spirometric and structured light plethysmography derived measures of airflow obstruction in asthma', *European Respiratory Journal*, 48(60), p. 4134. doi: 10.1183/13993003.congress-2016.PA4134.

Hmeidi, H. *et al.* (2017) 'Tidal breathing parameters measured using structured light plethysmography in healthy children and those with asthma before and after bronchodilator', *Physiological Reports*, 5(5). doi: 10.14814/phy2.13168.

Hmeidi, H. *et al.* (2018) 'Tidal breathing parameters measured by structured light plethysmography in children aged 2-12 years recovering from acute asthma/wheeze compared with healthy children', *Physiological Reports*, 6(12), pp. 1–21. doi: 10.14814/phy2.13752.

Hossack, W. (2006) 'Stereo Imaging'. The School of Physics and Astronomy,The University of Edinburgh. Available at: https://www2.ph.ed.ac.uk/~wjh/teaching/dia/documents/stereo.pdf.

Jackson, E. *et al.* (1995) 'A critical assessment of uncalibrated respiratory inductance

plethysmography (Respitrace®) for the measurement of tidal breathing parameters in newborns and infants', *Pediatric pulmonology*. Wiley Online Library, 20(2), pp. 119–124.

Johns, D. P. and Pierce, R. (2007) *Pocket Guide to Spirometry*. second edi, *The Measurement and Interpretation of Ventilatory Function in Clinical Practice*. second edi. Australia: McGraw-Hill. Available at: http://www.nationalasthma.org.au/uploads/content/211-spirometer_handbook_naca.pdf.

Kahaner, D. *et al.* (1989) 'Numerical methods and software'. NJ USA: Upper Saddle River, p. 495.

Kampschmidt *et al.* (2016) 'Feasibility of spirometry testing in preschool children', *Pediatric Pulmonology*, 51(3), pp. 258–266.

Kayvan, N. and Splinter, R. (2012) *Biomedical Signal and Image Processing*. US: Taylor and Francis.

Kesten, S. *et al.* (1990) 'Respiratory rate during acute asthma', *Chest*. Elsevier, 97(1), pp. 58–62.

Kim, E. S. *et al.* (2007) 'Basement membrane thickening and clinical features of children with asthma', *Allergy*. Wiley Online Library, 62(6), pp. 635–640.

Kloke, J. D. and Mckean, J. W. (2012) 'Rfit : Rank-based Estimation for Linear Models Rank-regression', *The R Journal*, 4(December), pp. 57–64.

Kondo, T. *et al.* (2000) 'A dynamic analysis of chest wall motions with MRI in healthy young subjects', *Respirology*. Wiley Online Library, 5(1), pp. 19–25.

Konno, K. and Mead, J. (1967) 'Measurement of the separate volume changes of rib cage and abdomen during breathing.', *Journal of Applied Physiology (Bethesda, Md. : 1985)*, 22(3), pp. 407–422.

Kostianev, S., Hristova, A. and Iluchev, D. (1999) 'Characteristics of tidal expiratory flow pattern in healthy people and patient with chronic obstructive pulmonary disease.', *Folia medica*, 41(3), pp. 18–25.

Kotani, T. *et al.* (2002) 'Three dimensional analysis of chest wall motion during breathing in healthy individuals and patients with scoliosis using an ultrasonography-based system.', *Studies in health technology and informatics*, 91, pp. 135–139.

Kotani, T. *et al.* (2004) 'An analysis of chest wall and diaphragm motions in patients with idiopathic scoliosis using dynamic breathing MRI', *Spine*. LWW, 29(3), pp. 298–302.

Kuratomi, Y. *et al.* (1985) 'Variability of breath-by-breath tidal volume and its characteristics in normal and diseased subjects', *Japanese journal of medicine*. The Japanese Society of Internal Medicine, 24(2), pp. 141–149.

Lafortuna, C. L. and Passerini, L. (1995) 'A new instrument for the measurement of rib cage and abdomen circumference variation in respiration at rest and during exercise', *European journal of applied physiology and occupational physiology*. Springer, 71(2–3), pp. 259–265.

Lall, C. A. *et al.* (2007) 'Airway resistance variability and response to bronchodilator in children with asthma', *European Respiratory Journal*. Eur Respiratory Soc, 30(2), pp. 260–268.

Langston, C. *et al.* (1984) 'Human lung growth in late gestation and in the neonate.', *The American review of respiratory disease*, 129(4), pp. 607–613.

Latzin, P. *et al.* (2009) 'Lung volume, breathing pattern and ventilation inhomogeneity in preterm and term infants', *PLoS ONE*, 4(2). doi: 10.1371/journal.pone.0004635.

Laveneziana, P. *et al.* (2015a) 'Disruption of tidal breathing in COPD by use of pneumotachograph and mouthpiece compared to non-contact measurement with structured light plethysmography (SLP)'. European Respiratory Society, 46(59), p. 511.

Laveneziana, P. *et al.* (2015b) 'Non-contact assessment of acute bronchodilator9 response during tidal breathing in COPD patients using structured light plethysmography (SLP)'. European Respiratory Society, 44(58), p. 4262.

Leach, R. M. (2008) 'Symptoms and signs of respiratory disease', *Medicine*, 36(3), pp. 119–125. doi: 10.1016/j.mpmed.2007.12.003.

Leonard, P. A. *et al.* (2006) 'An automated algorithm for determining respiratory rate by photoplethysmogram in children', *Acta Paediatrica, International Journal of Paediatrics*, 95(9), pp. 1124–1128. doi: 10.1080/08035250600612280.

Liu, C.-L. (2010) 'A Tutorial of the Wavelet Transform', *National Taiwan University, Department of Electrical Engineering (NTUEE), Taiwan*, pp. 1–72. doi: 10.1111/j.1600-0404.1995.tb01711.x.

Lodrup-Carlsen, K. C. and Carlsen, K. H. (1993) 'Lung function in awake healthy infants: the first five days of life', *European respiratory journal*. Eur Respiratory Soc, 6(10), pp. 1496–1500.

Lødrup, K. C. C. (2000) 'Tidal breathing at all ages.', *Monaldi archives for chest disease= Archivio Monaldi per le malattie del torace*, 55(5), pp. 427–434.

MacBean, V. O. (2014) 'The utility of surface parasternal intercostal electromyography in the assessment of paediatric respiratory disease For the degree of PhD Respiratory Muscle Laboratory of Respiratory Medicine King ' s College London School of Medicine'.

Malina, R. M., Bouchard, C. and Bar-Or, O. (2004) *Growth, maturation, and physical activity*. Leeds: Human kinetics.

Miller, M. R., Crapo, R., *et al.* (2005) 'General considerations for lung function testing', *European Respiratory Journal*. Eur Respiratory Soc, 26(1), pp. 153–161.

Miller, M. R., Hankinson, J., *et al.* (2005) 'Standardisation of spirometry', *European respiratory journal*. Eur Respiratory Soc, 26(2), pp. 319–338.

Monitoring, A. C. for A. (2008) 'Asthma in Australia', *Asthma in Australia*, 24(1), pp. 71–71. doi: 10.1111/j.1445-5994.1994.tb04436.x.

Moodley, T. *et al.* (2010) 'Acute viral bronchiolitis: aetiology and treatment implications in a population that may be HIV co-infected.', *Southern African Journal of Epidemiology & Infection*, 25(2), pp. 6–8. doi: 10.1080/10158782.2010.11441379.

Morgan, M. D. *et al.* (1985) 'Contribution of the rib cage to breathing in tetraplegia.', *Thorax*. BMJ Publishing Group Ltd, 40(8), pp. 613–617.

Morgan, M. D., Gourlay, A. R. and Denison, D. M. (1984) 'An optical method of studying the shape and movement of the chest wall in recumbent patients.', *Thorax*. BMJ Publishing Group Ltd, 39(2), pp. 101–106.

Morgan, W. *et al.* (1982) 'The measurement of total respiratory resistance in small children', *Journal of Asthma*. Taylor & Francis, 19(4), pp. 233–240.

Morris, M. J. *et al.* (2004) 'Changes in lung function and tidal airflow patterns after increasing extrathoracic airway resistance', *Respirology*. Wiley Online Library, 9(4), pp. 474–480.

Morris, M. J. and Lane, D. J. (1981) 'Tidal expiratory flow patterns in airflow obstruction.', *Thorax*. BMJ Publishing Group Ltd, 36(2), pp. 135–142.

Motamedi-Fakhr, S., Wilson, R. and Iles, R. (2017) 'Tidal breathing patterns derived from structured light plethysmography in COPD patients compared with healthy subjects', *Medical Devices: Evidence and Research*, 10, pp. 1–9. doi: 10.2147/MDER.S119868.

Motamedi-Fakhr, S. *et al.* (2017) 'Evaluation of the agreement of tidal breathing parameters measured simultaneously using pneumotachography and structured light plethysmography', *Physiological Reports*, 5(3), p. e13124. doi: 10.14814/phy2.13124.

Moxham, J. and Jolley, C. (2009) 'Breathlessness, fatigue and the respiratory muscles', *Clinical medicine*. Royal College of Physicians, 9(5), pp. 448–452.

Muller, N., Bryan, A. C. and Zamel, N. (1980) 'Tonic inspiratory muscle activity as a cause of hyperinflation in histamine-induced asthma', *Journal of Applied Physiology*. Am Physiological Soc, 49(5), pp. 869–874.

Muthuswamy, J. (2003) 'Biomedical Signal Analysis', in Kutz, M. (ed.) *Standard Handbook of Biomedical Engineering and Design*. McGRAW-HILL: London, p. 18.1. Available at: http://unhas.ac.id/tahir/BAHAN-KULIAH/BIO-MEDICAL/NEW/HANBOOK/18_Biomedical_Signal_Analysis.pdf (Accessed: 20 September 2017).

Narayanan, M. *et al.* (2012) 'Alveolarization continues during childhood and adolescence: new evidence from helium-3 magnetic resonance', *American journal of respiratory and critical care medicine*. Am Thoracic Soc, 185(2), pp. 186–191.

National Heart Lung, Institute, B. and others (2007) 'National Asthma Education and Prevention Program (2007) Expert panel report 3: guidelines for the diagnosis and management of asthma', *Full report. Washington (DC): US Department of Health and Human Services*.

Nationwide Children's Hospital (2018) *Asthma and Reactive Airway Disease (RAD) (Wheezing)*. Available at: https://www.nationwidechildrens.org/conditions/asthma-and-

reactive-airway-disease-rad-wheezing (Accessed: 28 July 2017).

Newth, C. J. L. and Hammer, J. (2005) 'Measurements of thoraco-abdominal asynchrony and work of breathing in children', in *Paediatric pulmonary function testing*. Karger Publishers, pp. 148–156.

NICE (2015) *Bronchiolitis in children: diagnosis and management*. Available at: https://www.nice.org.uk/guidance/ng9/chapter/1-Recommendations#management-of-bronchiolitis.

Nunes, C., Pereira, A. M. and Morais, M. (2017) 'Asthma costs and social impact', *Asthma Research and Practice*. Asthma Research and Practice, 3(1), p. 1. doi: 10.1186/s40733-016-0029-3.

Olden, C., Symes, E. and Seddon, P. (2010) 'Measuring tidal breathing parameters using a volumetric vest in neonates with and without lung disease', *Pediatric pulmonology*. Wiley Online Library, 45(11), pp. 1070–1075.

Øymar, K., Skjerven, H. O. and Mikalsen, I. B. (2014) 'Acute bronchiolitis in infants, a review', *Scandinavian journal of trauma, resuscitation and emergency medicine*. BioMed Central, 22(1), p. 23.

Papadopoulos, N. G. *et al.* (2012) 'International consensus on (ICON) pediatric asthma', *Allergy*. Wiley Online Library, 67(8), pp. 976–997.

Papastamelos, C. *et al.* (1995) 'Developmental changes in chest wall compliance in infancy and early childhood', *Journal of Applied Physiology*. Am Physiological Soc, 78(1), pp. 179–184.

Papiris, S. *et al.* (2001) 'Clinical review: severe asthma', *Critical Care*. BioMed Central, 6(1), p. 30.

Papiris, S. *et al.* (2002) 'Clinical review: severe asthma', *Critical Care*. BioMed Central, 6(1), p. 30.

Parker, R. A. *et al.* (2016) 'Application of mixed effects limits of agreement in the presence of multiple sources of variability: Exemplar from the comparison of several devices to measure respiratory rate in COPD patients', *PLoS ONE*, 11(12), pp. 1–15. doi: 10.1371/journal.pone.0168321.

Pedersen, S. E. *et al.* (2011) 'Global strategy for the diagnosis and management of asthma in children 5 years and younger', *Pediatric Pulmonology*, 46(1), pp. 1–17. doi: 10.1002/ppul.21321.

Petrus, N. C. M. *et al.* (2015) 'Accuracy of tidal breathing measurement of FloRight compared to an ultrasonic flowmeter in infants', *Pediatric pulmonology*. Wiley Online Library, 50(4), pp. 380–388.

Pickerd, N., Williams, E. M. and Kotecha, S. (2013) 'Electromagnetic inductance plethysmography to measure tidal breathing in preterm and term infants', *Pediatric pulmonology*. Wiley Online Library, 48(2), pp. 160–167.

Piippo-Savolainen, E. *et al.* (2004) 'Asthma and lung function 20 years after wheezing in infancy: Results from a prospective follow-up study', *Archives of Pediatrics and Adolescent Medicine*, 158(11), pp. 1070–1076. doi: 10.1001/archpedi.158.11.1070.

Pittman, J. E. *et al.* (2011) 'Age of Pseudomonas aeruginosa acquisition and subsequent severity of cystic fibrosis lung disease', *Pediatric pulmonology*. Wiley Online Library, 46(5), pp. 497–504.

PneumaCare (2013) *The Next Generation of Lung Function Imaging and Assessment Technology*. Available at: http://www.pneumacare.com/ (Accessed: 25 March 2018).

Polikar, R. (1994) 'The Wavelet Tutorial', *Internet Resources httpengineering rowan edu polikarWAVELETSWTtutorial html*, pp. 1–67. doi: 10.1088/1751-8113/44/8/085201.

Quanjer, P. H. (2003) 'Lung function tests', *Medicina (B Aires)*, 63(5), p. 459.

Raichura, N. *et al.* (2001) 'Breath-hold MRI in evaluating patients with pectus excavatum', *The British journal of radiology*. British Institute of Radiology, 74(884), pp. 701–708.

Ralston, S. L. *et al.* (2014) 'Clinical practice guideline: the diagnosis, management, and prevention of bronchiolitis', *Pediatrics*. Am Acad Pediatrics, p. peds--2014.

Rasmussen, F. *et al.* (2002) 'Risk factors for hospital admission for asthma from childhood to young adulthood: a longitudinal population study', *Journal of Allergy and Clinical Immunology*. Elsevier, 110(2), pp. 220–227.

Ratnovsky, A., Elad, D. and Halpern, P. (2008) 'Mechanics of respiratory muscles', *Respiratory physiology & neurobiology*. Elsevier, 163(1–3), pp. 82–89.

Régnier, S. A. and Huels, J. (2013) 'Association between respiratory syncytial virus hospitalizations in infants and respiratory sequelae: systematic review and meta-analysis', *The Pediatric infectious disease journal*. LWW, 32(8), pp. 820–826.

Reich, A. R. and McHenry, M. A. (1990) 'Estimating respiratory volumes from rib cage and abdominal displacements during ventilatory and speech activities', *Journal of Speech, Language, and Hearing Research*. ASHA, 33(3), pp. 467–475.

Rome, E. S. *et al.* (1987) 'Effect of sleep state on chest wall movements and gas exchange in infants with resolving bronchopulmonary dysplasia', *Pediatric pulmonology*. Wiley Online Library, 3(4), pp. 259–263.

Russell, N. J. *et al.* (1986) 'Quantitative assessment of the value of spirometry.', *Thorax*. BMJ Publishing Group Ltd, 41(5), pp. 360–363.

Russell, R. I. and Helms, P. J. (1994) 'Evaluation of three different techniques used to measure chest wall movements in children', *European respiratory journal*. Eur Respiratory Soc, 7(11), pp. 2073–2076.

Sackner, M. A. *et al.* (1989) 'Calibration of respiratory inductive plethysmograph during natural breathing', *Journal of Applied Physiology*, 66(1), pp. 410–420.

Sahambi, J. S., Tandon, S. N. and Bhatt, R. K. P. (1997) 'Using wavelet transfroms for ECG characterization', *IEEE Engineering Medicine and Biology Magazine.*, 16, pp. 77–83. doi: 10.1109/51.566158.

Sartene, R. *et al.* (1990) 'Respiratory cross-sectional area-flux measurements of the human chest wall', *Journal of Applied Physiology*, 68(4), pp. 1605–1614.

Schmalisch, G., Wilitzki, S. and Wauer, R. R. (2005) 'Differences in tidal breathing between infants with chronic lung diseases and healthy controls', *BMC pediatrics*. BioMed Central, 5(1), p. 36.

Schmidt, M. *et al.* (1998) 'Comparative investigations of algorithms for the detection of breaths in newborns with disturbed respiratory signals', *Computers and Biomedical Research*, 31(6), pp. 413–425. doi: 10.1006/cbmr.1998.1493.

Schultz, A. *et al.* (2010) 'The transient value of classifying preschool wheeze into episodic viral wheeze and multiple trigger wheeze', *Acta Paediatrica*. Wiley Online Library, 99(1), pp. 56–60.

Seddon, P. (2015) 'Options for Assessing and Measuring Chest Wall Motion', *Paediatric Respiratory Reviews*. doi: 10.1016/j.prrv.2014.10.006.

Seddon, P. C., Davis, G. M. and Coates, A. L. (1996) 'Do tidal expiratory flow patterns reflect lung mechanics in infants?', *American journal of respiratory and critical care medicine*. American Public Health Association, 153(4), pp. 1248–1252.

Seppa, V. (2013) 'European Respiratory Society Annual Congress 2013', 36, p. 1.

Shim, C. S. and Williams, M. H. (1980) 'Evaluation of the severity of asthma: patients versus physicians', *The American journal of medicine*. Elsevier, 68(1), pp. 11–13.

Shoeb, A. and Clifford, G. (2006) 'Wavelets ; Multiscale Activity in Physiological Signals Short-Time Fourier Transform', *Biomedical Signal and Image Processing*, pp. 1–29.

Sigurs, N. *et al.* (2010) 'Asthma and allergy patterns over 18 years after severe RSV bronchiolitis in the first year of life', *Thorax*. BMJ Publishing Group Ltd, 65(12), pp. 1045–1052.

Sivan, Y. and Newth, J. L. (1990) 'Thoracoabdominal Asynchrony in Acute Upper Airway Obstruction in Small Children1, 2', *Am Rev Respir Dis*. Am Thoracic Soc, 142, pp. 540–544.

Smith, I. and Mackay, J. (2011) 'Respiratory rate measurement: a comparison of methods', *British Journal of Healthcare Assistants*, 05(01), pp. 1–6. doi: 10.12968/bjha.2011.5.1.18.

Smith, S. W. (1997) *The scientist and engineer's guide to digital signal processing*. California Technical Pub. San Diego.

Sorkhabi, M. M. (2014) 'Emotion Detection from EEG signals with Continuous Wavelet Analyzing', *American Journal of Computing Research Repository*, 2(4), pp. 66–70. doi: 10.12691/ajcrr-2-4-3.

Spycher, B. D. *et al.* (2008) 'Distinguishing phenotypes of childhood wheeze and cough using latent class analysis', *European Respiratory Journal*. Eur Respiratory Soc, 31(5), pp. 974–981.

Stick, S. (1996) 'Measurements during tidal breathing', *Infant respiratory function testing. New York: Wiley-Liss*, 134.

Stick, S. M. *et al.* (1992) 'Validation of respiratory inductance plethysmography for the measurement of tidal breathing parameters in newborns', *Pediatric pulmonology*. Wiley Online Library, 14(3), pp. 187–191.

Stocks, J. (1996) *Infant respiratory function testing*. Edited by J. Stocks et al. John Wiley & Sons.

Stocks, J. (1999) 'Respiratory physiology during early life.', *Monaldi archives for chest disease= Archivio Monaldi per le malattie del torace*, 54(4), pp. 358–364.

Tauber, E. *et al.* (2003) 'Negative expiratory pressure: a new tool for evaluating lung function in children?', *Pediatric pulmonology*. Wiley Online Library, 35(3), pp. 162–168.

Taylor, T. (2013) *Respiratory System: Interactive Anatomy Guide-Human Anatomy.* Available at: www.innerbody.com/anatomy/respiratory (Accessed: 29 May 2014).

The Pt Group: Physical Therapy (2015) *Why Do Muscles Need Oxygen?* Available at: http://theptgroup.com/why-do-muscles-need-oxygen/ (Accessed: 2 May 2017).

Thien, F. (2013) 'Measuring and imaging small airways dysfunction in asthma', *Asia Pacific Allergy*, 3(4), p. 224. doi: 10.5415/apallergy.2013.3.4.224.

Tidy, C. (2016) *Spirometry*. Available at: https://patient.info/doctor/spirometry-pro (Accessed: 25 May 2018).

Tobin, M. J. *et al.* (1988) 'Variability of resting respiratory drive and timing in healthy subjects', *Journal of Applied Physiology*. Am Physiological Soc, 65(1), pp. 309–317.

Tokuda, J. *et al.* (2009) 'Lung motion and volume measurement by dynamic 3D MRI using a 128-channel receiver coil', *Academic radiology*. Elsevier, 16(1), pp. 22–27.

Totapally, B. R. *et al.* (1996) 'TIDAL BREATHING FLOW-VOLUME (TBFV) LOOPS IN INFANTS WITH BRONCHIOLITIS: EFFECT OF ALBUTEROL. 2331', *Pediatric Research*. Nature Publishing Group, 39(S4), p. 391.

Troyer, A. D. E. M. (1988) 'Functional anatomy of the respiratory muscles', *Clin Chest Med.*, 9(2), pp. 175–93.

Turner, S. *et al.* (2011) 'British guidelines on the management of asthma: What's new for 2011?', *Thorax*, 66(12), pp. 1104–1105. doi: 10.1136/thoraxjnl-2011-200213.

Unser, M. and Aldroubi, A. (1996) 'A review of wavelets in biomedical applications', *Proceedings of the IEEE*, 84(4), pp. 626–638. doi: 10.1109/5.488704.

Upadhyay, N. and Karmakar, A. (2015) 'Speech Enhancement using Spectral Subtraction-type

Algorithms: A Comparison and Simulation Study', *Procedia Computer Science*. Elsevier Masson SAS, 54, pp. 574–584. doi: 10.1016/j.procs.2015.06.066.

Vaseghi, S. (2000) 'Spectral Substraction', *Advanced Digital Signal Processing and Noise Reduction*, 9, pp. 333–354. doi: 10.1007/978-3-319-09659-9.

Vilozni, D. *et al.* (2009) 'FRC measurements using body plethysmography in young children', *Pediatric pulmonology*. Wiley Online Library, 44(9), pp. 885–891.

Walter, R. N. and Vaughn, B. V. (2013) 'Low frequency filtering of nasal pressure channel causes loss of flow limitation', *Neurodiagnostic Journal*, 53(1), pp. 58–62. doi: 10.1080/21646821.2013.11079885.

Warren, R. H. and Alderson, S. H. (1986) 'Breathing patterns in infants utilizing respiratory inductive plethysmography', *Chest*. Elsevier, 89(5), pp. 717–722.

Warren, R. H., Horan, S. M. and Robertson, P. K. (1997) 'Chest wall motion in preterm infants using respiratory inductive plethysmography', *European Respiratory Journal*. Eur Respiratory Soc, 10(10), pp. 2295–2300.

Webb, M. S. *et al.* (1985) 'Continuing respiratory problems three and a half years after acute viral bronchiolitis.', *Archives of disease in childhood*, 60(11), pp. 1064–7. Available at: http://www.pubmedcentral.nih.gov/articlerender.fcgi?artid=1777618&tool=pmcentrez&rendertype=abstract.

Weissman, C. *et al.* (1984) 'Effect of respiratory apparatus on respiration', *Journal of Applied Physiology*. Am Physiological Soc, 57(2), pp. 475–480.

Weldam, S. W. *et al.* (2014) 'Perceived quality of life in chronic obstructive pulmonary disease patients: a cross-sectional study in primary care on the role of illness perceptions', *BMC Family Practice*, 15(1), p. 140. doi: 10.1186/1471-2296-15-140.

Wijngaart, L. S., Roukema, J. and Merkus, P. J. F. M. (2015) 'Respiratory disease and respiratory physiology: putting lung function into perspective: paediatric asthma', *Respirology*. Wiley Online Library, 20(3), pp. 379–388.

Wilkens, H. *et al.* (2010) 'Breathing pattern and chest wall volumes during exercise in patients with cystic fibrosis, pulmonary fibrosis and COPD before and after lung transplantation', *Thorax*. BMJ Publishing Group Ltd, 65(9), pp. 808–814.

Williams, E. M. *et al.* (2011) 'Estimation of tidal ventilation in preterm and term newborn infants using electromagnetic inductance plethysmography', *Physiological measurement*. IOP Publishing, 32(11), p. 1833.

Williams, E. M. *et al.* (2014) 'A pilot study quantifying the shape of tidal breathing waveforms using centroids in health and COPD', *Journal of clinical monitoring and computing*. Springer, 28(1), pp. 67–74.

Williams, E. M., Madgwick, R. G. and Morris, M. J. (1998) 'Tidal expired airflow patterns in adults with airway obstruction', *European Respiratory Journal*. Eur Respiratory Soc, 12(5), pp. 1118–1123.

World Health Organisation (2013) ‘Chronic respiratory diseases - Asthma’, *WHO*. World Health Organization. Available at: http://www.who.int/respiratory/asthma/en/ (Accessed: 29 October 2018).

Zapletal, A., Samanek, M. and Paul, T. (1982) ‘Upstream and total airway conductance in children and adolescents.’, *Bulletin europeen de physiopathologie respiratoire*, 18(1), pp. 31–37.

Zeltner, T. B. *et al.* (1987) ‘The postnatal development and growth of the human lung. I. Morphometry’, *Respiration physiology*. Elsevier, 67(3), pp. 247–267.

12 Appendices

Appendix - A Matlab codes

- Code used for Spectral subtraction

This code was used to clean the SLP signal using spectral subtraction,
% For the original code see link:
% https://gist.github.com/jameslyons/554325efb2c05da15b31
% Copyright 2013 James Lyons , MIT License (MIT)

```
function [S_out]=spectral_sub(S_in,I_in,Fs)

NFFT = 1024;
WINLEN = 10; %frame length in seconds
WINSTEP = 0.5; % frame step in seconds

% converting the noisy signal to frames and getting its spectral
frames = frame_sig(S_in, WINLEN*Fs, WINSTEP*Fs, @hamming);
cspec = fft(frames,NFFT,2); % complex spectrum
pspec = abs(cspec).^2; % power spectrum of noisy signal
phase = angle(cspec);


% converting the noise to frames and getting its spectral
noise_frames = frame_sig(I_in, WINLEN*Fs, WINSTEP*Fs, @hamming);
noise_cspec = fft(noise_frames,NFFT,2); % complex spectrum
noise_pspec = abs(noise_cspec).^2; % power spectrum of noisy signal
noise_phase = angle(noise_cspec);


clean_spec = pspec - noise_pspec;
clean_spec(clean_spec < 0) = 0; % negative power spectrum is not allowed


reconstructed_frames = ifft(sqrt(clean_spec).*exp(i * phase),NFFT,2);
reconstructed_frames = real(reconstructed_frames(:,1:WINLEN*Fs)); % sometimes small
complex residuals stay behind
```

```
S_out                                                                    =
deframe_sig(reconstructed_frames,length(S_in),WINLEN*Fs,WINSTEP*Fs,@hamming);

Return

% For the original code see link:
% https://github.com/jameslyons/spl_featgen
% Copyright 2013 James Lyons, MIT License (MIT)

function win_frames = frame_sig(signal, frame_len, frame_step, winfunc)
%function win_frames = frame_sig(signal, frame_len, frame_step, wintype)
% takes a 1 by N signal, and breaks it up into frames. Each frame starts
% frame_step samples after the start of the previous frame. Each frame is
% windowed by wintype.
% - to specify window, use e.g. @hamming, @(x)chebwin(x,30), @(x)ones(x,1), etc.
if size(signal,1) ~= 1
   signal = signal';
end

signal_len = length(signal);
if signal_len <= frame_len  % if very short frame, pad it to frame_len
   num_frames = 1;
else
   num_frames = 1 + ceil((signal_len - frame_len)/frame_step);
end
padded_len = (num_frames-1)*frame_step + frame_len;
% make sure signal is exactly divisible into N frames
pad_signal = [signal, zeros(1,padded_len - signal_len)];


% build array of indices
indices = repmat(1:frame_len, num_frames, 1) + ...
   repmat((0: frame_step: num_frames*frame_step-1)', 1, frame_len);
frames = pad_signal(indices);

win = repmat(winfunc(frame_len)', size(frames, 1), 1);
% apply window
win_frames = frames .* win;
% For the original code see link:
% https://github.com/jameslyons/spl_featgen
% Copyright 2013 James Lyons , MIT License (MIT)

function rec_signal = deframe_sig(frames, signal_len, frame_len, frame_step, winfunc)
```

```
%rec_signal = deframe_sig(frames, signal_len, frame_len, frame_step, wintype)
% frames - a N by frame_len matrix of frames
% signal_len - the length of the original unframed signal (if unknown, use [])
% frame_len, frame_step - should be same as used by frame_sig (framing function)
% winfunc - the same used when framing, this is undone before overlap-add


num_frames = size(frames,1);
indices = repmat(1:frame_len, num_frames, 1) + ...
        repmat((0: frame_step: num_frames*frame_step-1)', 1, frame_len);
padded_len = num_frames*frame_step + frame_len;

if isempty(signal_len)
   signal_len = padded_len;
end

rec_signal = zeros(1,padded_len);
window_correction = zeros(1,padded_len);
%wsyn = 0.5-0.5*cos((2*pi*((0:frame_len-1)+0.5))/frame_len);

win = winfunc(frame_len)';

for i = 1:num_frames
   window_correction(indices(i,:)) = window_correction(indices(i,:)) + win + eps;

   rec_signal(indices(i,:)) = rec_signal(indices(i,:)) + frames(i,:);
end

rec_signal = rec_signal./window_correction;
rec_signal = rec_signal(1:signal_len); % discard any padded samples
```

- Code for abnormalities-removal algorithm

```
% function
[S_clean,S_zero,loc,rloc_zero,rloc_clean,y_rising,y_falling,t_rising,t_falling]=remove_abnor
mal(S_in,min_ratio,max_ratio,min_t_ratio,max_t_ratio,PK_TH)
% S_in:     The input signal with abnormalities
% min_ratio: Minimums ratio (with respect to median) of accepted
% rising or falling (difference in y value) in the signal
% max_ratio: Maximum ratio (with respect to median) of accepted
% rising or falling (difference in y value) in the signal
% min_t_ratio: Minimums time ratio (with respect to median) of accepted
% rising or falling in the signal
% max_t_ratio: maximums time ratio (with respect to median) of accepted
% rising or falling in the signal
% PK_TH: minimum value of the peaks that are included in median
% calculations
% S_clean:  The abnormalities are deleted, and the signal level is adjusted
%           to be matched at the deletion point
% S_zero:   The abnormalities are replaced with zero
% loc:      minima-location matrix
% rloc_zero: Rejected locations for S_zero matrix
% rloc_clean: Rejected locations for S_clean matrix
% y_rising: The value of y-difference (rising)
% y_falling: The value of y-difference (falling)
% t_rising: The value of t-difference in samples (rising)
% t_falling: The value of t-difference in samples (falling)
% Date:     01 June 2018
% Author:   Hamzah Hmeidi (h.hmeidi@keele.ac.uk)

function
[S_clean,S_zero,loc,rloc_zero,rloc_clean,y_rising,y_falling,t_rising,t_falling]=remove_abnor
mal(S_in,min_ratio,max_ratio,min_t_ratio,max_t_ratio,PK_TH)

% finding the minima by finding the maxima of the negative signal
[minimas,loc] = findpeaks(-S_in);

% storting location matrix
loc=sort(loc);

min_count = length(loc); % the number of minimas


% Finding the the y-difference for the rising period and failing period
```

```
y_rising  = zeros(1,min_count-1);
y_falling = zeros(1,min_count-1);

% Finding the the t-difference (in samples) for the rising period and failing period
t_rising  = zeros(1,min_count-1);
t_falling = zeros(1,min_count-1);

for index = 1:(min_count - 1)

    % The current and the next minima
    loc1 = loc(index);
    loc2 = loc(index+1);

    % Finding the value of the peak between the two minima
    [pk,lc] = findpeaks(S_in(loc1:loc2));

    y_rising (index) = pk - S_in(loc1);
    y_falling(index) = pk - S_in(loc2);

    % Finding the number of samples from first minima to the peak
    t_rising (index) = lc;
    % Finding the number of samples from the peak to the second minima
    t_falling(index) = (loc2-loc1) - lc;
end


% finding the median of y_rising and y_faling

% exculuding peaks which has small values
rising_med = median(y_rising(y_rising>PK_TH));
falling_med = median(y_falling(y_falling>PK_TH));

min_r = rising_med * min_ratio; % minimum accepted rising y difference
max_r = rising_med * max_ratio; % maximum accepted rising y difference

min_f = falling_med * min_ratio; % minimum accepted falling y difference
max_f = falling_med * max_ratio; % maximum accepted falling y difference


% finding the median of t_rising and t_falling
% execluding the time of the peaks that has small values
% notice that y_rising and y_falling are used to find those peaks
```

```
rising_t_med = median(t_rising(y_rising>PK_TH));
falling_t_med = median(t_falling(y_falling>PK_TH));

min_t_r = rising_t_med * min_t_ratio; % minimum accepted rising times
max_t_r = rising_t_med * max_t_ratio; % maximum accepted rising times

min_t_f = falling_t_med * min_t_ratio; % minimum accepted falling times
max_t_f = falling_t_med * max_t_ratio; % maximum accepted falling times


% The index of rejected minima location
rejected_loc_index = zeros(1,min_count-1);

% Finding the location of rejected breathing units (rising and falling)
for index  = 1:(min_count-1)
   if y_rising(index) < min_r | y_rising(index) > max_r
      rejected_loc_index(index) = index;
   elseif y_falling(index) < min_f | y_falling(index) > max_f
      rejected_loc_index(index) = index;
   elseif t_rising(index) < min_t_r | t_rising(index) > max_t_r
      rejected_loc_index(index) = index;
   elseif t_falling(index) < min_t_f | t_falling(index) > max_t_f
      rejected_loc_index(index) = index;
   end
end

% removing zeros values from rejected_loc_index
rejected_loc_index(rejected_loc_index==0) = [];

rloc_zero  = loc(rejected_loc_index);

LN = length(rejected_loc_index);

% Setting rejected breathing units to 0
S_zero = S_in;
for index = 1:LN
   % The start and end of the rejected breathing unit
   reject_start = loc(rejected_loc_index(index));
   reject_end = loc(rejected_loc_index(index)+1) -1;

   S_zero(reject_start:reject_end) = 0;
end
```

```
% Deleting the rejected breathing units
S_clean = S_in;
for index = LN:-1:1
   % The start and end of the rejected breathing unit
   reject_start = loc(rejected_loc_index(index));
   reject_end = loc(rejected_loc_index(index)+1) -1;

   % Deleting the rejected breathing unit
   S_clean(reject_start:reject_end) = [];

   % If part of the signal is still remaining after deletion point
   if reject_start < length(S_clean)
      % If delection point is not the first point in the signal
      if reject_start > 1
         % Finding the difference between the deletion point and the
         % point before it
         y_diff = S_clean(reject_start) - S_clean(reject_start-1);

         % Adjusting the level of the signal after deletion point
         S_clean(reject_start:end) = S_clean(reject_start:end) - y_diff;
      end
   end

   % Adjusting the location matrix to match S_clean
   % Finding the difference in locations
   loc_diff = reject_end-reject_start+1;
   loc(rejected_loc_index(index)+1:end) = loc(rejected_loc_index(index)+1:end) - loc_diff;
end


rloc_clean = loc(rejected_loc_index);

% Removing duplicate values in rloc_clean
rloc_clean = unique(rloc_clean);


return
```

Appendix - B Clinical Studies Demographic

12.1 Healthy Subjects

ID	Gender	Age	Height	Weight	BMI
HHN01	M	9	138.3	30	15.68472
HHN02	M	9	138.5	32.9	17.15127
HHN03	M	7	115	21.6	16.3327
HHN04	M	10	144	43	20.73688
HHN08	F	8	141	33	16.59876
HHN09	M	11	135.5	33	17.97361
HHN12	F	8	130.6	36	21.1065
HHN14	M	7	142	28	13.88613
HHN15	M	4	111	20	16.23245
HHN16	M	5	110.5	20	16.37968
HHN17	F	3	98.3	14	14.48842
HHN18	M	10	137	32	17.04939
HHN20	F	7	118	20	14.36369
HHN22	F	7	124.7	31.7	20.38573
HHN23	F	7	126.8	28.05	17.44594
HHN24	F	8	125.2	25.4	16.20411
HHN25	M	8	133	26.1	14.75493
HHN26	F	11	155	47	19.56296
HHN28	M	8	125.3	24.15	15.38208
HHN31	F	10	136.6	31	16.61347
HHN34	F	5	113.6	27.3	21.15466
HHN36	M	11	153.3	35.85	15.25474
HHN39	M	7	126.5	28.7	17.93498
HHN40	F	5	110.5	18.9	15.4788
HHN41	F	5	116.7	21.52	15.80158
HHN43	F	10	152.8	37.62	16.11284
HHN44	F	12	153.2	43.1	18.36368
HHN45	M	5	114.5	20.9	15.94172
HHN46	M	12	148.8	37.8	17.07206
HHN47	M	2	91.1	15.18	18.2909
HHN50	M	10	144.7	50.38	24.06141
HHN57	F	7	126.5	28.1	17.56003
Healthy 001	F	4	101	17	16.66503
Healthy 003	M	5	102	15	14.41753
Healthy 004	M	3	94	15	16.97601

Healthy 007	F	6	111	20	16.23245
Healthy 008	F	3	96	17	18.44618
Healthy 009	F	4	101	16	15.68474
Healthy 011	M	5	97	18	19.13062
Healthy 012	M	6	110	27	22.31405
Healthy 013	M	4	97	19	20.19343
Healthy 014	M	4	90	18	22.22222
Healthy 015	M	4	97	17	18.06781
Healthy 016	M	2	76	14	24.23823
Healthy 018	M	3	104	19	17.56657
Healthy 019	M	2	95	14	15.51247
Healthy 020	M	4	97	19	20.19343
Healthy 021	M	2	95	17	18.83657
Healthy 022	M	3	100	18	18
Healthy 023	F	3	88	17	21.95248
Healthy 024	M	2	82	15	22.30815
Healthy 025	M	6	118	23	16.51824
Healthy 026	F	6	115	23	17.3913
Healthy 027	M	2	86	14	18.92915

12.2 Acute Asthma:

ID	Gender	Age	Height	Weight	BMI
HHA01	M	5	109.9	18	14.90312
HHA02	M	5	112.7	19	14.95911
HHA03	F	11	143	34.54	16.8908
HHA04	M	6	117.2	22	16.01649
HHA07	F	3	100.6	15.5	15.31566
HHA08	M	4	103.5	16.2	15.12287
HHA09	F	6	126	33	20.78609
HHA10	M	3	102.7	14.4	13.6528
HHA11	M	5	112	19.8	15.78444
HHA13	M	3	154	37	15.60128
HHA16	M	8		25.5	
HHA17	F	3	95.7	14.3	15.61393
HHA21	F	6	109	18.8	15.82358
HHA22	M	8	138		0
HHA23	F	4	103	17.36	16.36346
HHA24	M	9	142	30	14.878
HHA27	F	12	139	35.4	18.32203
HHA29	M	7	128.3	24.3	14.76226
HHA30	M	3	97.7	15	15.71456
HHA31	F	8	121.5	25.26	17.11121
HHA33	M	5	117.8	23	16.57438
HHA34	F	3	94.8	13.36	14.86585
HHA35	M	2	85.7	11.88	16.17539
HHA36	M	8		31.2	
HHA38	M	3	98.9	14.58	14.90613
HHA39	F	5	111.6	20.4	16.37954
HHA42	F	8	127.2	26.5	16.37841
HHA43	M	9	142.4	38.2	18.83837
HHA44	F	4	108	20.14	17.2668
HHA45	M	2	91.2	12.7	15.26912
HHA46	M	2		15.2	
HHA48	M	2	96.9	13.4	14.27109
HHA49	M	2	93.85	16.58	18.82418
HHA51	M	2	86.7	13.76	18.30544
HHA52	M	4	103.3	14.36	13.45717
HHA53	F	5	107.9	17.9	15.37482
HHA55	M	4	107.2	16	13.92292
HHA56	M	10	144.1	34.46	16.59538
HHA58	M	6	122.8	20.85	13.82641

12.3 Stable asthma:

ID	Gender	Age	Weight	Heigth
HHS01	F	11	65.5	162
HHS02	F	8	20	119.4
HHS03	F	8	24.9	130.8
HHS04	F	9	29.8	133.2
HHS05	F	13	64.7	153.9
HHS06	M	12	29.8	133.2
HHS07	F	8	29.8	129.6
HHS08	M	13	62.5	165.4
HHS09	F	10	30.1	129.9
HHS10	M	13	45.7	151.4
HHS11	M	10	34.1	135.6
HHS12	F	13	56.15	160.2
HHS13	M	11	54.8	160.1
HHS14	F	12	45.8	150.9
HHS15	F	13	41.65	150.4
HHS16	F	13	56.8	173.7
HHS17	M	11	44	143.2
HHS18	M	4	15.1	97.1
HHS19	M	7	24.8	129
HHS20	M	13	73.85	159.8
HHS21	F	11	51.8	138.6
HHS22	M	13	40.25	155.2
HHS23	M	7	22.2	118.5
HHS24	M	8	28.8	128.4
HHS25	F	9	30	133.7
HHS26	M	13	49.2	158
HHS27	M	15	60.7	177.3
HHS28	F	9	33.95	128.7
HHS29	F	9	24.4	128.9
HHS30	M	9	27.8	131.3
HHS31	M	9	34.5	151.4
HHS32	M	16	61.4	181.4
HHS33	M	12	50.2	149.9

Appendix - C Bland-Altman Agreement Plots

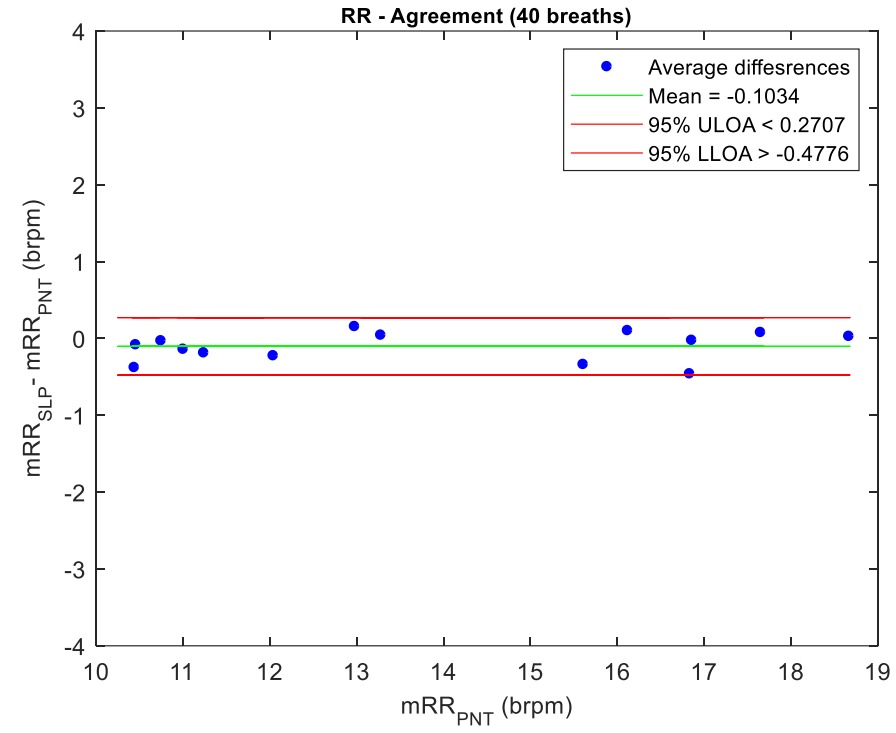

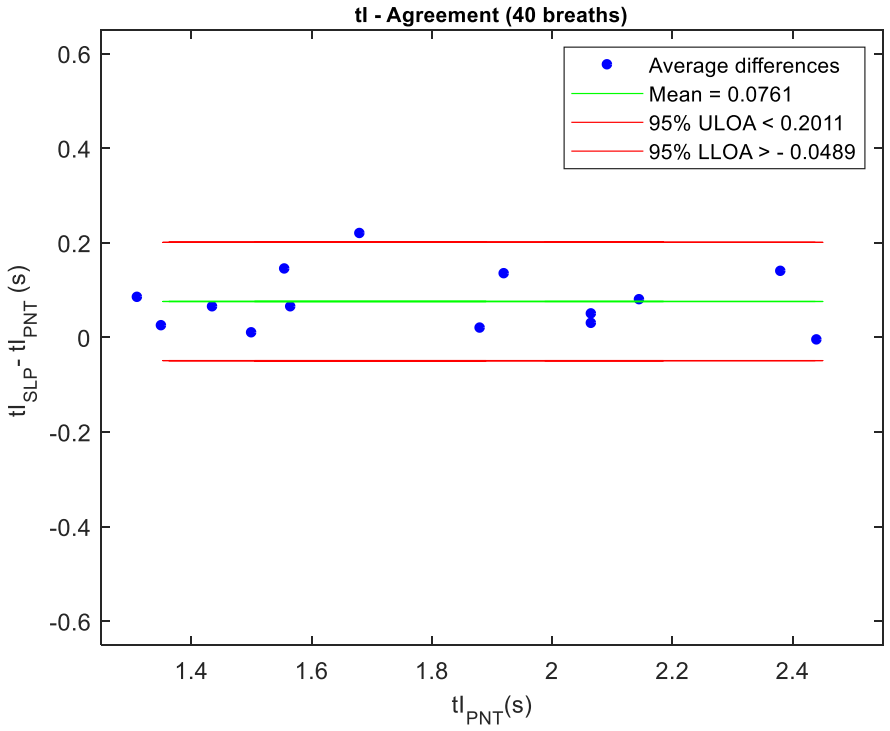

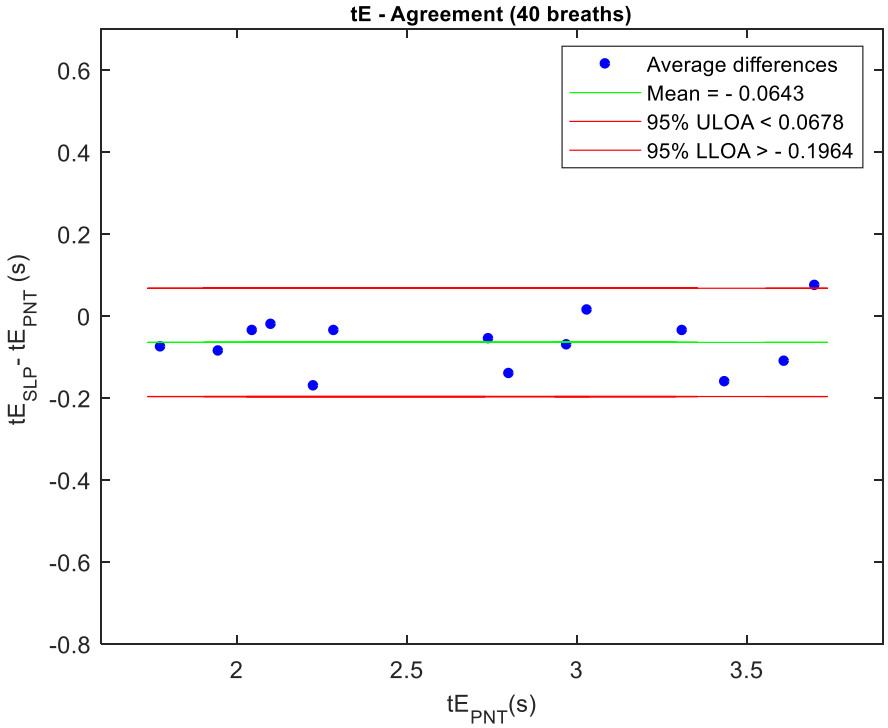
tE - Agreement (40 breaths)
Average differences
Mean = - 0.0643
95% ULOA < 0.0678
95% LLOA > - 0.1964
0.6
0.4
0.2
0
-0.2
-0.4
-0.6
-0.8
2
2.5
3
3.5
tE_SLP - tE_PNT (s)
tE_PNT(s)

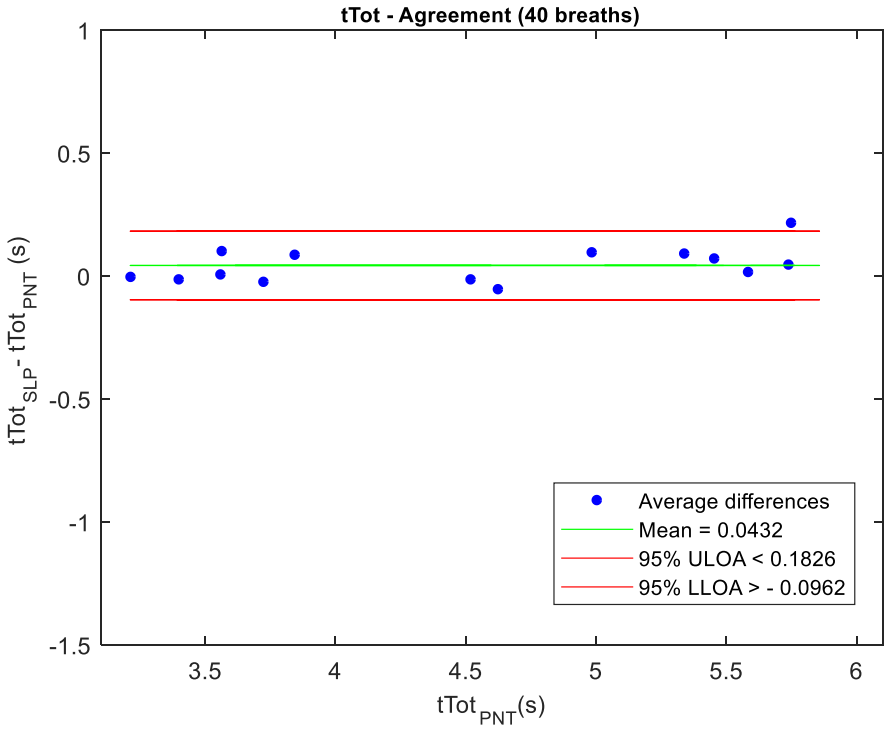
tTot - Agreement (40 breaths)
Average differences
Mean = 0.0432
95% ULOA < 0.1826
95% LLOA > - 0.0962
1
0.5
0
-0.5
-1
-1.5
3.5
4
4.5
5
5.5
6
tTot_SLP - tTot_PNT (s)
tTot_PNT(s)

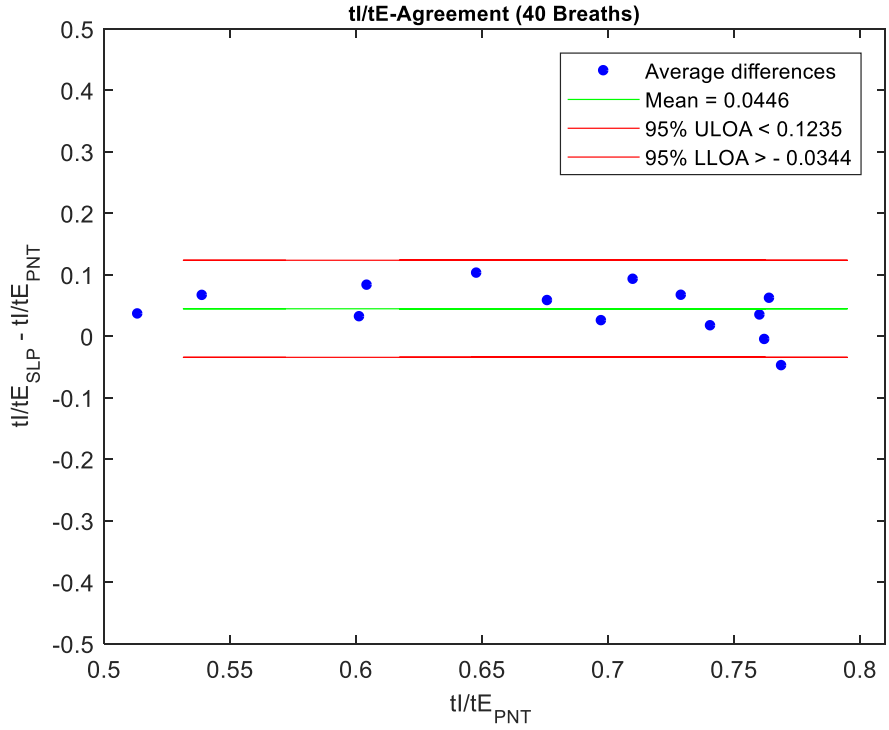
tI/tE-Agreement (40 Breaths)
Average differences
Mean = 0.0446
95% ULOA < 0.1235
95% LLOA > - 0.0344
tI/tE_SLP - tI/tE_PNT
tI/tE_PNT
0.5
0.4
0.3
0.2
0.1
0
-0.1
-0.2
-0.3
-0.4
-0.5
0.5
0.55
0.6
0.65
0.7
0.75
0.8

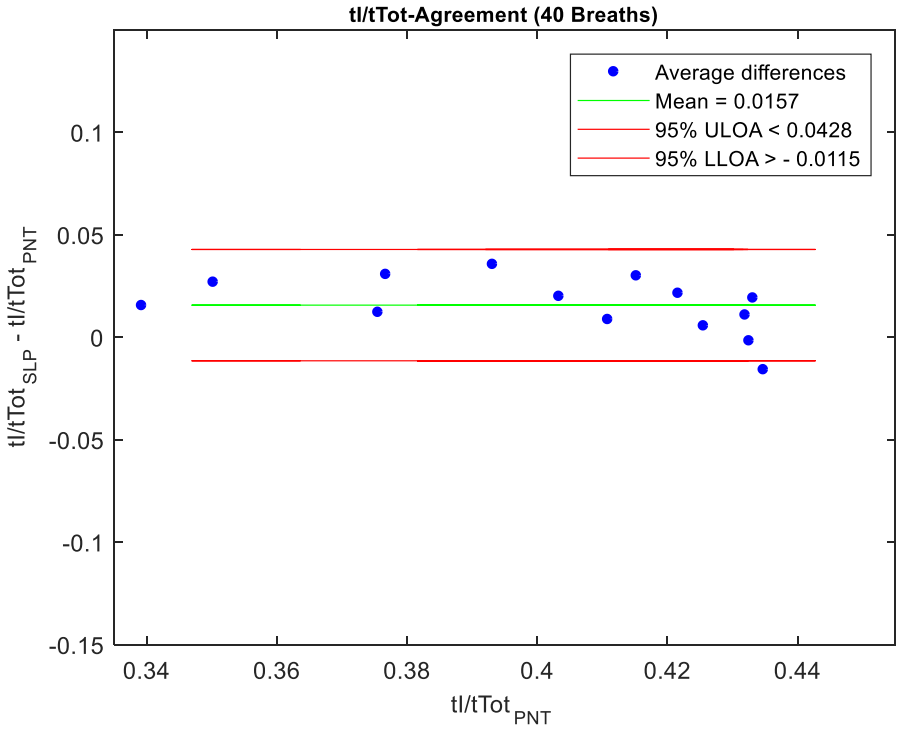
tI/tTot-Agreement (40 Breaths)
Average differences
Mean = 0.0157
95% ULOA < 0.0428
95% LLOA > - 0.0115
tI/tTot_SLP - tI/tTot_PNT
tI/tTot_PNT
0.1
0.05
0
-0.05
-0.1
-0.15
0.34
0.36
0.38
0.4
0.42
0.44

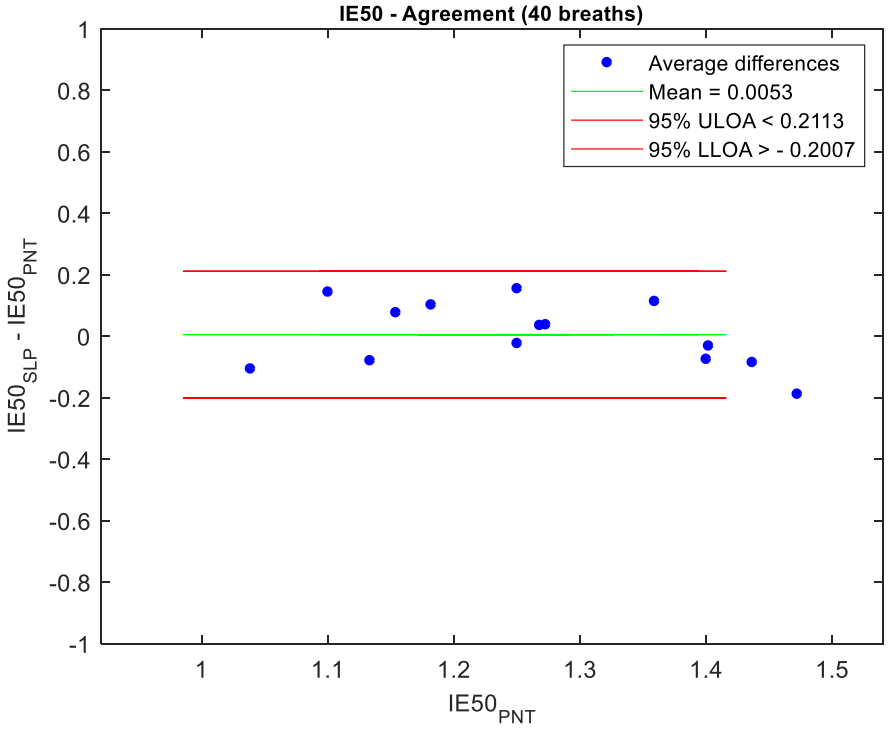
IE50 - Agreement (40 breaths)
Average differences
Mean = 0.0053
95% ULOA < 0.2113
95% LLOA > - 0.2007
IE50SLP - IE50PNT
IE50PNT
1
0.8
0.6
0.4
0.2
0
-0.2
-0.4
-0.6
-0.8
-1
1
1.1
1.2
1.3
1.4
1.5

Ethical Approvals:

Asthma studies in chapters five and six

Studies (ClinicalTrials.gov identifier: NCT02543333) were conducted in line with the International Conference on Harmonisation Good Clinical Practice guidelines and were approved by the UK Health Research Authority National Research Ethics Service (reference number 11/EE/00/37).
https://clinicaltrials.gov/ct2/show/NCT02543333?term=structured+light+plethysmography&cond=Asthma&rank=1

Acute Viral Bronchiolitis (AVB) study in Chapter seven

This study (ClinicalTrials.gov identifier: NCT02881632) was conducted in line with the International Conference on Harmonisation Good Clinical Practice guidelines and was approved by the UK Health Research Authority National Research Ethics Service (reference number 11/EE/00/37).
https://clinicaltrials.gov/ct2/show/NCT02881632?term=structured+light

Keele University

Ref: ERP1303 24th November 2016

Hamzah Hmeidi
Institute for Science and Technology in Medicine
Guy Hilton Research Centre
Thornburrow Drive
Stoke On Trent
ST4 7QB

Dear Hamzah,
Re: Improvement of the reliability of Structured Light Plethysmography measurements
Thank you for submitting your revised application for review.
I am pleased to inform you that your application has been approved by the Ethics Review Panel. The following documents have been reviewed and approved by the panel as follows:

Document(s)	Version Number	Date
Study Poster	4	16-11-2016
Consent Form	4	16-11-2016
Information Sheet	4	16-11-2016
Health Screening Questionnaire	4	16-11-2016

If the fieldwork goes beyond the date stated in your application, **28th December 2016**, or there are any other amendments to your study you must submit an 'application to amend study' form to the ERP administrator at research.erps@keele.ac.uk stating **ERP1** in the subject line of the email. This form is available via http://www.keele.ac.uk/researchsupport/researchethics/

If you have any queries, please do not hesitate to contact me via the ERP administrator on research.erps@keele.ac.uk stating **ERP1** in the subject line of the e-mail.

Yours sincerely

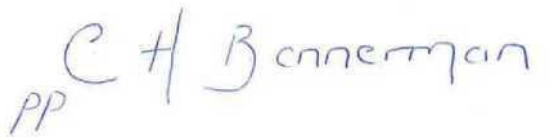

Dr Jackie Waterfield Chair - Ethical Review Panel

CC RI
Manager
Supervisor

Directorate of Engagement & Partnerships
T: +44(0)1782 734467

Keele University, Staffordshire ST5 5BG, UK

www.keele.ac.uk +44(0)1782 732000